8430-2-T

Report of BAMIRAC

THE LAMINAR NEAR WAKE BEHIND A SLENDER WEDGE AT SUPERSONIC SPEED AND HIGH REYNOLDS NUMBER

CHING-JU CHANG
ARTHUR F. MESSITER

November 1968

INFRARED PHYSICS LABORATORY
Willow Run Laboratories
INSTITUTE OF SCIENCE AND TECHNOLOGY

Contract DAHC15 67 C 0062

175

NOTICES

Sponsorship. The work reported herein is a part of the research under BAMIRAC (Ballistic Missile Research Analysis Center) conducted at the Willow Run Laboratories of the Institute of Science and Technology for the Advanced Research Projects Agency, Department of Defense, Washington, D. C., under Contract DAHC15 67 C 0062, ARPA Order 236, Amendment 26. Contracts and grants to The University of Michigan for the support of sponsored research are administered through the Office of the Vice-President for Research.

BAMIRAC. The Ballistic Missile Radiation Analysis Center is specifically concerned with electromagnetic radiation emanating from or caused by ICBM's or IRBM's in the powered and ballistic phases. In accordance with DoD Instruction 5100.45, BAMIRAC collects, processes, and disseminates information obtained from reports of field measurements and from laboratory and theoretical studies. In addition, it conducts its own theoretical and experimental investigations. BAMIRAC provides for visits of qualified persons and prepares bibliographies on request. Also, the facility aids ARPA by planning and conducting various technical conferences and by publishing the Proceedings of the Anti-Missile Research Advisory Council. This report represents one phase of the research being carried out as part of the BAMIRAC technical effort.

BAMIRAC is under the technical direction of the Infrared Physics Laboratory of Willow Run Laboratories, a unit of The University of Michigan's Institute of Science and Technology. It draws also upon the capabilities of the Infrared and Optical Sensor Laboratory and the Computation Department of Willow Run Laboratories, and upon those of the Department of Aerospace Engineering and of other departments of The University of Michigan, particularly within the College of Engineering.

Distribution. Initial distribution of this report has been approved by the Advanced Research Projects Agency and is indicated at the end of this document.

Final Disposition. After this document has served its purpose, it may be destroyed. Please do not return it to Willow Run Laboratories.

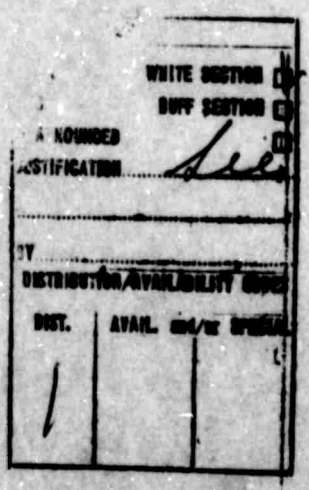

Laboratory copy
by A.H.

8430-2-T

Report of BAMIRAC

THE LAMINAR NEAR WAKE BEHIND A SLENDER WEDGE AT SUPERSONIC SPEED AND HIGH REYNOLDS NUMBER

CHING-JU CHANG
ARTHUR F. MESSITER

November 1968

Infrared Physics Laboratory
Willow Run Laboratories
INSTITUTE OF SCIENCE AND TECHNOLOGY
THE UNIVERSITY OF MICHIGAN
Ann Arbor, Michigan

BLANK PAGE

ACKNOWLEDGMENTS

The authors wish to express their gratitude and appreciation to the other members of Dr. Chang's doctoral committee: Professors T. C. Adamson, Jr., W. P. Graebel, A. M. Kuethe, and Vi-Cheng Liu. They also wish to thank Anna Pasternak and Carol Champagne for their aid in typing the manuscript.

ABSTRACT

The theoretical study presented is concerned with predicting the flow details in the region immediately behind a slender wedge moving at supersonic speed. An asymptotic solution is obtained for the laminar near wake, which is valid in the limit as Reynolds number based on external flow properties tends to infinity, with the external Mach number held fixed. In this limit, the interior of the recirculating flow is approximately incompressible and inviscid; the viscous layer is a continuous thin layer with large transverse velocity gradient; and the typical velocity of the recirculating flow must be of the same order as that of the external flow, although numerically it is small.

For the inviscid core, it is shown from consideration of the dissipative terms that the temperature and vorticity are nearly constant. These results demonstrate the fact that, even though the core flow is inviscid and nonconducting, and the primary effects of diffusive exchanges are limited to the continuous viscous layer enclosing the recirculating flow, the accumulative effects of very small diffusive exchanges are experienced throughout the entire recirculation region.

There exists an equilibrium vorticity for the inviscid core so as to satisfy the condition of conservation of angular momentum for the recirculating flow. At the rear stagnation point, a tentative reattachment condition similar to Chapman's is used but based on the minimum pressure increase attainable at the rear stagnation point from the turning of a streamline in the shear layer to a direction parallel to the wake center line. Based on these two conditions, a unique solution for the near wake flow can be obtained for a given upstream flow condition. Numerical results are in general agreement with the available experimental data.

TABLE OF CONTENTS

TABLE OF CONTENTS (CONT.)

TABLE OF CONTENTS (CONT.)

LIST OF ILLUSTRATIONS

LIST OF SYMBOLS

$A(\psi)$	Area inside the closed streamline ψ
$a_n(\tilde{x})$	n = 0, 1, 2. Coefficients in representation for $\tilde{g}(\tilde{\zeta})$, Eq. (VI-9)
$b_n(\tilde{x})$	n = 0, 1, ..., 4. Coefficients in representation for $\tilde{g}_{(+)}(\tilde{\zeta}_{(+)})$, Eq. (VI-10)
$b_{n,m}(\tilde{x})$	m = 0, 1, ..., 5; n = 0, 1, ..., 4. Defined in appendix
C_n	n = 1, 2... . Coefficients in Taylor's expansion for small θ, Eq. (V-33)
$c_n(\tilde{x})$	n = 0, 1, ..., 4. Coefficients in representation for $\tilde{g}_{(-)}(\tilde{\zeta}_{(-)})$, Eq. (VI-11)
$c_{nm}(\tilde{x})$	m = 0, 1, ..., 5; n = 0, 1, ...4. Defined in appendix
$\bar{c}_p$	Specific heat at constant pressure
$\bar{c}_v$	Specific heat at constant volume
D	Function defined in appendix
D_I	Coefficient in representation for Θ for X small, Eq. (V-35)
D_i	i = 0, 1, ..., 5. Functions defined in appendix
E	Function defined in appendix
E_i	i = 0, 1, ...5. Functions defined in appendix
F(U)	Weighting function, Eq. (V-6)
$F_{K,I}(U)$	I = 1, 2, ..., K. Weighting function in the Kth approximation
$f_0(\eta)$	Universal function, Eq. (VI-39)
$f_c(\eta_c)$	$f_0(\eta_c)$

$f_c^{(1)}(\eta_c)$	$\frac{df_c}{d\eta_c}$
$f_c^{(2)}(\eta_c)$	$\frac{df_c^{(1)}}{d\eta_c}$
G_i	i = 1, 2, 3. Functions defined in (VII, 1)
G_{ij}	i = 1, 2, 3; j = 1, 2, 3. Functions defined in (VII, 1)
$\tilde{g}(\tilde{\zeta})$	Velocity profile for the outer shear layer, Eq. (VI-9)
$\tilde{g}_{(+)}(\tilde{\zeta}_{(+)})$	Velocity profile for the upper shear sublayer, Eq. (VI-10)
$\tilde{g}_{(-)}(\tilde{\zeta}_{(-)})$	Velocity profile for the lower shear sublayer, Eq. (VI-11)
$\bar{H}$	Total enthalpy
H	$\bar{H}/\bar{c}_p\,\bar{T}_r$
$\tilde{H}$	$\bar{H}/\bar{u}_e^2$
h_1	$h_1\,d\xi$ is the element of length in the direction of increasing ξ
h_2	$h_2\,d\psi$ is the element of length in the direction of increasing ψ
l	l = 1, ...K. Index appearing in Eq. (V-10)
i	Index
$\vec{i}_q$	Unit vector along a streamline
$\vec{i}_\omega$	Unit vector normal to the plane of the flow
J	J = 0, 1, ...K-1. Index appearing in Eq. (V-13)
j	Index
K	Order of approximation appearing in equation (V-10)
$\bar{k}$	Coefficient of heat conductivity
$\bar{L}_c$	Length of the inclined surface of the wedge.

$\bar{L}_r$	Length of the near wake
M	Function defined in appendix
M_i	i = 0, 1...5. Functions defined in appendix
m	Index
N	Function defined in appendix
N_i	i = 0, 1, ..., 5. Functions defined in appendix
$\hat{N}$	Nondimensional vorticity appearing in (VI, 5)
n	Index
Pr	Prandtl number
$\bar{p}$	Pressure
Q_i	i = 1, 2, 3. Functions defined in (VII, 1)
Q_{ij}	i = 1, 2, 3; j = 1, 2, 3. Functions defined in (VII, 1)
$\bar{q}$	Velocity in the inviscid core flow
Re	Reynolds number
$\bar{R}_b$	Distance between the base of the wedge and the center of rotation
$\bar{R}_d$	Distance between the dividing streamline and the center of rotation
$\bar{r}$	Radial length (Fig. 3)
$\bar{r}_o$	Distance between the trailing edge and the rear stagnation points (Fig. 3)
r^*	Stretched radial length appearing in (IV, 2)
$\bar{S}$	Entropy
$\bar{T}$	Temperature

$\bar{U}$	$\bar{X}$ component of velocity appearing in (V, 1)
U	$\bar{U}/\bar{q}_b$
$\bar{u}$	$\bar{x}$ component of velocity appearing in (VI, 1)
$\bar{V}$	$\bar{Y}$ component of velocity appearing in (V, 1)
$\bar{v}$	$\bar{y}$ component of velocity appearing in (VI, 1)
W	$\left(\frac{\bar{V}}{\bar{q}_b} + \frac{1}{\bar{q}_b} \frac{d\bar{q}_b}{d\bar{X}} \bar{Y} \frac{\bar{U}}{\bar{q}_b} \right) \sqrt{Re_r}$
$\bar{X}$	Coordinate measured along the base of the wedge from the wake centerline (Fig. 3)
X	Transformed coordinate appearing in (V, 1)
$\bar{x}$	Coordinate measured along the dividing streamline from the trailing-edge stagnation point. (Fig. 3)
$\bar{Y}$	Coordinate measured normal to the base of the wedge (Fig. 3)
Y	Transformed coordinate appearing in (V, 1)
$\bar{y}$	Coordinate measured normal to the dividing streamline (Fig. 3)
$\bar{y}_c$	Coordinate measured normal to the wedge surface at the trailing edge
$\beta_u^{\uparrow}$	Constant proportional to the displacement thickness of the upper shear sublayer
$\beta_l^{\uparrow}$	Constant proportional to the displacement thickness of the lower shear sublayer
γ	Specific heat ratio

Δ	$\tilde{\delta}_{(+)}/\tilde{\delta}$ appearing in (VII, 1)
δ	$\tilde{\delta}_{(-)}/\tilde{\delta}_{(+)}$ appearing in (VII, 1)
$\tilde{\delta}$	Nondimensional outer shear-layer thickness
$\tilde{\delta}_{(+)}$	Nondimensional upper shear sublayer thickness
$\tilde{\delta}_{(-)}$	Nondimensional lower shear sublayer thickness
$\tilde{\delta}^*_{(+)}$	Nondimensional displacement thickness of the upper shear sublayer
ϵ	$(Re_u)^{-\frac{1}{2}}$
$\tilde{\zeta}$	$\tilde{y}/\tilde{\delta}$
$\tilde{\zeta}_{(+)}$	$\tilde{y}/\tilde{\delta}_{(+)}$
$\tilde{\zeta}_{(-)}$	$\tilde{y}/\tilde{\delta}_{(-)}$
η	Similarity variable defined in Eq. (VI-40)
η_c	Similarity variable defined in Eq. (V-34)
Θ	$\frac{\partial U}{\partial Y}^{-1}$
$\bar{\theta}$	Angle (Fig. 3)
$\bar{\theta}_o$	Wake angle (Fig. 3)
κ	$1 - \frac{\tilde{\delta}^*_{(+)}}{\tilde{\delta}_{(+)}}$
κ_n	n = 0, 1, . . . , 7. Defined in (VII, 1)
κ_{nm}	n = 0, 1, . . . , 6; m = 0, 1, . . . , 5. Defined in appendix
$\bar{\mu}$	First coefficient of viscosity
$\bar{\mu}'$	Second coefficient of viscosity
$\bar{\nu}$	Kinematic viscosity

ξ	Coordinate measured along closed streamline appearing in (III)
$\bar{\rho}$	Density
χ	Complementary solution for ψ^*
χ_i	$i = 1, 2, \ldots$. Expansion of χ in powers of $\bar{\theta}_o$
$\chi_2^{(c)}$	Complementary solution of χ_2
$\chi_2^{(p)}$	Particular solution for χ_2
Ψ	Particular solution for ψ^*
Ψ_i	$i = 1, 2, \ldots$. Expansion of Ψ in powers of $\bar{\theta}_o$
$\bar{\psi}$	Stream function
ψ^*	$\bar{\psi}/\bar{\omega}\bar{r}_o^2$
Ω	ω/ρ
Ω_i	$i = 0, 1, \ldots$. Expansion of Ω in powers of M_r^2
$\vec{\omega}$	Vorticity
ω_i	$i = 0, 1, \ldots$. Expansion of ω in powers of M_r^2

Subscripts

b	Denotes condition at $r = 1$
c	Denotes condition at trailing edge of the wedge and at the outer edge of the wedge boundary layer
d	Denotes condition at the dividing streamline
e	Denotes condition at the outer edge of the shear layer
r	Denotes typical condition in the recirculating flow
s	Denotes condition at $\theta = 1$

u	Denotes condition at the outer edge of the upper shear sublayer
∞	Denotes condition in the undisturbed free stream

Superscripts

—	Denotes dimensional quantity
~	Denotes modified Howarth transformation
^	Denotes condition in the approximated outer shear layer flow
†	Denotes condition in the shear sublayer

THE LAMINAR NEAR WAKE BEHIND A SLENDER WEDGE AT SUPERSONIC SPEED AND HIGH REYNOLDS NUMBER*

I

INTRODUCTION

Renewed effort has been directed recently to the theoretical and experimental investigation of the wake behind a body moving at high speeds through air. Considerable progress has been made in analytical studies of both the laminar and turbulent far wake (e.g., see the review paper of Lykoudis[1]). However, accurate prediction of the far-wake flow properties requires knowledge of these same properties at a distance of a few body heights behind the body. Because of the extreme complexity of the flow in the near-wake region, the attempts to obtain satisfactory analytical results have been only partially successful. Accordingly current studies are focusing on the near wake in the hope that an adequate analysis of the complex coupling processes occurring within this region can be carried out. The present investigation is concerned with the laminar near wake of a slender wedge at low supersonic Mach numbers and high Reynolds numbers.

Knowledge of experimental results is essential to the developing of a mathematical model, both as a guide for the choice of approximations and for a check on the accuracy of the results predicted using the model. At the base of the wedge it is known that the external flow expands to a lower pressure, through a Prandtl-Meyer expansion. The boundary layers along the wedge surfaces separate and form free shear layers which enclose a region of steady recirculating flow. These results are evident, for example, in the experiments

---

* This report is based on a dissertation submitted in partial fulfillment of the requirements for the degree of Doctor of Philosophy at The University of Michigan, 1968.

carried out by Hama[2], for various Mach numbers between about 2.0 and 4.0, and for a range of Reynolds numbers such that the free shear layer was laminar at the lower values. Among the results, it was shown that the pressure is almost constant on the base; the dividing streamline is nearly straight over most of its length from the base to the rear stagnation point; and a "lip shock" originates in the shear layer, very close to the corner. This lip shock may have considerable strength for flows with a large expansion ratio at the corner, but remains weak for flow over a slender wedge at low supersonic Mach numbers[3]. Batt[4] has made measurements in the wake behind a 20^{o} wedge at $M_{\infty} = 6$ and at various Reynolds numbers such that the free shear layer is laminar. The results indicate that the location of the rear stagnation point is not very sensitive to the variation in Reynolds number, and that the recirculating flow has a very low density. Martellucci et al.[5] have studied the turbulent near wake of a cone at $M_{\infty} = 6$. Their results show that the pressure at the base is nearly constant, but the velocity at the axis in the recirculation region may correspond to Mach numbers as high as 0.8. For a Mach number equal to 16 Todisco and Pallone[6] found that a region of constant temperature exists in the recirculating flow of the laminar near wake behind a slender wedge or cone.

These and other experimental results therefore suggest that the near wake of a slender body can be divided into regions of different physical character. An external inviscid flow results from the corner expansion of the flow outside the boundary layer. A free shear layer is formed by the expanded

boundary layer which mixes with the relatively low-speed recirculating flow. The velocity gradient is large near the dividing streamline, which separates the recirculating fluid from the fluid which passed over the wedge. Since the flow near the dividing streamline is directed toward the wake center line, an increase in pressure occurs in the vicinity of the rear stagnation point, in order that the flow may be turned. The fluid with total pressure higher than on the dividing streamline escapes downstream and forms the far wake, whereas the fluid with lower total pressure turns back toward the base and constitutes the recirculating flow. The shear stress along the dividing streamline drives the recirculating flow against the retarding force along the base of the wedge.

Since the near-wake flow field is determined by a complicated interaction between the flow in the shear layers, the inviscid external flow, and the internal recirculating flow, analytical descriptions have only been obtained by some rather rough approximation or through a semi-empirical formulation. Several simplified near-wake models have been proposed.

The Chapman[7,8,9] dividing-streamline model is based on the conservation of mass within the recirculating-flow region. The mass flow in the shear layer below the dividing streamline is balanced by the mass flow reversed by the pressure rise through the recompression zone near the rear stagnation point. The base pressure is determined by requiring that the total pressure along the dividing streamline be equal to the final static pressure, and the total pressure is assumed to be fully recovered at the rear stagnation point. It is

assumed that the viscous shear layer has zero initial thickness. The external flow mixes with the recirculating flow, which is considered to have zero velocity, and it is assumed that the thickness of the viscous shear layer remains small in comparison with the dimensions of the recirculation region. It is further assumed that the dividing streamline is straight and that the boundary-layer equations may be employed to solve the shear-layer problem. Baum, King and Denison[10] improve on Chapman's model by considering a nonzero initial viscous-layer thickness. They propose that the separated shear layer is a thin mixing region between the outer flow and the essentially stagnant recirculating flow with the suction of fluid along the inner edge of the shear layer made up by a source introduced at the rear stagnation point. Toba[11] makes a further improvement by taking into consideration not only the finite initial viscous-layer thickness but also the trailing-edge expansion. The shear layer is regarded as consisting of an outer shear layer where inertia effects are dominant and an inner mixing layer where both viscous and inertia forces are important. The velocity at the inner edge of the shear layer is again assumed zero.

A different model is used by Reeves and Lees[12] to analyze the near wake of a circular cylinder. The boundary-layer assumptions are regarded as valid for the flow in the near wake. Stewartson's reverse-flow profiles,[13] obtained by an extension of the Falkner-Skan similar solutions, are adopted to describe the region with reversed flow. In this application the profiles are

characterized by two length scales, the base height and the boundary-layer thickness at separation. A two-moment integral method is used to obtain the flow properties. Golik, Webb, and Lees[14] extend the method to study the near wake behind a wedge. A three-moment integral method is employed, in order that one more degree of freedom may be available in representing the flow, and the axis velocity is uncoupled from the Stewartson profiles. It is discovered that only one value for the base pressure allows the integral curve of the solution to pass through a saddle point of the system. The requirement that the solution curve pass through this critical point is regarded as a uniqueness criterion for the near wake.

Dean[15] and Oswatitsch[16] employ a double power-series expansion of the stream function about the separation and reattachment points for the study of the local behavior of incompressible and viscous flows near these points. These local solutions are extended by Reeves and Buss[17, 18] to the study of the near wake of a slender wedge, which is regarded as controlled by a thin shear layer of relatively low energy fluid. The stream function is expanded about the rear stagnation point and the coefficients of the series can be determined by substituting in the full Navier-Stokes equations, satisfying suitable conditions at separation and at the rear stagnation point, and matching with the downstream flow. Accordingly it is found that the geometrical and dynamical properties of the near wake are determined by the local Reynolds number and the velocity profile at the rear stagnation point.

Weiss[19] suggests a model which consists of three coupled regions: a vortical outer flow, which results from an approximately inviscid expansion of the boundary layer at the trailing edge of the wedge, is treated by the method of characteristics; the flow in a thin viscous layer above the dividing streamline, which has large velocity gradient and can be described by the boundary-layer equations, is solved by a modified Oseen linearization technique; and the recirculating flow, which contains flow of relatively low velocity and is described by the full Navier-Stokes equations, is solved by a finite-difference technique. A numerical iterative scheme is proposed such that the flow properties at the boundaries of the coupled region are properly matched. These conditions are obtained by demanding that velocity, shear, pressure, temperature and heat transfer be continuous for any given base pressure.

Prandtl[20, 21] suggests that, in steady incompressible laminar flows with closed streamlines at large Reynolds number, viscous effects can be disregarded wherever there are no large velocity gradients or accumulative effects. Thus the viscous effects are limited to narrow regions in the vicinity of boundary surfaces which enclose the recirculating flow. Since the net work done on a fluid particle moving along any closed streamline must be zero for a complete cycle, the vorticity can be shown to be distributed uniformly in the interior of the recirculation region of a two dimensional flow where convective effects are dominant. Batchelor[22, 23] obtains this result in essentially the same way, by taking the line integral of the complete equation of motion around a closed

streamline. He proposes that the value of vorticity may be determined by the condition that the boundary layers enclosing this recirculating flow must also be in steady motion. This implies that in incompressible and inviscid wakes behind two-dimensional bodies the vorticity must take such a value that the relative momentum of the viscous layer enclosing the recirculating flow is increased over part of its path and decreased over other parts, the net effect being to allow the viscous layer to have a steady motion. It is implied that as Reynolds number becomes large the velocity in the recirculation region remains of the same order as the velocity in the external flow.

Lenard[24] applies Batchelor's idea to the near wake of a slender cone at large Reynolds number and supersonic Mach number. The near wake is divided into the inviscid core region, the corner-expansion region, the external inviscid-flow region, the recompression region and the viscous-layer region, which in turn is subdivided into the base boundary layer and the free shear layer. The base boundary layer on the base surface of the cone is represented by an axially symmetric stagnation point boundary layer with highly vortical outer flow. The free shear layer which grows into the inviscid external flow and inner recirculating flow is described by the von Mises form of the boundary layer equations. The external flow is considered as an isentropic expansion of the flow upstream of the corner to the base pressure. The inviscid inner recirculating flow is regarded as having constant properties along streamlines. The integral relations which are obtained by integration of the govern-

ing differential equations along a closed streamline lying entirely within the viscous layers provide the necessary conditions for a unique solution. A numerical procedure is suggested for obtaining a solution to the equations.

Guderley and Greene[25] adopt Batchelor's proposal for the study of steady compressible swirl flow with closed streamlines at high Reynolds number. Some special conditions, which are determined by the dissipative terms and are deduced from the mathematical conditions for solvability of the equations for approximations of a higher order, can be obtained for the inviscid core flow. These conditions have the physical meaning of conservation of momentum, energy, and entropy for any control surface generated by rotating a streamline in the recirculating flow around the axis of symmetry.

The methods proposed by Golik, Webb, and Lees,[14] by Reeves and Buss,[17, 18] and by Weiss[19] have all provided results which compared favorably with experiment for one or more combinations of Mach number and Reynolds number. However, a difficulty remains in each case because there is no obvious procedure for estimating the error or for systematically improving the approximation. Therefore it appears of interest also to study asymptotic approximations for large Reynolds number which in principle can be extended to include higher-order terms. If a complete solution could be obtained in this manner, it is expected that the flow details would be predicted more accurately than by the solutions obtained in a more intuitive way. The range of validity of an asymptotic solution would probably be smaller, but the solution could pro-

vide a useful standard of comparison for solutions obtained by the other methods quoted.

In the present study the idea proposed by Batchelor[23] for imcompressible wakes is adopted, in the manner of Lenard[24] and Guderley and Greene,[25] to provide a model for the near wake behind a slender wedge at supersonic speed. That is, an attempt is made to obtain an asymptotic solution for the laminar near wake, which is valid in the limit as the Reynolds number based on external flow properties tends to infinity, with the external Mach number held fixed. Terms considered to be of higher order are not obtained here, but it is pointed out that a complete understanding of the problem requires knowledge of additional terms in the asymptotic expansions. It is important to emphasize that a solution obtained in this limit is not expected to describe effects associated with high Mach number. The solutions, of course, are to be used not at arbitrarily large Reynolds numbers but at Reynolds numbers such that the flow actually is laminar.

As suggested by Batchelor, it is expected that as the Reynolds number becomes large the velocity in the recirculation region remains of the same order as the velocity in the external flow, although numerically smaller. In this limit, therefore, the Reynolds number based on typical properties for the recirculating flow will also approach infinity, although in any application the numerical value will be far smaller than the Reynolds number based on external flow properties. It is believed nevertheless that the results will provide a

useful approximation at the larger values of Reynolds number for which the flow remains laminar.

Since experiments suggest that the Mach number in the recirculation region may not be very large, the recirculation region is assumed to have constant density, and an estimate is made to show that the effects of nonzero Mach number may reasonably be neglected. It is therefore also assumed that the dividing streamline is straight and that the pressure is nearly constant except in regions near the corner and near the rear stagnation point. In the limit it is assumed that the dimensions of these regions approach zero. Since the size of these regions will increase with increasing Mach number, it seems clear that the hypersonic problem would have to be studied by some different limit process such that the Mach number also approaches infinity and the size of these regions does not approach zero. Finally, for simplicity zero heat transfer to the wedge surfaces is assumed, and the Prandtl number is taken equal to one.

Solutions are derived for the recirculating flow, for a shear sublayer and for the outer part of the free shear layer, and for the base boundary layer. Two constants remain undetermined in these solutions, namely the base pressure and the vorticity of the recirculating flow. Therefore two additional conditions are needed. A balance is imposed between the torques exerted on the recirculating flow by the shear stress along the dividing streamline and the shear stress along the base. At the rear stagnation point a criterion similar

to Chapman's is used, but based on flow conditions for a particular streamline inside the shear layer, rather than on conditions outside the shear layer. It is pointed out that these conditions are considered as tentative, since they are not derived from the solutions obtained. If second approximations could be obtained in the asymptotic expansions of the flow properties for large Reynolds number, it is believed that these or similar criteria could be proposed with greater confidence. Numerical results are given for some of the cases studied by Hama, and rather good agreement is found between predicted and measured values of the base pressure.

II

DESCRIPTION OF THE PHYSICAL PROBLEM AND PROPOSED MODEL FOR ANALYSIS

1. General Description of the Near Wake

The flow in the near wake of a slender wedge is shown in figure (1). At the vertex the uniform supersonic stream on each side of the wedge is turned through an angle ϕ_c, through an oblique shock. Boundary layers are formed on the top and bottom surfaces of the wedge. At the base of the wedge, these boundary layers expand rapidly, and in a complex manner, to a low pressure. The separation point is believed to occur on the base at a small distance from the corner.[2,26] For low supersonic Mach numbers, the acceleration and pressure gradient are very large in a relatively small region near the separation point. Hence it is expected that the expansion process may be treated as an isentropic expansion and the flow may be regarded approximately as an inviscid rotational flow. In order that the no-slip condition along the wedge surface be satisfied as the flow approaches the trailing edge, there exists a viscous sublayer, having steep velocity gradient and with thickness small compared to the boundary-layer thickness. The effect of the sublayer on the outer part of boundary layer is small[27]. Since the flow is actually overexpanded and then recompressed by a lip shock, deeply embedded within the shear layer[2], the expansion processes at the trailing edge are further complicated. The strength of the lip shock is small only if the ratio of the base pressure to wedge surface pressure is not too small. Therefore, for flow over a slender wedge at low

supersonic Mach numbers the lip shock is rather weak and the accompanying entropy changes may be neglected[3].

The expanded boundary-layer flow, separating from the wedge, mixes under nearly constant pressure with the relatively low-speed recirculating flow[2,4]. Viscous effects are important primarily near the dividing streamline, where the velocity gradient is large. For most of the distance from the base to the rear stagnation point, the dividing streamline has small curvature. The shear layer remains rather thin provided, again, that the wedge is slender and the Mach number is not very large. Eventually the shear-layer flow approaches the wake center line at the rear stagnation point, which is located at a distance of a few body heights downstream of the base of the wedge[2,4].

In the vicinity of the rear stagnation point, the flow outside the dividing streamline is turned to a direction approximately parallel to the wake center line. This fluid has momentum larger than the momentum at the dividing streamline, and therefore moves downstream to form the far wake. A compression accompanies the turning of the flow, and the compression waves coalesce to form the wake shock. A fluid particle along the dividing streamline is brought to rest at the rear stagnation point, since it has a total pressure just large enough to sustain the recompression. The fluid with lower momentum turns back to the base region and recirculates. The velocity of the recirculating flow is relatively small compared with the velocity of the external flow. The shear force acting on the recirculating flow along the dividing stream-

line produces an accelerating torque, whereas the shear force acting along the base of the wedge produces a retarding torque. The net effect of the accelerating and retarding torques is to allow a steady motion in the recirculation region.

2. Motivation, Assumptions and Description of the Present Model.

As suggested before, the near-wake flow comprises three flow regions of different physical character, each described by approximate flow equations of a different mathematical type. These regions are the inviscid external flow, the viscous-layer flow, and the recirculating flow, and are described approximately by pure hyperbolic equations, parabolic equations and elliptic equations respectively. A description of the interactions between the regions will be an essential part of any analysis of the near-wake flow field. However, it seems clear that the solution of the problem depends largely on the success in formulating essentially separate problems for the different regions which may be studied independently, and then using some matching procedure to obtain a unique solution for the whole near-wake flow.

In the study of the recirculating flow the idea proposed by Batchelor[23] for incompressible laminar wakes is adopted, in the manner of Lenard[24] and Guderley and Greene[25]. That is, an attempt is made to obtain an asymptotic solution for the recirculation region which is valid in the limit as the Reynolds number based on external flow properties tends to infinity, with the external Mach number held fixed. Because the Reynolds number is large the viscous

forces acting on the fluid are small everywhere except in the neighborhood of certain surfaces where the velocity gradient is large These surfaces enclose the recirculating flow. The region where the viscous effects are not negligible becomes smaller and smaller as the Reynolds number increases. Thus. in the limit, the flow in the interior of the recirculation region may be regarded as inviscid. The solution, of course, is to be used not at arbitrarily large Reynolds numbers but at Reynolds numbers such that the flow actually is laminar.

From experimental evidence[2, 4], it is clear that the length of the viscous layer which accelerates the fluid in the inviscid core is greater than the length of the viscous layer which decelerates this fluid. It is expected, as proposed by Batchelor[23], that as the free-stream Reynolds number becomes large the velocity in the recirculation region is of the same order as the velocity in the external flow, although numerically smaller. In the limit, therefore, the Reynolds number based on the typical properties for the recirculation region will also approach infinity, although in any application the numerical value will be considerably smaller than the Reynolds number based on external flow properties. However, it is believed that the results will provide a useful approximation at the larger values of Reynolds number for which the flow remains laminar.

Since experiments suggest that the thermal energy of the fluid in the recirculating flow is of the same order as the kinetic energy in the external flow, which is numerically considerably larger than the kinetic energy of the

recirculating flow, the Mach number based on typical properties for the recirculating flow may be assumed small. This assumption implies that the recirculation region may be treated approximately as an incompressible rotational flow. The effects of nonzero Mach number may be shown to be rather small. If the energy and momentum equations are operated on in the manner of Prandtl[20] and Batchelor[22], one may obtain the result that the flow in the interior of the recirculation region is inviscid and incompressible with constant vorticity and temperature.

In order to study the complex flow outside the dividing streamline certain simplifications are needed to provide a simple but meaningful solution. The most important omissions are the details of the flow near the trailing-edge stagnation point, where the lip shock is formed, and the details of the flow near the rear stagnation point, where the wake shock originates. Experiments suggest that for a slender wedge at low supersonic Mach number the lip shock is rather weak[3], and in the limit of large Reynolds number the dimensions of these omitted regions are of higher order than the wake length. Therefore, the expansion near the trailing-edge stagnation point and the recompression near the rear stagnation point may be assumed to be shock-free and may be replaced by isentropic processes. It is also assumed that the dividing streamline is straight and that the pressure is nearly constant except in the omitted regions.

Finally, for simplicity it is assumed that there is no heat transfer to the wedge surfaces; the Prandtl number is unity; the product of density and

viscosity is constant throughout the viscous layers; and the velocity profile prior to the corner expansion is a Blasius velocity profile in suitable transformed coordinates.

Based on the simplifications and approximations mentioned above, the configuration of the present model of the near-wake flow field is shown in figure (2). The thin boundary-layer flow separating from the trailing edge of the wedge expands rapidly and isentropically to a base pressure. This expanded boundary-layer flow then mixes under nearly constant pressure with the relatively low-speed recirculating flow, confined in a right triangular region with a wake angle $\bar{\theta}_0$ between the dividing streamline and the wake center line. The mixing is limited to a narrow band around the dividing streamline which has a negligible curvature. Eventually this shear-layer flow reaches the wake center line, and as it begins to turn compression waves are emitted. The low-momentum fluid below the dividing streamline is turned back and recirculates in the recirculation region. The high-momentum fluid above the dividing streamline escapes downstream and constitutes the far wake region. The compression continues until the external flow turns parallel to the wake center line. The flow in the right triangular region may be regarded as incompressible and inviscid with constant vorticity and temperature. Since the no-slip condition must be satisfied at the base, a base boundary layer is formed at the base of the wedge. This base boundary layer is thin in the limit of large Reynolds number, and produces resistance to the recirculating flow against the driving force of the

shear layer.

3. Criterion for a Unique Near-Wake Solution.

Since a fluid particle in the recirculation region undergoes a laminar steady motion along closed streamlines, the net gain in angular momentum of each fluid particle, as it moves through a complete cycle, must be zero. This condition should be true for all particles in either the inviscid core flow or in the continuous viscous layers enclosing the recirculating flow. When a streamline is taken as a control surface, then the above condition implies that the angular momentum of the fluid bounded by this control surface must be conserved. For convenience the control surface may be chosen as the streamline enclosing the whole recirculation region, which consists of the dividing streamline, the wake center line and the base of the wedge. The shear along the dividing streamline produces an accelerating torque whereas the shear along the base of wedge produces a retarding torque. Since the wake behind a symmetric wedge is symmetric with respect to the wake center line, there is no shear along the wake center line. Therefore, the accelerating torque from the shear layer should always be equal to the retarding torque from the base boundary layer, because there should be no change in total angular momentum of the recirculating flow. This implies that for a given flow condition before the trailing edge expansion and for a given wake angle there exists an equilibrium vorticity in the core flow so as to satisfy the requirement of conservation of angular mo-

mentum for the recirculation region.

When the shear-layer flow approaches the wake center line it starts to turn and the pressure begins to increase. The recompression has been assumed to take place in a region having dimensions of higher order than the wake length. In this region the pressure and inertia effects are much larger than the viscous effects, and so the flow near and on the dividing streamline may be assumed to be recompressed approximately isentropically. A fluid particle along the dividing streamline is brought isentropically from a large velocity, corresponding to the condition prior to the recompression, to rest at the rear stagnation point. Accordingly, its static pressure increases from the base pressure to the stagnation pressure. Experimental results show that at the rear stagnation point the flow is partially recompressed[2], and the turning of the external flow to the direction parallel to the wake center line is not yet completed. Hence, further recompression is required downstream of the rear stagnation point until the external flow is parallel to the wake center line.

If a uniform supersonic flow is turned through a given angle from a specified initial static pressure, the final value of the pressure depends on the initial value of the Mach number, and it is known that the final pressure has a minimum value for a particular initial Mach number.[28] Near the rear stagnation point, for a streamline just outside the dividing streamline , the velocity of a fluid particle is decreased and the flow is turned to a direction almost parallel to the wake center line. Since the turning actually is completed downstream of

the rear stagnation point, the pressure rise would be overestimated if it were assumed that the streamline becomes parallel to the center line at a point very close to the rear stagnation point. To compensate partially for this error, the streamline having a minimum pressure rise is considered. It is assumed that this streamline is turned through a simple wave to a direction parallel to the wake center line, and that the pressure thus attained is equal to the pressure at the rear stagnation point. This requirement will be referred to as the reattachment condition. It is similar to Chapman's criterion of reattachment[9] but is based on flow conditions for a particular streamline inside the shear layer rather than outside the entire shear layer. Since for a given flow condition before the trailing-edge expansion, the shear-layer velocity distribution is dependent both on the vorticity of the inviscid core flow and on the wake angle, the reattachment condition must also be dependent on the same factors.

For a given flow condition before the trailing-edge expansion, the shear-layer velocity distribution varies with the change in both the inviscid flow velocity at the inner edge of the shear layer and the external-flow velocity; in other words, it depends on the vorticity of the inviscid core flow and on the wake angle. The velocity distribution in the base boundary layer is determined by the velocity distribution at the outer edge of the base boundary layer which is, in turn, a function of the wake angle and the vorticity of the inviscid core flow. Hence, if the wake angle and the vorticity of the inviscid core flow are obtainable, the near-wake flow properties may be determined. Therefore, two inde-

pendent conditions, which involve both the wake angle and the vorticity of the inviscid core flow, are needed to provide a unique solution for the near-wake flow. These independent conditions are the conservation of angular momentum for the recirculation region, and the reattachment condition at the rear stagnation point. It should be pointed out that the reattachment condition is considered as tentative, since it is not derived from the solutions obtained. In the present context, solutions for the flow details near separation and near the rear stagnation point are regarded as part of a higher approximation. A solution valid near the rear stagnation point, and perhaps other parts of the next approximation, would have to be studied in order to devise some sort of reattachment condition in a systematic way. Presumably it could then also be shown that the error really is of higher order in the present formulation of the condition that angular momentum must be conserved.

III

GENERAL RESULTS FOR RECIRCULATING FLOW WITH LARGE LOCAL REYNOLDS NUMBER AND SMALL LOCAL MACH NUMBER

1. General Remarks and Formulation

The arguments given by Prandtl[20, 21] and by Batchelor[22, 23] for incompressible flow are extended here for the steady flow at large local Reynolds number in the confined region behind a blunt-based body immersed in a uniform supersonic stream. The derivation is also an extension of Lenard's[24] work, because an estimate is obtained to demonstrate that the effect of nonzero Mach number in the recirculating flow is probably quite small. Diffusive exchanges are supposed to be so small that they may be disregarded wherever there are no large velocity and temperature gradients or accumulative effects. That is, for steady laminar motion along closed streamlines at large local Reynolds number, viscous forces acting on a fluid element and thermal exchanges between the element and its surroundings are small everywhere except in thin viscous layers where large gradients in flow properties are encountered. Such thin layers enclose the recirculating flow behind the blunt-based body. Hence, for large local Reynolds number, the flow in the interior of the recirculation region may essentially be considered as inviscid and nonconducting. The assumption of small diffusive exchanges implies that the nondimensional forms of the viscous forces and of the thermal exchanges are small compared with unity, provided that the characteristic values used in the definition of local

Reynolds number and local Mach number for the recirculating flow are chosen as typical values for nondimensionalization.

For the present model, it is assumed that the Reynolds number Re_e, based on the external-flow conditions and the wake length, is large, and the flow is laminar. Thus as Re_e approaches infinity as a limit, the thickness of the laminar viscous layers, at the wedge surfaces and the boundary surfaces of the wake, is calculable and is of order $Re_e^{-\frac{1}{2}}$. In the limit $Re_e \to \infty$, these viscous layers reduce to a number of singular stream surfaces of the fluid. Across such singular stream surfaces the flow properties may be discontinuous. For the laminar wake of a wedge, the portion of the wake boundary which yields resistance to the recirculating flow is shorter than the portion of the boundary which produces driving forces, and the vorticity of the inviscid core flow must take up an equilibrium value such that the flow is steady. Therefore, the typical velocity of the recirculating flow must be fairly high. In the limit of large Re_e, the typical velocity of the recirculating flow must be of the same order as that of the external flow, although numerically it is smaller. Since the flow properties in the recirculation region differ from those of the external flow primarily through factors involving powers of the Mach number M_e, based on external flow properties, then the Reynolds number Re_r, based on the typical flow properties of the recirculating flow, differs from Re_e through factors involving powers of M_e. In the limit $Re_e \to \infty$ with M_e held fixed, Re_r will also approach infinity.

Let the typical length, velocity magnitude, temperature, density, pres-

sure and total enthalpy for the recirculating flow be denoted by $\bar{L}_r$, $\bar{q}_r$, $\bar{T}_r$, $\bar{\rho}_r$, $\bar{p}_r$ and $\bar{H}_r = \bar{c}_p \bar{T}_r$ respectively. The coefficients of viscosity and thermal conductivity corresponding to the typical temperature $\bar{T}_r$ are $\bar{\mu}_r$ and $\bar{k}_r$ respectively. The following is a list of nondimensional variables for the recirculation region:

$$q = \frac{\bar{q}}{\bar{q}_r} \; ; \; T = \frac{\bar{T}}{\bar{T}_r} \; ; \; \rho = \frac{\bar{\rho}}{\bar{\rho}_r} \; ; \; p = \frac{\bar{p}}{\bar{p}_r} \; ; \; H = T + [\,(\gamma-1)M_r^2\,]\,\frac{q^2}{2}$$

$$\mu = \frac{\bar{\mu}}{\bar{\mu}_r} \; ; \; \mu' = \frac{\bar{\mu}'}{\bar{\mu}_r} \; ; \; k = \frac{\bar{k}}{\bar{k}_r} \; ; \; S = \frac{\bar{S}}{\bar{c}_v} \; ; \; \gamma = \frac{\bar{c}_p}{\bar{c}_v}$$

where $M_r = \dfrac{\bar{q}_r}{\sqrt{\gamma R \bar{T}_r}}$ = reference Mach number for the recirculation region. The bar above any symbol denotes a dimensional quantity. The first and second viscosity coefficients are denoted by $\bar{\mu}$ and $\bar{\mu}'$ respectively, and $\bar{S}$ is the specific entropy. The spatial coordinates are made nondimensional by the typical length $\bar{L}_r$ which is taken equal to the base height. Later it will be clear that the obvious choice for $\bar{q}_r$ is $|\,\bar{\omega}_r \bar{L}_r/2\,|$, where $\bar{\omega}_r$ is the reference vorticity in the inviscid core flow. Also $\bar{T}_r$ is the stagnation temperature of the free stream, $\bar{p}_r$ is the pressure after the trailing edge expansion, and $\bar{\rho}_r$ is the density corresponding to $\bar{T}_r$. It is assumed that the Prandtl number $Pr = \dfrac{\bar{c}_p \bar{\mu}_r}{\bar{k}_r}$ is equal to one and the specific heats are constants. In a later part of the derivation the coefficients of viscosity and conductivity will be taken to be linear functions of temperature, and so $\bar{\mu}_r$ and $\bar{k}_r$ are proportional to $\bar{T}_r$.

The nondimensional equations which describe the laminar motion can

be derived from the general form of these equations given by Lagerstrom[29]:

$$\nabla \cdot (\rho \vec{q}) = 0 \qquad \text{(III-1)}$$

$$\rho \vec{q} \times (\nabla \times \vec{q}) = \frac{1}{\gamma M_r^2} \nabla p + \rho \nabla \frac{q^2}{2} - \frac{1}{Re_r} \left\{ \nabla (\mu' \nabla \cdot \vec{q}) \right.$$

$$+ 2\nabla [\mu (\nabla \cdot \vec{q})] + \nabla (\vec{q} \cdot \nabla \mu) - \vec{q} \nabla^2 \mu$$

$$\left. + (\nabla \mu) \times (\nabla \times q) - (\nabla \cdot \vec{q})(\nabla \mu) - \nabla \times \nabla \times (\mu \vec{q}) \right\}$$

(III-2)

$$\rho \vec{q} \cdot \nabla H = \frac{1}{Re_r} \left[\nabla \cdot (\mu \nabla H) \right] + \frac{(\gamma - 1) M_r^2}{Re_r} \left\{ \nabla \cdot \left[\mu' \vec{q} (\nabla \cdot \vec{q}) \right. \right.$$

$$\left. \left. + \mu \nabla (\tfrac{1}{2} q^2) + \mu (\nabla \times \vec{q}) \times \vec{q} \right] \right\} \qquad \text{(III-3)}$$

$$\rho \vec{q} \cdot \nabla S = \frac{\gamma}{Re_r} \left\{ \frac{1}{T} \nabla \cdot (\mu \nabla T) \right\} + \frac{\gamma(\gamma - 1) M_r^2}{Re_r} \left\{ \frac{\mu'}{T} (\nabla \cdot \vec{q})^2 \right.$$

$$+ \frac{\mu}{T} \nabla^2 (\vec{q} \cdot \vec{q}) + \frac{2\mu}{T} \nabla \cdot \left[(\nabla \times \vec{q}) \times \vec{q} \right.$$

$$\left. \left. - 2\vec{q} \cdot \nabla (\nabla \cdot \vec{q}) + | \nabla \times \vec{q} |^2 \right] \right\} \qquad \text{(III-4)}$$

$$\frac{p}{\rho^\gamma} = e^{\Delta S} \qquad \text{(III-5)}$$

where $Re_r = \frac{\bar{\rho}_r \bar{q}_r \bar{L}_r}{\bar{\mu}_r}$ = Reynolds number for the recirculation region, $\Delta S = S - S_r$, and $S_r = \frac{\bar{S}_r}{c_v}$ = the typical entropy for the recirculation region corresponding to $\bar{T}_r$, $\bar{p}_r$ and $\bar{\rho}_r$. When Re_e is $O(10^4)$, then Re_r is $O(10^2)$, as will be shown later when the numerical results are presented.

In the limit $Re_r \to \infty$, following Prandtl[20] and Batchelor[22], the non-dimensional equations (III-2) to (III-4) valid for the interior of the region of recirculating flow become

$$\rho \vec{q} \times \nabla \times \vec{q} = \frac{1}{\gamma M_r^2} \nabla p + \rho \nabla \frac{q^2}{2} \qquad \text{(III-6)}$$

$$\rho \vec{q} \cdot \nabla H = 0 \qquad \text{(III-7)}$$

$$\rho \vec{q} \cdot \nabla S = 0 \qquad \text{(III-8)}$$

Thus in the interior of the recirculation region the flow is regarded as inviscid and nonconducting. However, since the gradients in flow properties are large near the boundary surfaces which enclose the recirculating flow, the viscous effects are important in thin layers adjacent to these surfaces. As the local Reynolds number grows, these layers become thinner, and the typical length in the direction normal to the flow direction is not $\bar{L}_r$ but should instead be of the order $\bar{L}_r / Re_r^{\frac{1}{2}}$. Therefore in the limit of large local Reynolds number the appropriate viscous-stress terms may be retained and these regions are described by boundary-layer equations.

Nondimensional orthogonal streamline coordinates ξ and ψ are now

introduced, where ξ is measured in the streamline direction and ψ is measured normal to the streamline direction. The elements of length in the direction of increasing ξ, ψ are $h_1 d\xi$, $h_2 d\psi$ respectively.

The integral conditions which arise from the effect of diffusive exchanges, and which are valid no matter how small the coefficients of viscosity and thermal conductivity may be, can be derived from the energy equation and the momentum equation. The operations applied to these equations should be performed in such a way that the contributions from all terms other than the terms involving diffusive exchanges vanish identically. Such an operation is to take the line integral around a closed streamline in the two-dimensional flow.

Since experimental results show that M_r is fairly small, it will be assumed that the flow variables can be expanded in power series of M_r^2, as in the Janzen-Rayleigh method (e.g., van Dyke[30], 1964):

$$\vec{q} \sim \vec{q}_o + M_r^2 \vec{q}_1 + \ldots$$

$$T \sim T_o + M_r^2 T_1 + \ldots$$

$$\rho \sim \rho_o + M_r^2 \rho_1 + \ldots$$

$$p \sim p_o + M_r^2 p_1 + \ldots$$

$$H \sim H_o + M_r^2 H_1 + \ldots$$

$$\mu \sim \mu_o + M_r^2 \mu_1 + \ldots$$

$$\mu' \sim \mu'_o + M_r^2 \mu_1 + \ldots$$

The effects of compressibility may, in principle, be studied by perturbing a basic solution for incompressible flow. The first order corrections are pro-

portional to the square of the typical local Mach number M_r, and higher approximations proceed by successive powers of M_r^2.

2. Integral Condition Obtained from Energy Equation.

The integral condition arising from the distribution of thermal energy within the recirculating flow is now considered. The energy equation (III-3) may be rewritten in the following form:

$$\vec{i}_q \cdot \nabla H = \left(\frac{1}{Re_r}\right)\left(\frac{1}{\rho q}\right)\left\{\nabla \cdot (\mu \nabla H) + (\gamma-1) M_r^2 \nabla \cdot \left[\mu' \vec{q}\,(\nabla \cdot \vec{q}) + \mu(\vec{q} \cdot \nabla)\vec{q}\right]\right\} \tag{III-9}$$

where $\vec{i}_q$ is a unit vector along a streamline and $\vec{q}$ may be replaced by $q\vec{i}_q$. Integration of equation (III-9) around a closed streamline inside the recirculation region gives

$$\oint \left[\vec{i}_q \cdot \nabla H\right] h_1 d\xi = \left(\frac{1}{Re_r}\right)\oint\left(\frac{1}{\rho q}\right)\left\{\nabla \cdot \mu \nabla H + (\gamma-1) M_r^2 \nabla \cdot \left[\mu' \vec{q}\,(\nabla \cdot \vec{q}) + \mu(\vec{q} \cdot \nabla)\vec{q}\right]\right\} h_1 d\xi \tag{III-10}$$

The left-hand side of this equation may be written as $\oint \left[\nabla H\right] \cdot h_1 d\vec{\xi}$, which vanishes because H is a single-valued function of position. Then the exact integral condition to be satisfied for every closed streamline is

$$\oint\left(\frac{1}{\rho q}\right)\left[\nabla \cdot (\mu \nabla H)\right] h_1 d\xi = -(\gamma-1) M_r^2 \oint\left(\frac{1}{\rho q}\right)\left\{\nabla \cdot \left[\mu' \vec{q}\,(\nabla \cdot \vec{q}) + \mu(\vec{q} \cdot \nabla)\vec{q}\right]\right\} h_1 d\xi \tag{III-11}$$

Substitution of the expansion in powers of M_r^2 into this equation gives

$$\oint\left(\frac{1}{\rho_0 q_0}\right)\left[\nabla\cdot(\mu_0\nabla H_0)\right]h_1 d\xi$$

$$+\left[M_r^2\right]\oint\left(\frac{1}{\rho_0 q_0}\right)\left\{\nabla\cdot(\mu_0\nabla H_1)+\nabla\cdot(\mu_1\nabla H_0)-\left(\frac{q_1}{q_0}+\frac{\rho_1}{\rho_0}\right)\nabla\cdot(\mu_0\nabla H_0)\right.$$

$$\left.+(\gamma-1)\nabla\cdot\left[\mu_0'\vec{q}_0(\nabla\cdot\vec{q}_0)+\mu_0(\vec{q}_0\cdot\nabla)\vec{q}_0\right]\right\}h_1 d\xi = O(M_r^4) \qquad \text{(III-12)}$$

Therefore the integral condition from the energy equation may be written as

$$\oint\left(\frac{1}{\rho_0 q_0}\right)\left[\nabla\cdot(\mu_0\nabla H_0)\right]h_1 d\xi = O(M_r^2) \qquad \text{(III-13)}$$

when Re_r is large, the energy equation (III-7) for the inviscid core flow can be reduced to

$$H = H(\psi) = H_0(\psi) + M_r^2 H_1(\psi) + \ldots \qquad \text{(III-14)}$$

This means that total enthalpy is constant along a streamline. If equation (III-14) is substituted into equation (III-13), the resulting integral condition from the equation for the inviscid core may be rewritten as

$$\oint\left(\frac{1}{\rho_0 q_0}\right)\left(\frac{1}{h_1 h_2}\right)\left[\frac{\partial}{\partial\psi}\left(\mu_0\frac{h_1}{h_2}\frac{dH_0(\psi)}{d\psi}\right)\right]h_1 d\xi = O(M_r^2) \qquad \text{(III-15)}$$

From the definition of the stream function it follows that

$$\rho_0 q_0 h_2 = 1$$

Hence the operator $\frac{d}{d\psi}$ may be taken outside the integral, and equation (III-15) becomes

$$\frac{d}{d\psi} \oint \left(\frac{dH_0(\psi)}{d\psi} \right) \rho_0 q_0 \mu_0 h_1 \, d\xi = 0$$

Integration with respect to ψ gives

$$\frac{dH_0(\psi)}{d\psi} \oint \rho_0 q_0 \mu_0 h_1 \, d\xi = \text{constant} \qquad \text{(III-16)}$$

Equation (III-16) should be valid for any streamline lying entirely in the inviscid core flow, including streamlines arbitrarily close to the center of rotation, where $q_0 = 0$. This indicates that the constant in equation (III 16) can only be zero. Because

$$\oint \rho_0 q_0 \mu_0 h_1 \, d\xi \neq 0$$

except for $q_\eta = 0$, equation (III-16) becomes

$$\frac{dH_0(\psi)}{d\psi} = 0 \qquad \text{(III-17)}$$

That is, H_0 = constant, or

$$T_0 = \text{constant} \qquad \text{(III-18)}$$

From the definition of $\overline{T}_r$, one gets $T_0 = 1$. This condition states that in the limit $Re_r \to \infty$ the contribution from the diffusive exchanges to the rate of change of enthalpy in the inviscid core of the recirculating flow must be zero when terms of order M_r^2 are neglected.

The existence of a constant temperature region in the wake of a body is evident both from theoretical analysis and from experimental results. Burggraf[31], in a study of the structure of the two-dimensional flow inside a square, has solved the Navier-Stokes equations numerically for a constant-density fluid. The highest Reynolds number for which results are presented is 400, which is comparable to values anticipated for Re_r in the present analysis. Both vorticity and temperature are found to be approximately constant in an inviscid core flow. The result of constant temperature in the inviscid core is obtained by taking the integral of the constant-density energy equation around a closed streamline. Todisco and Pallone[6] have made near-wake flow field measurements, and found the existence of a temperature plateau in the recirculating flow.

3. Integral Condition Obtained from Momentum Equation

The integral condition arising from the velocity distribution may be obtained by integrating the momentum equation around a closed streamline inside the recirculating flow. For convenience the momentum equation (III-2)

can be rewritten as

$$\vec{q} \times (\nabla \times \vec{q}) = \left(\frac{1}{\gamma M_r^2}\right)\frac{\nabla p}{\rho} + \nabla\left(\frac{q^2}{2}\right) - \left(\frac{1}{Re_r}\right)\left(\frac{1}{\rho}\right)\Big[\nabla(\mu' \nabla \cdot \vec{q})$$

$$+ (\nabla \cdot 2\mu\nabla)\vec{q} + \nabla \times (\mu\nabla \times \vec{q})\Big]$$

The integration of the above equation around a closed streamline gives

$$\oint\Big[\vec{q} \times (\nabla \times \vec{q})\Big] \cdot h_1 \, d\vec{\xi} = \left(\frac{1}{\gamma M_r^2}\right)\oint\Big[\frac{\nabla p}{\rho}\Big] \cdot h_1 \, d\vec{\xi} + \oint\Big[\nabla\left(\frac{q^2}{2}\right)\Big] \cdot h_1 \, d\vec{\xi}$$

$$-\left(\frac{1}{Re_r}\right)\oint \frac{1}{\rho}\Big[\nabla(\mu'\nabla \cdot \vec{q}) + (\nabla \cdot 2\mu\nabla)\vec{q} + \nabla \times (\mu\nabla \times \vec{q})\Big] \cdot h_1 \, d\vec{\xi}$$

(III-19)

The integral $\oint\Big[\vec{q} \times (\nabla \times \vec{q})\Big] \cdot h_1 \, d\vec{\xi}$ vanishes, because the contour of integration is a streamline. The second term on the right-hand side vanishes since $\frac{q^2}{2}$ is a single-valued function of position. Then equation (III-19) becomes:

$$\left(\frac{1}{Re_r}\right)\oint\frac{1}{\rho}\Big[\nabla(\mu' \nabla \cdot \vec{q}) + (\nabla \cdot 2\mu\nabla)\vec{q}$$

$$+ \nabla \times (\mu\nabla \times \vec{q})\Big] \cdot h_1 \, d\vec{\xi} = \left(\frac{1}{\gamma M_r^2}\right)\oint\Big[\frac{\nabla p}{\rho}\Big] \cdot h_1 \, d\vec{\xi}$$

(III-20)

When the expansions in powers of M_r^2 are substituted into the above equation, there results:

$$\left(\frac{1}{Re_r}\right)\left\{\oint\frac{1}{\rho_0}\left[\nabla\times\mu_0(\nabla\times\vec{q}_0)+\nabla(\mu_0'\nabla\cdot\vec{q}_0)+(\nabla\cdot 2\mu_0\nabla)\vec{q}_0\right]\cdot h_1\,d\vec{\xi}\right.$$

$$+\left(M_r^2\right)\oint\frac{1}{\rho_0}\Big[\ \nabla\times\mu_1(\nabla\times\vec{q}_0)+\nabla(\mu_1'\nabla\cdot\vec{q}_0)+(\nabla\cdot 2\mu_1\nabla)\vec{q}_0$$

$$-\left(\frac{\rho_1}{\rho_0}\right)\nabla\times\mu_0(\nabla\times\vec{q}_0)-\left(\frac{\rho_1}{\rho_0}\right)\nabla(\mu_0'\nabla\cdot\vec{q}_0)-\left(\frac{\rho_1}{\rho_0}\right)(\nabla\cdot 2\mu_0\nabla)\vec{q}_0$$

$$+\nabla\times\mu_0(\nabla\times\vec{q}_1)+\nabla(\mu_0'\nabla\cdot\vec{q}_1)+(\nabla\cdot 2\mu_0\nabla)\vec{q}_1\Big]\cdot h_1\,d\xi$$

$$\left.+O(M_r^4)\right\}=\left(\frac{1}{\gamma M_r^2}\right)\oint\frac{\nabla p}{\rho}\cdot h_1\,d\vec{\xi} \qquad \text{(III-21)}$$

For the interior of the recirculation region, an estimate of the variation in entropy along a closed streamline can be derived from equation (III-4) and the condition of constant temperature in the inviscid core:

$$\frac{\partial}{\partial\xi}(\Delta S)=O\left(\frac{M_r^2}{Re_r}\right) \qquad \text{(III-22)}$$

Now the estimate of the right-hand side of equation (III-20) may be obtained by substituting the estimate of the entropy variation from equation (III-22) into the equation of state (III-5). Because equation (III-5) can be expanded as

$$\frac{1}{\rho}=\frac{1}{p^{1/\gamma}}\left(1+\frac{1}{\gamma}\Delta S+\ldots\right)$$

$$\cong \frac{1}{p^{1/\gamma}} + \frac{1}{\gamma}\left(\Delta S \frac{1}{\rho}\right) + O\left[(\Delta S)^2\right] \qquad \text{(III-23)}$$

the right-hand side of equation (III-20) has the following expansion:

$$\oint\left(\frac{\nabla p}{\rho}\right)\cdot h_1 d\vec{\xi} = \oint\left(\frac{\nabla p}{p^{1/\gamma}}\right)\cdot h_1 d\vec{\xi}$$

$$+ \oint \frac{1}{\gamma}\left(\frac{\nabla p}{\rho}\ \Delta S\right)\cdot h_1 d\vec{\xi} + O\left[(\Delta S)^2\right] \qquad \text{(III-24)}$$

The first term on the right-hand side of the above equation is zero. By substituting the expansions in powers of M_r^2 and the estimate of equation (III-22) into equation (III-24), one finds

$$\oint\left(\frac{\nabla p}{\rho}\right)\cdot h_1 d\vec{\xi} = O\left\{\left(\frac{M_r^2}{Re_r}\right)\left[\oint\left(\frac{\nabla p_0}{\rho_0}\right)\cdot h_1 d\vec{\xi}\right.\right.$$

$$\left.\left. + (M_r^2)\oint\left(\frac{\nabla p_1}{\rho_0} - \frac{\rho_1 \nabla p_0}{\rho_0^2}\right)\cdot h_1 d\vec{\xi} + \ldots\right]\right\} \qquad \text{(III-25)}$$

Since $T_0 = 1$, and $S \cong$ constant along a streamline, it follows from the equation of state and the relation between S and $\frac{p}{\rho^\gamma}$ that p_0 and ρ_0 are constant along a streamline. From the component of the momentum equation normal to streamlines it is found that the changes in pressure normal to streamlines are $O(M_r^2)$. Therefore p_0 and ρ_0 are constant throughout the core region. Hence one obtains

$$\oint\left(\frac{\nabla p}{\rho}\right)\cdot h_1\, d\vec{\xi} = O\left(\frac{M_r^6}{Re_r}\right) \qquad \text{(III-26)}$$

Since $\mu_0 = \mu_0(T_0)$, $\mu_0' = \mu_0'(T_0)$, and $p_0 =$ constant, the resulting integral condition from the momentum equation can be rewritten, to order one, as

$$\oint\left[\nabla\times(\nabla\times\vec{q}_0)\right]\cdot h_1\, d\vec{\xi} = -\left(\frac{\mu_0' + 2\mu_0}{\mu_0}\right)\oint\left[\nabla(\nabla\cdot\vec{q}_0)\right]\cdot h_1\, d\vec{\xi} \qquad \text{(III-27)}$$

The term on the right-hand side vanishes because $\nabla\cdot\vec{q}_0 = 0$. Therefore

$$\oint\left[\nabla\times(\nabla\times\vec{q}_0)\right]\cdot h_1\, d\vec{\xi} = 0 \qquad \text{(III-28)}$$

It is clear that to order one the recirculating flow may be considered as incompressible because both T_0 and p_0 are constants. The result of equation (III-28) may, of course, be obtained by operating on the incompressible flow momentum equation. In order to obtain a condition which is valid for the entire inviscid core, rather than for a single streamline, equation (III-6) is used. By taking the curl, and using $\nabla\cdot(\nabla\times\vec{q}) = 0$ and also $\rho = \rho(p)$, equation (III-6) can be reduced to the vorticity equation for inviscid flow

$$(\vec{q}\cdot\nabla)\frac{\vec{\omega}}{\rho} = \left(\frac{\vec{\omega}}{\rho}\cdot\nabla\right)\vec{q} \qquad \text{(III-29)}$$

where $\vec{\omega} = \nabla\times\vec{q}$ and $\omega = \dfrac{\bar{\omega}\,\bar{L}_r}{2\bar{q}_r} = \dfrac{\bar{\omega}}{|\bar{\omega}_r|}$. For the two-dimensional recir-

culating flow, the right-hand side is identically zero, because $\vec{\omega}$ is always perpendicular to $\vec{q}$. Thus it follows that

$$\frac{\omega}{\rho} = \Omega(\psi)$$

Let the expansion of vorticity in powers of M_r^2 be defined by

$$\omega \sim \omega_0 + M_r^2 \omega_1 + \cdots$$

and

$$\Omega \sim \Omega_0(\psi) + M_r^2 \Omega_1(\psi) + \cdots$$

hen

$$\omega \sim \rho_0 \Omega_0(\psi) + (M_r^2) \left[\rho_1 \Omega_0(\psi) + \rho_0 \Omega_1(\psi) \right] + \cdots$$

hen the above result is applied to equation (III-28) there results

$$\oint \left[\nabla \times \rho_0 \Omega_0(\psi) \vec{i}_\omega \right] \cdot h_1 \, d\vec{\xi} = 0 \qquad \text{(III-30)}$$

where $\vec{i}_\omega$ is the unit vector normal to the plane of the flow and $\vec{\omega} = \omega \vec{i}_\omega$. Since ρ_0 is a constant, equation (III-30) can be rewritten as

$$\oint \left[\frac{d}{d\psi} \Omega_0(\psi) \right] q_0 h_1 \, d\xi = 0 \qquad \text{(III-31)}$$

Since $\oint q_0 h_1 \, d\xi \neq 0$ except when $q_0 = 0$, the condition obtained from the mo-

mentum equation for the inviscid core flow can be written, to order one, as

$$\omega_0 = \text{constant} \qquad \text{or} \qquad \Omega_0 = \text{constant} \qquad \text{(III-32)}$$

From the definition of $|\bar{\omega}_r|$, ω_0 must be equal to -1. This condition states that in the limit $Re_r \to \infty$ the contribution from viscous forces to the rate of change of vorticity in the two-dimensional recirculating flow must be zero when terms of order M_r^2 are neglected. Prandtl[20] and Batchelor[22] have found that for incompressible flow with closed streamlines the vorticity is uniformly distributed in the inviscid core flow. Since the conditions ω_0 = constant and T_0 = constant for the inviscid core flow are obtained by studying the dissipative terms, they demonstrate the fact that even though the core flow is inviscid and nonconducting, and the primary effects of diffusive exchanges are limited to the continuous viscous layer enclosing the recirculating flow, the accumulative effects of very small diffusive exchanges are experienced throughout the entire recirculating region. In other words, the reason for the existence of these integral conditions are that, in the exact steady motion, the net effects of diffusive exchanges must be exactly zero. Therefore, for two-dimensional flows with closed streamlines, the fluid motion cannot be exactly steady until the effects of the small but persistent diffusive exchanges have evened out any variation of temperature and vorticity that may have been present initially.

4. Discussion of Errors in the Incompressible-flow Approximation for the Inviscid Core.

The solutions obtained in the preceding sections are based on the assumption that the density of the recirculating flow is approximately constant.

The errors resulting from this approximation depend on the magnitude of the reference Mach number M_r for the recirculation region, which is known to be numerically small. Accordingly the higher-order terms in M_r, which have been neglected in the previous incompressible-flow analysis, should be examined so that an estimate of the compressibility effect on the recirculating flow can be obtained.

If terms of order M_r^2 are retained, the next approximation to the integral condition from the energy equation can be obtained from equation (III-3):

$$\oint\left(\frac{1}{\rho_0 q_0}\right)\left[\nabla\cdot(\mu_0\nabla H_1)\right]h_1\,d\xi$$

$$= -(\gamma-1)\oint\left(\frac{1}{\rho_0 p_0}\right)\left\{\nabla\cdot\left[\mu_0\left(\nabla\frac{q_0^2}{2}+\vec{\omega}_0\times\vec{q}_0\right)\right]\right\}h_1\,d\xi \qquad \text{(III-33)}$$

Since $H_1 = H_1(\psi)$ for the inviscid core flow, the left-hand side becomes

$$\oint\left(\frac{1}{\rho_0 q_0}\right)\left[\nabla\cdot(\mu_0\nabla H_1)\right]h_1\,d\xi$$

$$= \mu_0\oint\left(\frac{1}{\rho_0 p_0}\right)\left(\frac{1}{h_1 h_2}\right)\left[\frac{\partial}{\partial\psi}\left(\frac{h_1}{h_2}\frac{dH_1}{d\psi}\right)\right]h_1\,d\xi$$

$$= \mu_0\oint\left(\frac{1}{h_1}\right)\left[\frac{\partial}{\partial\psi}\left(\rho_0 q_0 h_1\frac{dH_1}{d\psi}\right)\right]h_1\,d\xi$$

where $\rho_0 q_0 h_2 = 1$. The right-hand side of equation (III-33) may be rearranged

as

$$-(\gamma-1)\oint\left(\frac{1}{\rho_0 q_0}\right)\left\{\nabla\cdot\left[\mu_0\left(\nabla\frac{q_0^2}{2}+\vec{\omega}_0\times\vec{q}_0\right)\right]\right\}h_1\,d\xi$$

$$=-(\gamma-1)\,\mu_0\oint\left[\frac{1}{h_1}\frac{\partial}{\partial\psi}\left(\rho_0 q_0 h_1\frac{\partial\, q_0^2/2}{\partial\psi}\right)-\frac{\omega_0^2}{\rho_0 q_0}\right]h_1\,d\xi$$

where $\omega_0 = -\frac{1}{h_1 h_2}\frac{\partial h_1 q_0}{\partial\psi}$. Hence equation (III-33) can be written as

$$\frac{d}{d\psi}\oint\left[\frac{\partial}{\partial\psi}\left(H_1(\psi)+\frac{\gamma-1}{2}\,q_0^2\right)\right]\rho_0 q_0 h_1\,d\xi$$

$$=\left[(\gamma-1)\,\omega_0^2\right]\oint\frac{1}{\rho_0 q_0}\,h_1\,d\xi \qquad \text{(III-34)}$$

Integrating equation (III-34) with respect to ψ,

$$\oint\left[\frac{\partial}{\partial\psi}\left(H_1(\psi)+\frac{\gamma-1}{2}\,q_0^2\right)\right]\rho_0 q_0 h_1\,d\xi$$

$$=\left[(\gamma-1)\,\omega_0^2\right]\int\oint\frac{1}{\rho_0 q_0}\,h_1\,d\xi\,d\psi$$

Changing the order of integration on the right-hand side term and using $\rho_0 q_0 h_2 = 1$,

$$\oint\left(\frac{d}{d\psi}H_1(\psi)\right)\rho_0 q_0 h_1\,d\xi=(\gamma-1)\,\omega_0^2\,A(\psi)-(\gamma-1)\oint\left(\frac{\partial\, q_0^2/2}{\partial\psi}\right)\rho_0 q_0 h_1\,d\xi$$

(III-35)

where $A(\psi) = \int \oint \frac{1}{\rho_0 q_0} h_1 \, d\xi \, d\psi = \int \oint h_2 h_1 \, d\xi \, d\psi$. Hence $A(\psi)$ is the area inside the closed streamline. Also

$$\left(\frac{\partial q_0^2/2}{\partial \psi}\right)_{\rho_0 q_0} = q_0 \frac{1}{h_2}\left(\frac{\partial q_0}{\partial \psi}\right)$$

$$= \frac{1}{h_1 h_2} q_0\left(\frac{\partial h_1 q_0}{\partial \psi}\right) - \left(\frac{q_0}{h_1}\right)^2 \frac{1}{h_2} \frac{\partial}{\partial \psi}\left(\frac{h_1^2}{2}\right)$$

Since Stokes' theorem gives

$$\oint q_0 h_1 \, d\xi = -\omega_0 A(\psi)$$

then equation (III-35) can be reduced to

$$\frac{dH_1(\psi)}{d\psi} = (\gamma-1)\left\{\frac{\oint\left(\frac{q_0}{h_1}\right)^2\left[\frac{\partial}{h_2 \partial \psi}\left(\frac{h_1^2}{2}\right)\right] h_1 \, d\xi}{\left[\oint \rho_0 q_0 h_1 \, d\xi\right]}\right\} \qquad \text{(III-36)}$$

Integrating the above equation with respect to ψ and rearranging,

$$T_1 = \frac{\gamma-1}{2} q_0^2 + (\gamma-1)\int\left\{\frac{\oint\left(\frac{q_0}{h_1}\right)^2\left[\frac{\partial}{h_2 \partial \psi}\left(\frac{h_1^2}{2}\right)\right] h_1 \, d\xi}{\int \rho_0 q_0 h_1 \, d\xi}\right\} d\psi \qquad \text{(III-37)}$$

In order to obtain the exact value of T_1, it would be necessary to evaluate the second term on the right-hand side of equation (III-37). Since the exact functional dependence of h_1 is not known, the value of the integral can not be obtained analytically. However an estimate of the integral can be performed, so that the contribution of T_1 may be estimated. The term in the curly bracket

of the integral of equation (III-37) will be estimated as

$$\left\{ \frac{\oint \left(\frac{q_0}{h_1}\right)^2 \left[\frac{1}{h_2} \frac{\partial}{\partial \psi}\left(\frac{h_1^2}{2}\right)\right] h_1 \, d\xi}{\int \rho_0 q_0 h_1 \, d\xi} \right\}$$

$$\cong \left\{ \frac{\left[\left(\frac{q_0}{h_1}\right)^2 \frac{\partial}{\partial \psi}\left(\frac{h_1^2}{2}\right)\right]_{\text{typical of } A(\psi)} \oint \rho_0 q_0 h_1 \, d\xi}{\int \rho_0 q_0 h_1 \, d\xi} \right\}$$

$$\cong \left[\left(\frac{q_0}{h_1}\right)^2 \frac{\partial}{\partial \psi}\left(\frac{h_1^2}{2}\right)\right]_{\text{typical of } A(\psi)}$$

therefore the integral of equation (III-37) will be estimated as

$$(\gamma-1) \int \left\{ \frac{\oint \left(\frac{q_0}{h_1}\right)^2 \left[\frac{1}{h_2} \frac{\partial}{\partial \psi}\left(\frac{h_1^2}{2}\right)\right] h_1 \, d\xi}{\int \rho_0 q_0 h_1 \, d\xi} \right\} d\psi$$

$$\cong \left(\frac{\gamma-1}{2}\right) \left[\left(\frac{q_0}{h_1}\right)^2 \frac{\partial}{\partial \psi}\left(h_1^2\right)\right]_{\text{typical of } A(\psi)} \Delta\psi$$

$$\cong \left(\frac{\gamma-1}{2}\right) \left[\left(\frac{q_0^2}{h_1^2}\right)\left(\frac{\Delta h_1^2}{\Delta \psi}\right)\right]_{\text{typical of } A(\psi)} \Delta\psi$$

$$\cong \left(\frac{\gamma-1}{2}\right) \left[q_0^2\right]_{\text{typical of } A(\psi)}$$

It is assumed that $\frac{\Delta h_1^2}{h_1^2} \cong 1$ hence an estimate of T_1 may be obtained from equation (III-37) as

$$T_1 \cong -\left(\frac{\gamma-1}{2}\right) \left\{ q_0^2 - \left[q_0^2\right]_{\text{typical of } A(\psi)} \right\} \qquad \text{(III-38)}$$

From the solution for the inviscid core flow, which will be treated in (IV), one may show that q_0 is always less than unity. Actually $|q_0|_{max} \cong 0.85$, and so the quantity in the curly bracket of equation (III-38) must be always smaller than unity, with maximum value probably less than 0.5. Furthermore, for $\gamma = 1.4$, the numerical factor is equal to 0.2. Therefore, the term $M_r^2 T_1$ is believed to be very small in comparison with T_0, and for all practical purpose $M_r^2 T_1$ may be considered as zero.

It is known that in the inviscid core flow p_0 = constant. Thus the momentum equation can be written as

$$q_0 \frac{1}{h_1}\left(\frac{\partial q_0}{\partial \xi}\right) = -\frac{1}{\gamma \rho_0}\frac{1}{h_1}\left(\frac{\partial p_1}{\partial \xi}\right) \qquad \text{(III-39)}$$

$$\frac{1}{h_2}\left(\frac{\partial q_0^2/2}{\partial \psi}\right) + \omega_0 q_0 = -\frac{1}{\gamma \rho_0}\frac{1}{h_2}\left(\frac{\partial p_1}{\partial \psi}\right) \qquad \text{(III-40)}$$

Solving these equations

$$p_1 = -\gamma\left[\frac{\rho_0 q_0^2}{2} + \omega_0(\psi - \psi_c)\right] = -\gamma\left[\frac{\rho_0 q_0^2}{2} - (\psi - \psi_c)\right] \qquad \text{(III-41)}$$

where $\psi_c = \frac{\bar{\psi}_c}{\bar{q}_r \bar{L}_r}$, and $|\psi_c|$ is the mass flow per unit time between the center of rotation and the enclosing boundary surface. Since $\bar{q}_r \cong \bar{q}_{0\,max}$ and the distance between the center of rotation and the location where $\bar{q}_0 = \bar{q}_{0\,max}$ is approximately equal to $\bar{L}_r/2$, the mean velocity between

these two points will be estimated as $\frac{1}{2}q_r$. Therefore ψ_c will be estimated as -0.5. By the definition of the typical values of density, temperature and pressure, it is clear that $\rho_0 = p_0 = T_0 = 1$, and so the equation of state may be written as

$$p_1 = \rho_1 + T_1 \tag{III-42}$$

Since $T_1 \cong 0$,

$$\rho_1 = -\gamma\left[\frac{q_0^2}{2} - (\psi - \psi_c)\right] \tag{III-43}$$

By using equation (III-43) and the expansion of Ω in powers of M_r^2, there results

$$\omega_0 = \Omega_0 = -1$$

$$\Omega_1(\psi) = -\gamma\left[\frac{q_0^2}{2} - (\psi - \psi_c)\right] + \omega_1$$

or

$$\omega_1 = \Omega_1(\psi) + \gamma\left[\frac{q_0^2}{2} - (\psi - \psi_c)\right]$$

From the energy equation, the equation of state, and the results so far obtained, it has been shown that along a streamline the variation in entropy is $\Delta S = O\left(\frac{M_r^2}{Re_r}\right)$ and therefore $\oint\left(\frac{\Delta p}{\rho}\right)h_1\,d\xi = O\left(\frac{M_r^6}{Re_r}\right)$. In the expanded integral condition (III-21) all but one of the terms of order M_r^2 are zero, and so the next approximation to the condition becomes

$$\oint\left[\nabla \times \omega_1 \vec{i}_\omega\right] \cdot h_1\,d\vec{\xi} = 0 \tag{III-44}$$

Substituting the expression derived for ω_1 into equation (III-44) one obtains

$$\oint \left[\nabla \times \Omega_1(\psi)\, \vec{i}_\omega \right] \cdot h_1 \, d\vec{\xi} = -\gamma \oint \left\{ \nabla \times \left[\frac{q_0^2}{2} - (\psi - \psi_c) \right] \vec{i}_\omega \right\} \cdot h_1 \, d\vec{\xi} \qquad \text{(III-45)}$$

which may be rewritten as

$$\frac{d\Omega_1(\psi)}{d\psi} \oint q_0 h_1 \, d\xi = \gamma \oint q_0 h_1 \, d\xi - \gamma \oint \left[q_0 \frac{\partial q_0}{\partial \psi} \right] q_0 h_1 \, d\xi$$

$$= \gamma \oint q_0 h_1 \, d\xi - \gamma \oint \left[1 - \left(\frac{q_0}{h_1} \right)^2 \frac{\partial}{\partial \psi} \left(\frac{h_1^2}{2} \right) \right] q_0 h_1 \, d\xi$$

$$= \gamma \oint \left[\left(\frac{q_0}{h_1} \right)^2 \frac{\partial}{\partial \psi} \left(\frac{h_1^2}{2} \right) \right] q_0 h_1 \, d\xi$$

After rearranging and then integrating with respect to ψ,

$$\Omega_1(\psi) = \gamma \int \left\{ \frac{\oint \left[\left(\frac{q_0}{h_1} \right)^2 \frac{\partial}{\partial \psi} \left(\frac{h_1^2}{2} \right) \right] q_0 h_1 \, d\xi}{\oint q_0 h_1 \, d\xi} \right\} d\psi \qquad \text{(III-46)}$$

the integral of equation (III-46) will be estimated as

$$\int \left\{ \frac{\oint \left[\left(\frac{q_0}{h_1} \right)^2 \frac{\partial}{\partial \psi} \left(\frac{h_1^2}{2} \right) \right] q_0 h_1 \, d\xi}{\oint q_0 h_1 \, d\xi} \right\} d\psi$$

$$\cong \int \left\{ \frac{\left[\left(\frac{q_0}{h_1} \right)^2 \frac{\partial}{\partial \psi} \left(\frac{h_1^2}{2} \right) \right]_{\text{typical of } A(\psi)} \oint q_0 h_1 \, d\xi}{\oint q_0 h_1 \, d\xi} \right\} d\psi$$

$$\cong \left[\left(\frac{q_0}{h_1}\right)^2 \frac{\partial}{\partial\psi}\left(\frac{h_1^2}{2}\right)\right]_{\text{typical of } A(\psi)} \Delta\psi$$

$$\cong \left(\frac{q_0^2}{2}\right)_{\text{typical of } A(\psi)}$$

Then equation (III-46) will be estimated as

$$\Omega_1 \cong \gamma\left(\frac{q_0^2}{2}\right)_{\text{typical in } A(\psi)}$$

$$\omega_1 \cong \gamma\left\{\left[\frac{q_0^2}{2} + \left(\frac{q_0^2}{2}\right)_{\text{typical in } A(\psi)}\right] - (\psi - \psi_c)\right\}$$

Nearing the center of rotation, $\psi \to \psi_c$ and $q_0 \to 0$, and so

$$\omega_1 \to 0$$

Approaching the edge of the inviscid core flow, $\psi \to 0$ and $0 \leq q_0 \leq q_{0\,max} \cong 0.85$. Since $\psi_c \cong -0.5$, $|\omega_1|$ might be as large as 0.5 near the stagnation points. Elsewhere in the inviscid core flow,it would be expected that $|\omega_1|$ is considerably smaller than 0.5. Thoughout most of the region, therefore $M_r^2 |\omega_1|$ is believed to be quite small in comparison with $|\omega_0|$.

IV

THE INVISCID CORE FLOW

1. General Description and Formulation of the Problem

The results from previous sections have shown that when the wake Reynolds number Re_r is large and the wake Mach number M_r is small, the model proposed by Prandtl[20] and Batchelor[22] should correctly describe the interior of the recirculation region. Accordingly two conditions, which imply uniform temperature and vorticity, have been deducted for this inviscid core flow.

The static pressure in the near wake is known to be nearly constant, except in the vicinity of the trailing-edge stagnation point and the rear stagnation point. However, the regions near these points are assumed to be small in comparison with the length of the wake, provided that the Mach number is not too large. Away from the stagnation points, the curvature of the dividing streamline may be regarded as small. Furthermore, since the wake Reynolds number is large, the regions near the enclosing surfaces, where the diffusive exchanges are large, can be considered small. Consequently, the interior of the recirculation region, where the recirculating flow is inviscid and incompressible with uniform vorticity, may be approximated as a right triangle bounded by the base of the symmetric wedge, the wake center line and the dividing streamline.

It is convenient to work with a stream function $\bar{\psi}$ and to use cylindrical

coordinates $\bar{\theta}$ and $\bar{r}$, with origin at the rear stagnation point and $\bar{\theta}$ measured clockwise from the center line of the recirculation region (see figure 3). For plane incompressible flow the stream function is defined by

$$d\bar{\psi} = \frac{\partial \bar{\psi}}{\partial \bar{r}} d\bar{r} + \frac{\partial \bar{\psi}}{\partial \bar{\theta}} d\bar{\theta}$$

where $\frac{\partial \bar{\psi}}{\partial \bar{r}}$ and $-\frac{1}{\bar{r}} \frac{\partial \bar{\psi}}{\partial \bar{\theta}}$ are the velocity components in the $\bar{\theta}$ and $\bar{r}$ directions respectively. Therefore the governing differential equation is the Poisson equation

$$\nabla^2 \bar{\psi} = \bar{\omega} \qquad \text{(IV-1)}$$

where $\bar{\omega} = \bar{\omega}_r$ and is a constant. This equation expresses the physical fact that the flow is incompressible and inviscid with a uniform distribution in vorticity. The boundary conditions to be satisfied are

$$\bar{\psi}(\bar{r}, 0) = \bar{\psi}(\bar{r}, \bar{\theta}_o) = \bar{\psi}\left(\frac{\bar{r}_o \cos \bar{\theta}_o}{\cos \bar{\theta}}, \bar{\theta} \right) = 0 \qquad \text{(IV-2)}$$

where $\bar{r}_o$ is the length of the dividing streamline and $\bar{\theta}_o$ is the wake angle. These boundary conditions indicate that in the triangular region the mass is conserved; that is, there is no mass exchange with the surroundings. In order to nondimensionalize and normalize the governing differential equation and boundary conditions, new variables are introduced in the following manner:

$$\psi^* = \frac{\bar{\psi}}{\bar{\omega}\bar{r}_o^2} \; ; \; r = \frac{\bar{r}}{\bar{r}_o} \; ; \; \theta = \frac{\bar{\theta}}{\bar{\theta}_o}$$

Then the nondimensional form of equations (IV-1) and (IV-2) can be written as

$$\frac{\partial^2 \psi^*}{\partial r^2} + \frac{1}{r} \frac{\partial \psi^*}{\partial r} + \frac{1}{r^2 \bar{\theta}_o^2} \frac{\partial^2 \psi^*}{\partial \theta^2} = 1 \qquad \text{(IV-3)}$$

$$\psi^*(r,0) = \psi^*(r,1) = \psi^*\left(\frac{\cos \bar{\theta}_o}{\cos(\bar{\theta}_o \theta)} , \theta \right) = 0 \qquad \text{(IV-4)}$$

2. Method of Solution

In this problem a particular integral of the differential equation (IV-3) can be obtained by defining

$$\psi^*(r, \theta; \bar{\theta}_o) = \Psi(r, \theta; \bar{\theta}_o) + \chi(r, \theta; \bar{\theta}_o) \qquad \text{(IV-5)}$$

where $\Psi(r, \theta; \bar{\theta}_o)$ is the particular integral and satisfies the following differential equation and boundary conditions:

$$\frac{\partial^2 \Psi}{\partial r^2} + \frac{1}{r} \frac{\partial \Psi}{\partial r} + \frac{1}{r^2 \bar{\theta}_o^2} \frac{\partial^2 \Psi}{\partial \theta^2} = 1 \qquad \text{(IV-6)}$$

$$\Psi(r, 0; \bar{\theta}_o) = \Psi(r, 1; \bar{\theta}_o) = 0 \qquad \text{(IV-7)}$$

A solution of equations (IV-6) and (IV-7) is

$$\Psi(r, \theta; \bar{\theta}_o) = \left[\frac{-r^2}{4 \sin 2\bar{\theta}_o}\right]\left\{\sin\left[2\bar{\theta}_o(1-\theta)\right] + \sin\left[2\bar{\theta}_o\theta\right] - \sin\left[2\bar{\theta}_o\right]\right\} \tag{IV-8}$$

If equations (IV-5) and (IV-8) are substituted into equation (IV-3) and boundary conditions (IV-4), the differential equation becomes

$$\frac{\partial^2\chi}{\partial r^2} + \frac{1}{r}\frac{\partial\chi}{\partial r} + \frac{1}{r^2\bar{\theta}_o^2}\frac{\partial^2\chi}{\partial\theta^2} = 0 \tag{IV-9}$$

and the boundary conditions reduce to

$$\chi(r, 0; \bar{\theta}_o) = \chi(r, 1; \bar{\theta}_o) = 0 \tag{IV-10a,b}$$

$$\chi\left(\frac{\cos\bar{\theta}_o}{\cos(\theta_o\theta)}, \theta; \bar{\theta}_o\right) = \left[\frac{\cos^2\bar{\theta}_o}{4 \sin 2\bar{\theta}_o \cos^2(\bar{\theta}_o\theta)}\right]\left\{\sin\left[2\bar{\theta}_o(1-\theta)\right]\right.$$

$$\left. + \sin\left[2\bar{\theta}_o\theta\right] - \sin\left[2\bar{\theta}_o\right]\right\} \tag{IV-10c}$$

Although it may be possible by standard methods to obtain a solution which satisfies (IV-9) and (IV-10) to any desired degree of accuracy, it appears that any such solution would be very complicated. Since the wake angle $\bar{\theta}_c$ is known to be rather small, a further simplification can be made by expanding ψ in a power series in $\bar{\theta}_o$. Equation (IV-8) has the following series expansion in $\bar{\theta}_o$:

$$\Psi(r, \theta; \bar{\theta}_o) = \bar{\theta}_o^2\Psi_1(r, \theta) + \bar{\theta}_o^4\Psi_3(r, \theta) + O(\bar{\theta}_o^6)$$

$$= \bar{\theta}_o^2 \left[(\theta^2 - \theta) \frac{r^2}{2} \right] + \bar{\theta}_o^4 \left[(\theta - 2\theta^3 + \theta^4) \frac{r^2}{6} \right] + O(\bar{\theta}_o^6) \qquad \text{(IV-11)}$$

The solution for χ must satisfy equations (IV-9) and (IV-10). Since the boundary condition given by equation (IV-10c) may be approximated by a Fourier sine series, the method of separation of variables can be employed.[32] The largest term of the solution is of the form

$$r^{\pi/\bar{\theta}_o} \sin \pi\theta$$

where $\pi/\bar{\theta}_o \gg 1$ because $0 < \bar{\theta}_o \ll 1$. Therefore the solution decays fairly rapidly as (1-r) increases. Consequently, the contribution of $\chi(r, \theta; \bar{\theta}_o)$ to ψ^* may be considered as limited to the region where (1-r) is small. Since $r^{\pi/\bar{\theta}_o} \sim - \exp[-\pi(1-r)/\bar{\theta}_o]$ as $r \to 1$, it appears that, for $\bar{\theta}_o \to 0$, χ is a function of the stretched coordinate

$$r^* = \frac{1-r}{\bar{\theta}_o}$$

With this new independent variable, the expansion of $\chi(r, \theta; \bar{\theta}_o)$ is

$$\chi(r, \theta; \bar{\theta}_o) = \bar{\theta}_o^2 \chi_1(r^*, \theta) + \bar{\theta}_o^3 \chi_2(r^*, \theta) + \bar{\theta}_o^4 \chi_3(r^*, \theta) + O(\bar{\theta}_o^5) \qquad \text{(IV-12)}$$

Hence the expansion of ψ^* is

$$\psi^*(r, \theta; \bar{\theta}_o) = \bar{\theta}_o^2[\Psi_1 + \chi_1] + \bar{\theta}_o^3[\chi_2] + \bar{\theta}_o^4[\Psi_3 + \chi_3] + \ldots \quad \text{(IV-13)}$$

When equation (IV-12) is substituted into equation (IV-9) and (IV-10a, b, c), there results

$$\chi_{1r^*r^*} + \chi_{1\theta\theta} + \bar{\theta}_o[\chi_{2r^*r^*} - \chi_{1r^*} + \chi_{2\theta\theta} + 2r^*\chi_{1\theta\theta}] + \ldots = 0 \quad \text{(IV-14)}$$

$$\chi_1(r^* 0) + \bar{\theta}_o\chi_2(r^*, 0) + \ldots = 0 \quad \text{(IV-15a)}$$

$$\chi_1(r^*, 1) + \bar{\theta}_o\chi_2(r^*, 1) + \ldots = 0 \quad \text{(IV-15b)}$$

$$\chi_1(0, \theta) + \bar{\theta}_o\left[\chi_2(0,\theta) + \tfrac{1}{2}(1-\theta^2)\chi_{1r^*}(0,\theta)\right] + \bar{\theta}_o^2\left[\chi_3(0,\theta) + \frac{(1-\theta^2)^2}{8}\chi_{1r^*r^*}(0,\theta) + \frac{(1-\theta^2)}{2}\chi_{2r^*}(0,\theta)\right] + \ldots = \tfrac{1}{2}\left[\theta - \theta^2\right] + \bar{\theta}_o^2\left[-\tfrac{1}{3}\theta + \tfrac{1}{2}\theta^2 + \tfrac{1}{6}\theta^3 - \tfrac{1}{3}\theta^4\right] + \ldots \quad \text{(IV-15c)}$$

3. The Solution for the Inviscid Core Flow

From equations (IV-14) and (IV-15a, b, c), the governing differential equation and boundary conditions for $\chi_1(r, \theta)$ can be written as

$$\chi_{1r^*r^*} + \chi_{1\theta\theta} = 0 \quad \text{(IV-16)}$$

$$\chi_1(r^*, 0) = \chi_1(r^*, 1) = 0 \qquad \text{(IV-17a, b)}$$

$$\chi_1(0, \theta) = \tfrac{1}{2}(\theta - \theta^2) \qquad \text{(IV-17c)}$$

The above differential equation and boundary conditions describe inviscid incompressible flow in a semi-infinite strip bounded by walls at $\theta = 0$ and $\theta = 1$; the boundary condition at $r^* = 0$ is prescribed by equation (IV-17c); the other condition needed for the solution of the above problem can be obtained by the requirement that the solution must be bounded as $r^* \to \infty$. Since the boundary condition at $r^* = 0$ has the Fourier series expansion

$$\tfrac{1}{2}(\theta - \theta^2) = \frac{4}{\pi^3} \sum_0^\infty \frac{1}{(2n+1)^3} \sin(2n+1)\pi\theta \qquad \text{(IV-18)}$$

and since the method of separation of variables can be applied, the solution for $\chi_1(r^*, \theta)$ is

$$\chi_1(r^*, \theta) = \frac{4}{\pi^3} \sum_0^\infty \left\{ \frac{1}{(2n+1)^3} \exp\left[-(2n+1)\pi r^*\right] \right\} \sin(2n+1)\pi\theta \qquad \text{(IV-19)}$$

Therefore the solution to order $\bar{\theta}_o^2$ can be written as

$$\psi^*(r, \theta; \bar{\theta}_o) = \bar{\theta}_o^2 \left\{ \frac{r^2}{2}(\theta^2 - \theta) + \frac{4}{\pi^3} \sum_0^\infty \left[\frac{\exp\left[-(2n+1)(1-r)\pi/\bar{\theta}_o\right]}{(2n+1)^3} \right] \sin(2n+1)\pi\theta \right\} + O(\bar{\theta}_o^3) \qquad \text{(IV-20)}$$

For small values of the wake angle $\bar{\theta}_o$, this solution is equivalent to the solution for the flow in a circular sector with angle $\bar{\theta}_o$ and radius $\bar{r}_o$. The flow in the circular sector with constant vorticity would be described approximately as follows:

$$\psi^*(r, \theta; \bar{\theta}_o) \cong \left[-\frac{r^2}{2} (\theta - \theta^2)\, \bar{\theta}_o^2 + \chi_1(r, \bar{\theta}) \right] + O(\bar{\theta}_o^3)$$

$$\frac{\partial^2 \chi_1}{\partial r^2} + \frac{1}{r} \frac{\partial \chi_1}{\partial r} + \frac{1}{r^2} \frac{\partial^2 \chi_1}{\partial \bar{\theta}^2} = 0$$

$$\chi_1(r, 0) = \chi_1(r, 1) = 0$$

$$\chi_1(1, \theta) = \tfrac{1}{2}(\theta - \theta^2)$$

and $\chi_1(r, \bar{\theta})$ would be obtained by using the method of separation of variables. The solution is

$$\psi^* = \bar{\theta}_o^2 \left[\frac{r^2}{2}(\theta^2 - \theta) + \frac{4}{\pi^3} \sum_0^\infty \frac{r^{[(2n+1)\pi/\bar{\theta}_o]}}{(2n+1)^3} \sin(2n+1)\pi\theta \right] + O(\bar{\theta}_o^3)$$

Since the contribution from the series terms diminishes as (1-r) grows and since the powers of the nondimensional radius $r^{(2n+1)\pi/\bar{\theta}_o}$ for (1-r) small may be approximated by the exponential form $e^{-(2n+1)(1-r)\pi/\bar{\theta}_o}$, the above solution may be approximated by equation (IV-20) or vice versa.

The differential equation and boundary conditions for χ_2 can be obtained from equations (IV-14) and (IV-15) and the solutions for $\chi_1(r^*, \theta)$:

$$\chi_{2r^*r^*} + \chi_{2\theta\theta} = \chi_{1r^*} - 2r^*\chi_{1\theta\theta} \qquad \text{(IV-21)}$$

$$\chi_2(r^*, 0) = \chi_2(r^*, 1) = 0 \qquad \text{(IV-22a, b)}$$

$$\chi_2(0, \theta) = -\tfrac{1}{2}(1 - \theta^2)\chi_{1r^*}(0, \theta) \qquad \text{(IV-22c)}$$

$$= \frac{2}{\pi^2}(1 - \theta^2)\sum_0^\infty \frac{1}{(2n+1)^2}\sin(2n+1)\pi\theta$$

In this problem a particular integral that accounts for the terms on the right-hand side of the differential equation can be expressed in terms of the known solution $\chi_1(r^*, \theta)$. Let

$$\chi_2 = \chi_2^{(p)} + \chi_2^{(c)} \qquad \text{(IV-23a)}$$

where $\chi_2^{(p)}$ and $\chi_2^{(c)}$ denote the particular integral and the complementary solution for equations (IV-21) and (IV-22) respectively. A particular solution is given by

$$\chi_2^{(p)} = \tfrac{1}{2}r^{*2}\chi_{1r^*} \qquad \text{(IV-23b)}$$

Since $\chi_2^{(p)}$ satisfies homogeneous boundary conditions, $\chi_2^{(c)}$ satisfies the following differential equation and boundary conditions:

$$\chi^{(c)}_{2r^*r^*} + \chi^{(c)}_{2\theta\theta} = 0 \qquad \text{(IV-24)}$$

$$\chi_2^{(c)}(r^*, \theta) = \chi_2^{(c)}(r^*, 1) = 0 \qquad \text{(IV25a, b)}$$

$$\chi_2^{(c)}(0, \theta) = \frac{2}{\pi^2}(1-\theta^2)\sum_0^{\infty} \frac{1}{(2n+1)^2} \sin(2n+1)\pi\theta \qquad \text{(IV-25c)}$$

The other boundary condition is the condition that the solution must be bounded as $r^* \to \infty$.

The boundary condition for $\chi_2^{(c)}(r^*, 0)$ at $r^* = 0$ is expressed as the product of a polynomial and an infinite sine series. This sine series is known to converge uniformly in the region $0 \leq \theta \leq 1$, because the coefficients are $O(1/n^2)$ as $n \to \infty$. Equations (IV-24) and (IV-25) can be solved by the method of separation of variables provided that an appropriate Fourier series representation of the boundary condition at $r^* = 0$ can be obtained. Since the boundary condition is epxressed by a uniformly convergent series which converges fairly rapidly, only a small number of terms are needed to provide a quite good approximation. If the sine series appearing in $\chi_2^{(c)}(0, \theta)$ is approximated in this manner, a number of ways might be suggested to expand the resulting expression in Fourier series. However, for a good fit with a small

number of terms, with term-by-term differentiation permitted, a Fourier series which converges rapidly is desirable. The procedure adopted here will provide a series with coefficients which are $O(1/n^3)$ as $n \to \infty$.

For the present purpose the boundary condition $\chi_2^{(c)}(0, \theta)$ may first be approximated quite accurately by a fourth-degree polynomial in θ:

$$\chi_2^{(c)}(0, \theta) \cong \sum_0^4 A_n \theta^n$$

Its coefficients are determined by solving a set of five algebraic equations

$$\sum_0^4 A_n \left(\frac{j}{4}\right)^n = \frac{2}{\pi^2}\left[1 - \left(\frac{j}{4}\right)^2\right] \sum_0^\infty \frac{1}{(2n+1)^2} \sin(2n+1)\pi\left(\frac{j}{4}\right)$$

$$j = 0, 1, \ldots, 4$$

The resulting approximated boundary condition may be written as

$$\chi_2^{(c)}(0, \theta) = \frac{2}{\pi^2}\left[4.59\theta - 7.83\theta^2 + 2.49\theta^3 + 0.75\theta^4\right]$$

which can be expressed by a Fourier sine series

$$\chi_2^{(c)}(0, \theta) = \frac{4}{\pi^2}\left\{\sum_0^\infty\left[\frac{7.4}{(2n+1)^3\pi^3} + \frac{36}{(2n+1)^5\pi^5}\right]\sin(2n+1)\pi\theta\right.$$

$$\left. + \sum_1^\infty\left[\frac{23.9}{(2n\pi)^3}\right]\sin 2n\pi\theta\right\} \qquad \text{(IV-26)}$$

Consequently the problem of equations (IV-24),(IV-25a, b) and(IV-26) can be solved by the method of separation of variables. The solution is

$$\chi_2^{(c)}(r^*, \theta) = \frac{4}{\pi^2} \sum_0^\infty \left[\left(\frac{7.4}{[(2n+1)\pi]^3} + \frac{36}{[(2n+1)\pi]^5} \right) \exp[-(2n+1)\pi r^*] \right] \sin(2n+1)\pi\theta$$

$$+ \frac{4}{\pi^2} \sum_1^\infty \left[\left(\frac{23.9}{(2n\pi)^3} \right) \exp[-2n\pi r^*] \right] \sin 2n\pi\theta \qquad \text{(IV-27)}$$

Thus the solution for $\chi_2(r^*, \theta)$ is expressed by

$$\chi_2(r^*, \theta) = \frac{4}{\pi^2} \left\{ \sum_0^\infty \left[\left(-\frac{r^{*2}}{2(2n+1)^2} + \frac{7.4}{(2n+1)^3 \pi^3} \right.\right.\right.$$

$$\left.\left.\left. + \frac{36}{(2n+1)^5 \pi^5} \right) \exp[-(2n+1)\pi r^*] \right] \sin(2n+1)\pi\theta \right.$$

$$\left. + \sum_1^\infty \left[\left(\frac{23.9}{(2n\pi)^3} \right) \exp[-2n\pi r^*] \right] \sin 2n\pi\theta \right\} \qquad \text{(IV-28)}$$

Because of the presence of terms involving $\sin 2n\pi\theta$, the solution $\chi_2(r^*, \theta)$ is not symmetric with respect to the line $\bar{\theta} = \frac{1}{2}\bar{\theta}_o$. The complete solution for the inviscid core flow may be written as

$$\psi^*(r, \theta) = \bar{\theta}_o^2 \left[\frac{r^2}{2}(\theta^2 - \theta) + \frac{4}{\pi^3} \sum_0^\infty \left(\frac{\exp[-(2n+1)(1-r)\pi/\bar{\theta}_o]}{(2n+1)^3} \right) \sin(2n+1)\pi\theta \right]$$

$$+ \bar{\theta}_o^3 \left\{ \frac{4}{\pi^2} \sum_0^\infty \left[\left(-\frac{(1-r)^2}{2(2n+1)^2 \bar{\theta}_o^2} + \frac{7.4}{(2n+1)^3 \pi^3} \right.\right.\right.$$

$$\left.\left.\left. + \frac{36}{(2n+1)^5 \pi^5} \right) \exp[-(2n+1)(1-r)\pi/\bar{\theta}_o] \right] \sin(2n+1)\pi\theta \right.$$

$$\left. + \frac{4}{\pi^2} \sum_1^\infty \left[\left(\frac{23.9}{(2n\pi)^3} \right) \exp[-2n(1-r)\pi/\bar{\theta}_o] \right] \sin 2n\pi\theta \right\} + (\bar{\theta}_o^4) \qquad \text{(IV-29)}$$

The velocity component in the $\bar{\theta}$ direction is

$$\frac{\partial \bar{\psi}}{\partial \bar{r}} = \bar{\omega}_r \bar{r}_o \bar{\theta}_o \left\{ r(\theta^2 - \theta)\bar{\theta}_o + \frac{4}{\pi^2} \sum_0^\infty \left[\frac{\exp\left[-(2n+1)(1-r)\pi/\bar{\theta}_o\right]}{(2n+1)^2} \right] \sin(2n+1)\pi\theta \right.$$

$$+ \frac{4}{\pi^2} \sum_0^\infty \left[\left(\frac{(1-r)\pi}{(2n+1)^2} - \frac{(1-r)^2\pi}{2(2n+1)\bar{\theta}_o} + \frac{7.4\bar{\theta}_o}{(2n+1)^2\pi^2} \right.\right.$$

$$\left.\left. + \frac{36\bar{\theta}_o}{(2n+1)^4\pi^4} \right) \exp\left[-(2n+1)(1-r)\pi/\bar{\theta}_o\right] \right] \sin(2n+1)\pi\theta$$

$$\left. + \frac{4}{\pi^2} \sum_1^\infty \left[\left(\frac{23.9\bar{\theta}_o}{(2n\pi)^2} \right) \exp\left[-2n(1-r)\pi/\bar{\theta}_o\right] \right] \sin 2n\pi\theta \right\} \qquad \text{(IV-30)}$$

The velocity component in the $\bar{r}$ direction is

$$-\frac{1}{\bar{r}} \frac{\partial \bar{\psi}}{\partial \bar{\theta}} = -\bar{\omega}_r \bar{r}_o \bar{\theta}_o \left\{ \frac{r}{2}(2\theta - 1) + \frac{4}{\pi^2} \sum_0^\infty \frac{1}{r} \left[\frac{\exp\left[-(2n+1)(1-r)\pi/\bar{\theta}_o\right]}{(2n+1)^2} \right] \cos(2n+1)\pi\theta \right.$$

$$+ \frac{4}{\pi^2} \sum_0^\infty \frac{1}{r} \left[\left(-\frac{(1-r)^2\pi}{2(2n+1)\bar{\theta}_o} + \frac{7.4\bar{\theta}_o}{(2n+1)^2\pi^2} \right.\right.$$

$$\left.\left. + \frac{36\bar{\theta}_o}{(2n+1)^4\pi^4} \right) \exp\left[-(2n+1)(1-r)\pi/\bar{\theta}_o\right] \right] \cos(2n+1)\pi\theta$$

$$\left. + \frac{4}{\pi^2} \sum_1^\infty \frac{1}{r} \left[\left(\frac{23.9\bar{\theta}_o}{(2n\pi)^2} \right) \exp\left[-2n(1-r)\pi/\bar{\theta}_o\right] \right] \cos 2n\pi\theta \right\} \qquad \text{(IV-31)}$$

From the boundary condition specified by equation (IV-15c) it has been shown that the higher-order terms involve the radial derivatives of $\chi_1(r^*, \theta)$, which are

represented by infinite series. For reasons already mentioned these infinite-series representations are approximated by polynomials in θ. If these polynomial approximations are to be fairly accurate at every point, it is necessary to ensure that the original series be uniformly convergent. Since $\chi_{1r^*r^*}$ evaluated at $r^* = 0$ has the following series expression

$$\chi_{1r^*r^*}(0, \theta) = \frac{4}{\pi} \sum_{0}^{\infty} \frac{1}{(2n+1)} \sin(2n+1)\pi\theta$$

then $\chi_{1r^*r^*}(0, \theta) = 1 \qquad 0 < \theta < 1$

but if θ is set equal to zero or one, the series gives

$$\chi_{1r^*r^*}(0, 0) = \chi_{1r^*r^*}(0, 1) = 0$$

Obviously the series expansion of $\chi_{1r^*r^*}(0, \theta)$ does not converge uniformly at $\theta = 0$ and $\theta = 1$. For the third or higher order radial derivatives of χ_1, the resulting series expressions evaluated at $r^* = 0$ are no longer convergent series. Therefore the approximate polynomial representation of the boundary condition can only be applied to $\chi_{1r^*}(0, \theta)$ with sufficient accuracy.

V

BASE BOUNDARY LAYER

1. Formulation

As the wake Reynolds number approaches infinity, for a first approximation the recirculation region can be divided into the inviscid core flow and the viscous-layer flow. Since the wake Mach number is small, the recirculating flow may be regarded as incompressible. The inviscid core flow has already been studied in (IV). The viscous layers enclosing the inviscid core flow form a thin continuous layer for large Reynolds number. In order to obtain an approximate solution, it is necessary to break up this continuous layer into separate sections which may be solved approximately. These sections are the shear layer which separates the external flow from the recirculating flow; the base boundary layer along the base of the wedge; and, as mentioned by Batchelor[23], the viscous layer along the wake center line between the upper recirculating flow and the lower recirculating flow (which will not be studied here).

In studying the base boundary layer near the wake center line, the velocity distribution of the flow impinging on the base may be approximated by the velocity of the inviscid core flow, because as the Reynolds number grows the viscous layer along the wake center line becomes thinner, and because the velocity gradient across this layer decreases as the fluid moves toward the base. In the vicinity of the stagnation point at the center of the base, the velocity components

parallel and perpendicular to the base for the inviscid core flow are linear functions of the distance from the wake center line and the distance from the base of the wedge respectively. This type of flow is therefore a two-dimensional stagnation-point flow for which the solution is known[33, 34]. The pressure in the inviscid core flow is given by the Bernoulli's equation for rotational flow. For the stagnation-point viscous-layer flow the component of the momentum equation in the direction parallel to the base is independent of the component normal to the base, and is the same as the boundary-layer equation for incompressible flow. Since the base is flat and the boundary-layer assumptions are satisfied in the viscous layer everywhere along the base except very near the stagnation point or the point of separation just below the corner, the governing differential equations for this layer are identical to the flat-plate boundary-layer equations for incompressible flow:

$$\frac{\partial \bar{U}}{\partial \bar{X}} + \frac{\partial \bar{V}}{\partial \bar{Y}} = 0 \qquad \text{(V-1)}$$

$$\bar{U}\frac{\partial \bar{U}}{\partial \bar{X}} + \bar{V}\frac{\partial \bar{U}}{\partial \bar{Y}} = \bar{q}_b \frac{d\bar{q}_b}{d\bar{X}} + \bar{\nu}\frac{\partial^2 \bar{U}}{\partial \bar{Y}^2} \qquad \text{(V-2)}$$

where $\bar{U}$, $\bar{V}$ are velocity components parallel and perpendicular to the base respectively; $\bar{X}$, $\bar{Y}$ are the coordinates parallel and perpendicular to the base, and are measured from the wake center line and the base of the wedge respectively; and $\bar{q}_b$ is the velocity in the inviscid core flow evaluated at the base. Because

the no-slip condition must be satisfied at the base, and the flow velocity at the outer edge of the viscous layer approaches the inviscid-flow velocity evaluated at the base, the boundary conditions can be written as

$$\bar{U} = \bar{V} = 0 \qquad \text{at } \bar{Y} = 0$$

$$\bar{U} = \bar{q}_b \qquad \text{at the outer edge of viscous layer}$$

(V-3)

This system of governing differential equations for a plane, incompressible, laminar boundary layer may be transformed by introducing the appropriate form of the Dorodnitsyn variables[35], ;

$$X = \frac{1}{\bar{q}_r \bar{L}_r} \int_0^{\bar{X}} \bar{q}_b \, d\bar{X} \; ; \qquad Y = \frac{\sqrt{Re_r}}{\bar{L}_r \bar{q}_r} \bar{q}_b \bar{Y}$$

$$U = \frac{\bar{U}}{\bar{q}_b} \; ; \quad W = \left(\frac{\bar{V}}{\bar{q}_b} + \frac{1}{\bar{q}_b} \frac{d\bar{q}_b}{d\bar{X}} \bar{Y} \frac{\bar{U}}{\bar{q}_b} \right) \sqrt{Re_r}$$

One then obtains

$$\frac{\partial U}{\partial X} + \frac{\partial W}{\partial Y} = 0 \qquad \text{(V-4)}$$

$$U \frac{\partial U}{\partial X} + W \frac{\partial U}{\partial Y} = \frac{\dot{q}_b}{q_b} (1-U^2) + \frac{\partial^2 U}{\partial Y^2} \qquad \text{(V-5)}$$

where $\dot{q}_b = \frac{dq_b}{d\bar{X}}$. The boundary conditions are transformed to

$$U = W = 0 \qquad \text{at } Y = 0$$

$$U \to 1 \qquad \text{as } Y \to \infty$$

Hence in the Dorodnitsyn variables the boundary conditions are normalized.

The method of integral relations[35] is employed to solve the system of transformed boundary-layer equations. This method converts the system of partial differential equations into a system of ordinary differential equations and permits the use of well-developed numerical methods of solution of ordinary differential equations. In order to apply the method of integral relations, the system of partial differention equations is integrated across the layer, after multiplication by appropriate weighting functions. Hence the partial derivatives with respect to one variable are eliminated, and in the resulting ordinary differential equations there appear only integrals of functions of the dependent variables. These functions are approximated by suitable interpolation formulas.

2. Integral Relations

To obtain the integral relations for the system of transformed equations[35], equation (V-4) is multiplied by a weighting function F(U) which approaches zero sufficiently rapidly as $Y \rightarrow \infty$, equation (V-5) is multiplied by $\frac{dF(U)}{dU}$, and the resulting equations are added:

$$\frac{\partial}{\partial X}\left[UF(U)\right] + \frac{\partial}{\partial Y}\left[WF(U)\right] = \frac{\dot{q}_b}{q_b}\frac{dF(U)}{dU}(1-U^2) + \frac{dF(U)}{dU}\frac{\partial^2 U}{\partial Y^2} \qquad \text{(V-6)}$$

After integrating the above equation with respect to Y from 0 to ∞, one obtains the integral relation

$$\frac{d}{dX}\int_0^\infty U\,F(U)\,dY = \frac{\dot{q}_b}{q_b}\int_0^\infty \frac{dF(U)}{dU}(1-U^2) - \frac{dF(U)}{dU}\,\frac{\partial U}{\partial Y}\Big|_{Y=0}$$

$$-\int_0^\infty \frac{d^2F(U)}{dU^2}\left(\frac{\partial U}{\partial Y}\right)^2 dY \qquad (V\text{-}7)$$

This equation is rewritten in terms of the quantities

$$\Theta = \left(\frac{\partial U}{\partial Y}\right)^{-1} \qquad \text{and} \qquad \Theta_0 = \left(\frac{\partial U}{\partial Y}\right)^{-1}\Big|_{Y=0} \qquad (V\text{-}8)$$

Changing the variable of integration from Y to U then gives

$$\frac{d}{dX}\int_0^1 \Theta\,U F(U)\,dU = \frac{\dot{q}_b}{q_b}\int_0^1 \Theta\frac{dF(U)}{dU}(1-U^2)dU - \frac{1}{\Theta_0}\,\frac{dF(U)}{dU}\Big|_{U=0}$$

$$-\int_0^1 \frac{1}{\Theta}\,\frac{d^2F(U)}{dU^2}\,dU \qquad (V\text{-}9)$$

It is clear that Θ approaches infinity as $U \to 1$. From the Blasius solution for a flat-plate boundary layer with no pressure gradient, evaluated as the similarity variable approaches infinity[34], one obtains a singularity of the form[27]

$$\Theta = \left(\frac{\partial U}{\partial Y}\right)^{-1} \sim \text{constant}\,\frac{1}{(1-U)}\left[-\log(1-U)\right]^{-\frac{1}{2}} \qquad \text{as } Y \to \infty$$

In most previous applications of the method, this form is simplified by omitting

the logarithmic factor and so, for $U \to 1$, θ is approximated by

$$\Theta = O[(1-U)^{-1}] \qquad \text{as } U \to 1$$

If the same behavior is assumed in the present case, then an obvious simple choice for the weighting functions is

$$F_{K,I}(U) = (1-U)^I \qquad \text{(V-10)}$$

As in other applications, the functions Θ and $1/\Theta$ in the Kth approximation are represented by the following expressions

$$\Theta = \frac{1}{(1-U)} (A_0 + A_1 U + \ldots + A_{K-1} U^{K-1}) \qquad \text{(V-11)}$$

$$\Theta^{-1} = (1-U)(B_0 + B_1 U + \ldots + B_{K-1} U^{K-1}) \qquad \text{(V-12)}$$

The coefficients $A_0, A_1, \ldots; B_0, B_1 \ldots$ are functions of X and are related by the condition that for

$$U = U_J = \frac{J}{K}$$

where $J = 0, 1, 2, \ldots, K-1$, the representation of Θ and Θ^{-1} should be consistent:

$$\left(A_0 + A_1 U_J + \ldots + A_{K-1} U_J^{K-1}\right) = \left(B_0 + B_1 U_J + \ldots + B_{K-1} U_J^{K-1}\right)^{-1} \tag{V-13}$$

When K = 1 the approximate expressions for Θ and Θ^{-1} are

$$\Theta = \frac{\Theta_0(X)}{1-U} \quad , \quad \Theta^{-1} = \Theta_0^{-1}(X)(1-U) \tag{V-14}$$

if

$$F_1(U) = (1-U) \quad , \quad \frac{dF_1(U)}{dU} = -1 \quad , \quad \frac{d^2F_1(U)}{dU^2} = 0 \tag{V-15}$$

then equation (V-9) becomes

$$\frac{d}{dX}\int_0^1 U\Theta_0\, dU = -\frac{\dot{q}_b}{q_b}\int_0^1 (1+U)\Theta_0\, dU + \frac{1}{\Theta_0}$$

The resulting approximate differential equation is

$$\frac{d\Theta_0}{dX} + 3\frac{\dot{q}_b}{q_b}\Theta_0 = \frac{2}{\Theta_0} \tag{V-16}$$

which may be integrated directly. The solution can be written as

$$\Theta_0 = \frac{2}{3q_b}\left[\int_0^X q_b^6\, dX\right]^{\frac{1}{2}} \tag{V-17}$$

Substituting equations (V-14) and (V-17) into equation (V-8) and rearranging, one obtains

$$\frac{\partial U}{\partial Y} = (1-U)\, q_b^3 \left\{ 2\left[\int_0^X q_b^6\, dX \right]^{\frac{1}{2}} \right\}^{-1} \qquad \text{(V-18)}$$

Integrating the above equation with respect to Y for fixed X, there results

$$U = 1 - \exp\left\{ - \frac{q_b^3\, Y}{\left[2\left(\int_0^X q_b^6\, dX \right)^{\frac{1}{2}} \right]} \right\} \qquad \text{(V-19)}$$

From the solution of the inviscid core flow the velocity component in the $\bar{\theta}$ direction is $\frac{\partial \bar{\psi}}{\partial r}$ and is given by equation (IV-30). In nondimensional form it can be written as:

$$\begin{aligned} \frac{1}{\bar{q}_r}\frac{\partial \bar{\psi}}{\partial \bar{r}} = {} & 2r\bar{\theta}_o(\theta^2 - \theta) + \frac{8}{\pi^2}\sum_0^\infty \left[\frac{\exp\left[-(2n+1)(1-r)\pi/\bar{\theta}_o \right]}{(2n+1)^2} \right] \sin(2n+1)\pi\theta \\ & + \frac{8}{\pi^2}\sum_0^\infty \left\{ \left[\frac{(1-r)\pi}{(2n+1)^2} - \frac{(1-r)^2\pi}{2(2n+1)\bar{\theta}_o} + \frac{7.4\bar{\theta}_o}{(2n+1)^2\pi^2} \right. \right. \\ & \left. \left. + \frac{36\bar{\theta}_o}{(2n+1)^4\pi^4} \right] \exp\left[-(2n+1)(1-r)\pi/\bar{\theta}_o \right] \right\} \sin(2n+1)\pi\theta \\ & + \frac{8}{\pi^2}\sum_1^\infty \left\{ \left[\frac{23.9\bar{\theta}_o}{(2n\pi)^2} \right] \exp\left[-2n(1-r)\pi/\bar{\theta}_o \right] \right\} \sin 2n\pi\theta \end{aligned} \qquad \text{(V-20)}$$

The velocity of the inviscid core flow along the base can be evaluated by setting $r = 1 - \bar{\theta}_o^2(1-\theta^2)/2$, and is given by the expression

$$q_b = 2\bar{\theta}_o(\theta^2 - \theta) + \frac{8}{\pi^2}\sum_0^\infty\left[\frac{1}{(2n+1)^2}\right]\sin(2n+1)\pi\theta$$

$$+ \frac{8}{\pi^2}\sum_0^\infty\left[\frac{7.4\bar{\theta}_o}{(2n+1)^2\pi^2} + \frac{36\bar{\theta}_o}{(2n+1)^4\pi^4} - \frac{\pi\bar{\theta}_o}{2(2n+1)}\right]\sin(2n+1)\pi\theta$$

$$+ \frac{8}{\pi^2}\sum_1^\infty\left[\frac{23.9\bar{\theta}_o}{(2n\pi)^2}\right]\sin 2n\pi\theta \qquad \text{(V-21)}$$

For $\bar{\theta}_o$ sufficiently small, $\bar{X}$ can be approximated by $\bar{r}_o\,\bar{\theta}$. Since also $\bar{r}_o\,\bar{\theta}_o \cong \bar{L}_r$,

$$X = \int_0^{\frac{\bar{X}}{\bar{L}_r}} q_b\, d\left(\frac{\bar{X}}{\bar{L}_r}\right)$$

$$= \int_0^\theta q_b\, d\theta \qquad \text{(V-22)}$$

Since $\bar{\theta}_o$ is small, $\bar{Y} \cong \bar{r}_o - \bar{r}$. Then

$$Y = \frac{\sqrt{Re_r}}{\bar{r}_o\,\bar{\theta}_o}\, q_b(\bar{r}_o - \bar{r})$$

$$= \frac{\sqrt{Re_r}}{\bar{\theta}_o}\, q_b(1-r) \qquad \text{(V-23)}$$

From equations (V-19) through (V-23), the solution for U can be written as:

$$\bar{U} = 1 - \exp\left\{\left[-\frac{\sqrt{Re_r}}{\bar{\theta}_o}(1-r)\,q_b^4\right]\left[\int_0^\theta q_b^7\, d\theta\right]^{-\frac{1}{2}}\right\} \qquad \text{(V-24)}$$

When K = 2 the approximate expressions for Θ and Θ^{-1} are

$$\Theta = \frac{1}{(1-U)} \left[\Theta_0(1-2U) + \Theta_1 U \right] \qquad \text{(V-25a)}$$

$$\Theta^{-1} = (1-U) \left[\frac{1}{\Theta_0} (1-2U) + \frac{1}{\Theta_1} 4U \right] \qquad \text{(V-25b)}$$

If

$$F_1 = (1-U), \quad \frac{dF_1(U)}{dU} = -1, \quad \frac{d^2F_1(U)}{dU^2} = 0 \qquad \text{(V-26a)}$$

$$F_2 = (1-U)^2, \quad \frac{dF_2(U)}{dU} = -2(1-U), \quad \frac{d^2F_2(U)}{dU^2} = 2 \qquad \text{(V-26b)}$$

then equation (V-9) becomes

$$\frac{d}{dX} \int_0^1 U \left[\Theta_0(1-2U) + \Theta_1 U \right] dU$$

$$= -\frac{\dot{q}_b}{q_b} \int_0^1 (1+U) \left[\Theta_0(1-2U) + \Theta_1 U \right] dU + \frac{1}{\Theta_0} \qquad \text{(V-27)}$$

$$\frac{d}{dX} \int_0^1 U(1-U) \left[\Theta_0(1-2U) + \Theta_1 U \right] dU$$

$$= -\frac{2\dot{q}_b}{q_b} \int_0^1 (1-U^2) \left[\Theta_0(1-2U) + \Theta_1 U \right] dU$$

$$+ \frac{2}{\Theta_0} - 2 \int_0^1 (1-U) \left[\frac{1-2U}{\Theta_0} + \frac{4U}{\Theta_1} \right] dU \qquad \text{(V-28)}$$

The resulting approximate system of differential equations is

$$\frac{d\Theta_0}{dX} = -\frac{\dot{q}_b}{q_b}(9\Theta_0 + 7\Theta_1) + \frac{34}{\Theta_0} - \frac{32}{\Theta_1} \qquad \text{(V-29)}$$

$$\frac{d\Theta_1}{dX} = \frac{\dot{q}_b}{q_b}(4\Theta_0 + 6\Theta_1) + \frac{20}{\Theta_0} - \frac{16}{\Theta_1} \qquad \text{(V-30)}$$

Since q_b and $\dot{q}_b$ can be obtained from the solution for the inviscid core flow evaluated at the base of the wedge, the above systems of ordinary differential equations can be integrated numerically to give $\Theta_0(X)$ and $\Theta_1(X)$, provided that the initial conditions can be obtained. Since the first of equations (V-25) can be rewritten as

$$dY = \left[(\Theta_1 - 2\Theta_0)\left(\frac{U}{1-U}\right) + \Theta_0\left(\frac{1}{1-U}\right)\right] dU \qquad \text{(V-31)}$$

then for **X** fixed the above equation can be integrated to give

$$Y = -(\Theta_1 - \Theta_0)\ln(1-U) - (\Theta_1 - 2\Theta_0)U \qquad \text{(V-32)}$$

In order to provide initial conditions for the systems of approximate equations, it is necessary to examine the behavior of these equations near the wake center line. For θ sufficiently small the velocity of the inviscid core flow along the base, given by equation (V-21), possesses a power-series expansion in

θ and has the following form:

$$q_b = C_1\theta + C_2\theta^2 + \cdots\cdots$$

$$\cong C_1\theta \qquad \text{for } \theta \text{ very small}$$

Hence from equation (V-22)

$$X \cong \tfrac{1}{2}C_1\theta^2;\ q_b \cong \sqrt{2C_1X} \qquad \text{(V-33)}$$

$$\frac{\dot{q}_b}{q_b} \cong \frac{1}{2X} \qquad \text{for } \theta \text{ very small} \qquad \text{(V-34)}$$

For this value of $\dot{q}_b/q_b$, the approximate system of differential equations, which possesses a singularity at $X = 0$, can be shown to yield an exact solution of the form

$$\Theta_I = D_I\sqrt{X} \qquad \text{for } X \ll 1 \qquad \text{(V-35)}$$

The constants D_I are determined by the solutions of the algebraic equations which are obtained by substituting equation (V-35) into the original approximate system of differential equations. For $K = 1$, then

$$\Theta_0 = D_0\sqrt{X}$$

$$D_0 = 1 \; ; \; \Theta_0 = \sqrt{X} \qquad \text{for } X \ll 1 \qquad \text{(V-36)}$$

For K = 2, then

$$\Theta_0 = D_0\sqrt{X} \; ; \; \Theta_1 = D_1\sqrt{X}$$

$$10D_0 + 7D_1 = \frac{68}{D_0} - \frac{64}{D_1} \qquad \text{(V-37)}$$

$$4D_0 + 7D_1 = \frac{40}{D_0} - \frac{32}{D_1} \qquad \text{(V-38)}$$

Solving the above system of algebraic equations, one obtains

$$D_0 = 1.147 \; ; \; D_1 = 1.822$$

$$\Theta_0 = 1.147\sqrt{X} \; ; \; \Theta_1 = 1.822\sqrt{X} \quad \text{for } X \ll 1 \qquad \text{(V-39)}$$

The solution given by equation (V-39) provides the initial values for the quantities Θ_0 and Θ_1, if evaluated at very small X. Numerical integration of the systems of ordinary differential equations can now be carried out.

VI

LAMINAR FREE SHEAR LAYER

1. General Description and Formulation

The simplified model of the shear-layer flow, which retains the main physical features of the exact flow, is described here. The inviscid supersonic flow expands at the trailing edge of the wedge through a centered Prandtl-Meyer expansion fan to the base pressure. The boundary-layer flow along the wedge surface separates at the trailing edge of the wedge and expands isentropically to the base pressure in a very short distance. Subsequently it mixes under nearly constant pressure with the relatively low-speed recirculating flow. The expanded boundary-layer velocity profile forms the upper part of the initial velocity profile of the shear layer. The remaining part of the initial velocity profile is given approximately by the similarity profile obtained by assuming a mixing between a uniform stream, with velocity equal to the velocity at the inner edge of the expanded boundary layer, and a stagnant region. The velocity in this portion of the profile is evaluated at a very small distance from the trailing edge of the wedge. Near the dividing streamline, which separates the recirculating flow from the expanded boundary layer, the velocity gradient is considerably larger than the velocity gradient in the remaining part of the profile, over the entire length of the shear layer. The thickness of the shear layer is of higher order than $\bar{r}_o$, and the curvature of the dividing streamline is small except near the stagnation points.

From the description of the simplified shear-layer model, the relative orders of magnitude of individual terms in the Navier-Stokes equations are estimated in the same manner as in the derivation of the boundary-layer equations. For the two-dimensional case the resulting differential equations are identical to the flat-plate boundary-layer equations with pressure gradient:

$$\frac{\partial \bar{\rho}\bar{u}}{\partial \bar{x}} + \frac{\partial \bar{\rho}\bar{v}}{\partial \bar{y}} = 0 \qquad \text{(VI-1)}$$

$$\bar{\rho}\bar{u}\frac{\partial \bar{u}}{\partial \bar{x}} + \bar{\rho}\bar{v}\frac{\partial \bar{u}}{\partial \bar{y}} = -\frac{d\bar{p}}{d\bar{x}} + \frac{\partial}{\partial \bar{y}}\left(\bar{\mu}\frac{\partial \bar{u}}{\partial \bar{y}}\right) \qquad \text{(VI-2)}$$

$$\bar{\rho}\bar{u}\frac{\partial \bar{h}}{\partial \bar{x}} + \bar{\rho}\bar{v}\frac{\partial \bar{h}}{\partial \bar{y}} = \bar{u}\frac{d\bar{p}}{d\bar{x}} + \frac{\partial}{\partial \bar{y}}\left(\bar{k}\frac{\partial \bar{T}}{\partial \bar{y}}\right) + \bar{\mu}\left(\frac{\partial \bar{u}}{\partial \bar{y}}\right)^2 \qquad \text{(VI-3)}$$

where $\bar{x}$ is measured along the dividing streamline and $\bar{y}$ is measured normal to the dividing streamline. The dividing streamline is really slightly curved, but the curvature affects only the higher approximations to the equations for the mixing region. To simplify the problem further, it is assumed that $\bar{\rho}\bar{\mu}$ is constant across the shear layer and $Pr = \frac{\bar{c}_p \bar{\mu}}{\bar{k}}$ is equal to unity. The stream function $\bar{\psi}$ is defined in the usual manner by

$$\bar{\rho}\bar{u} = \bar{\rho}_e \frac{\partial \bar{\psi}}{\partial \bar{y}} \qquad \bar{\rho}\bar{v} = -\bar{\rho}_e \frac{\partial \bar{\psi}}{\partial \bar{x}}$$

and a modified Howarth transformation[34] is introduced as follows:

$$\tilde{\rho} = \frac{\bar{\rho}}{\bar{\rho}_e} \; ; \; \tilde{T} = \frac{\bar{T}}{\bar{T}_e} \; ; \; \tilde{p} = \frac{\bar{p}}{\bar{\rho}_e \bar{u}_e^2} \; ; \; \tilde{h} = \frac{\bar{h}}{\bar{u}_e^2} \; ; \; \tilde{H} = \frac{\bar{H}}{\bar{u}_e^2}$$

$$\tilde{\psi} = \frac{\bar{\psi} Re_e^{\frac{1}{2}}}{(\bar{u}_e \bar{r}_o)} \; ; \; \tilde{u} = \frac{\bar{u}}{\bar{u}_e} = \frac{\partial \tilde{\psi}}{\partial \tilde{y}} \; ; \; \tilde{v} = \frac{Re_e^{\frac{1}{2}}}{\bar{u}_e} \; \tilde{\rho} \tilde{v} = - \frac{\partial \tilde{\psi}}{\partial \tilde{x}}$$

$$\tilde{x} = \frac{\bar{x}}{\bar{r}_o} \; ; \; \tilde{y} = \frac{Re_e^{\frac{1}{2}}}{\bar{r}_o} \int_0^{\bar{y}} \tilde{\rho} \, d\bar{y}$$

When this transformation is applied to equations (VI-1), (VI-2) and (VI-3), there results a system of equations similar in form to the incompressible boundary-layer equations:

$$\frac{\partial \tilde{u}}{\partial \tilde{x}} + \frac{\partial \tilde{v}}{\partial \tilde{y}} = 0 \qquad \text{(VI-4)}$$

$$\tilde{u} \frac{\partial \tilde{u}}{\partial \tilde{x}} + \tilde{v} \frac{\partial \tilde{u}}{\partial \tilde{y}} = - \frac{1}{\tilde{\rho}} \frac{d\tilde{p}}{d\tilde{x}} + \frac{\partial^2 \tilde{u}}{\partial \tilde{y}^2} \qquad \text{(VI-5)}$$

$$\tilde{u} \frac{\partial \tilde{h}}{\partial \tilde{x}} + \tilde{v} \frac{\partial \tilde{h}}{\partial \tilde{y}} = \frac{\tilde{\partial}^2 \tilde{h}}{\partial \tilde{y}^2} + \left(\frac{\partial \tilde{u}}{\partial \tilde{y}} \right)^2 + \frac{1}{\tilde{\rho}} \tilde{u} \frac{d\tilde{p}}{dx} \qquad \text{(VI-6)}$$

Assuming that $\tilde{H}$ = constant in the initial profile, a solution of equation (VI-6) is

$$\tilde{h} = \tilde{H} - \frac{\tilde{u}^2}{2} \qquad \text{(VI-7)}$$

which reduces equation (VI-6) to (VI-5). This result implies that the energy

equation is automatically satisfied once the momentum equation is satified. The density in the shear layer can be written as:

$$\tilde{\rho} = \left(\frac{\tilde{p}}{p_e}\right)\left[(\gamma-1)M_e^2\left(\tilde{H} - \frac{\tilde{u}^2}{2}\right)\right]^{-1}$$

Since $\bar{p}_e$ has been defined as the pressure immediately after the corner expansion has been completed, the Bernoulli equation for the boundary $\bar{\theta} = \bar{\theta}_o$ of the inviscid core flow can be written as

$$\bar{p}_e = \bar{p} + \tfrac{1}{2}\bar{\rho}_r \bar{q}_r^2 q_s^2$$

or

$$\tilde{p} = \frac{1}{\gamma M_e^2} - \tfrac{1}{2}\tilde{\rho}_r\left(\frac{\bar{q}_r}{\bar{u}_e}\right)^2 q_s^2$$

where q_s is the nondimensional velocity of the inviscid core flow evaluated at $\bar{\theta} = \bar{\theta}_o$. Hence the density in the shear layer can be rewritten as

$$\tilde{\rho} = \left[\frac{(1 - \frac{\gamma}{2}M_r^2 q_s^2)}{(\gamma-1)M_e^2(\tilde{H} - \frac{\tilde{u}^2}{2})}\right] \qquad \text{(VI-8)}$$

The momentum equation (VI-5) is therefore independent of the energy equation (VI-6).

An integral method of the Kármán-Pohlhausen[33, 34] type is applied to analyze the shear layer, because it is simple and permits the treatment of the

case when the shear layer is not thin and has non-zero inner-edge velocity. This method involves approximation by polynomials with undetermined coefficients for the velocity profiles. The boundary conditions, continuity conditions, integrals of the momentum equation, momentum equation along the dividing streamline, and momentum equation along the inner edge of the outer shear layer yield a sufficient number of conditions for the complete determination of the profile coefficients and thicknesses.

2. Velocity Profile

The shear layer will be divided into an outer shear layer and a shear sublayer. The outer shear layer is the portion of the shear layer where the kinetic energy of the fluid is large and the velocity gradient is not too large. The initial velocity profile is determined by the boundary-layer velocity profile after the corner expansion. This portion of the shear layer grows into the inviscid high-speed outer flow, and flows downstream of the rear stagnation point to consitute a part of the far wake. The shear sublayer is the portion of the shear layer with larger velocity gradient, in the vicinity of the dividing streamline. The sublayer flow above the dividing streamline diffuses into the outer shear layer and flows downstream of the rear stagnation point forming a part of the far wake. The sublayer flow below the dividing streamline grows into the relatively low-speed inviscid recirculating flow, and in the vicinity of the rear stagnation point it turns back toward the base of the wedge. The initial velocity profile for the shear sublayer is given by the similarity profile resulting

from the mixing of a uniform flow with fluid at rest.

Obviously the velocity profile has different character in the different parts of the shear layer and the dominant factors influencing the change of velocity profile are not the same. Hence it is difficult to describe the shear-layer velocity profile as a whole by a single expression. In the study of mixing between a separated boundary-layer flow and a fluid at rest, Kubota and Dewey[36] represent the shear-layer velocity profile by two polynomials, one used above and one below the dividing streamline, because the initial velocity profile is noticeably different from the subsequent profiles. Similarly the shear layer discussed here will be divided into three layers, two above and one below the dividing streamline. They are the outer shear layer, the upper shear sublayer, and the lower shear sublayer. Each layer is represented by a polynomial with undetermined coefficients as functions of the coordinate measured along the dividing streamline.

Since the velocity profile for the shear-layer flow always possesses an inflection point, a polynomial of at least third degree must be employed to represent the portion of the velocity profile where the inflection point is most likely to occur[37]. It is known that there is no point of inflection in the initial velocity profile for the outer shear layer. Since the small pressure variation induced by the recirculating flow and the relatively small viscous force have little effect on the outer shear layer flow where the kinetic energy is very large, the point of inflection will occur in the shear sublayer.

For simplicity the outer shear layer may be approximately represented by a second-degree polynomial. To achieve sufficient accuracy where the velocity gradients are large, the shear sublayers are represented by fourth-degree polynomials. The velocity profile for the outer shear layer is expressed as

$$\tilde{u} = \tilde{g}(\tilde{\zeta}) = a_0 + a_1\tilde{\zeta} + a_2\tilde{\zeta}^2 \qquad \text{(VI-9)}$$

where $\tilde{\zeta} = \frac{\tilde{y}}{\tilde{\delta}} - \tilde{\zeta}_0$ and $\tilde{\delta}$ is the thickness of the outer shear layer. It is convenient to introduce the quantity $\tilde{\zeta}_0$ because of the small displacement effect of the shear sublayer. It will be shown in section 5 that $\tilde{\zeta}_0$ should be taken to equal $\tilde{\delta}^*_{(+)}/\tilde{\delta}$, where $\tilde{\delta}^*_{(+)}$ is the displacement thickness of the upper shear sublayer measured in terms of the $\tilde{y}$ coordinate. The upper shear sublayer is represented by

$$\frac{\tilde{u}}{\tilde{g}(0)} = \tilde{g}_{(+)}\left(\tilde{\zeta}_{(+)}\right) = \sum_0^4 b_n \tilde{\zeta}^n_{(+)} \qquad \text{(VI-10)}$$

where $\tilde{\zeta}_{(+)} = \frac{\tilde{y}}{\tilde{\delta}_{(+)}}$ and $\tilde{\delta}_{(+)}$ is the thickness of the upper shear sublayer. The lower shear sublayer is represented by

$$\frac{\tilde{u}}{\tilde{g}(0)} = \tilde{g}_{(-)}\left(\tilde{\zeta}_{(-)}\right) = \sum_0^4 c_n \tilde{\zeta}^n_{(-)} \qquad \text{(VI-11)}$$

where $\tilde{\zeta}_{(-)} = \frac{\tilde{y}}{\tilde{\delta}_{(-)}}$ and $\tilde{\delta}_{(-)}$ is the thickness of the lower shear sublayer.

The profile coefficients a_0, a_1, a_2, b_0, b_1, b_2, b_3, b_4, c_0, c_1, c_2, c_3, c_4, and the layer thicknesses $\tilde{\delta}$, $\tilde{\delta}_{(+)}$, $\tilde{\delta}_{(-)}$ are all functions of $\tilde{x}$. They are determined by the boundary conditions at the inner and outer edges of the shear layer, the continuity conditions between the layers, and appropriate differential equations.

Since at the outer and inner edges of the shear layer the velocity must be continuous and the first derivative of velocity with respect to $\tilde{y}$ must be zero (in the approximation of boundary-layer theory), the boundary conditions are

$$\tilde{g}(1) = 1 \qquad \text{(VI-12a)}$$

$$\frac{\partial \tilde{g}}{\partial \zeta}(1) = 0 \qquad \text{(VI-12b)}$$

and the boundary conditions at $\tilde{y} = -\tilde{\delta}_{(-)}$ are

$$\tilde{g}_{(-)}(-1) = \left(\frac{\bar{q}_r}{\bar{u}_e}\right)\left(\frac{q_s}{\tilde{g}(0)}\right) \qquad \text{(VI-13a)}$$

$$\frac{\partial \tilde{g}_{(-)}}{\partial \zeta_{(-)}}(-1) = 0 \qquad \text{(VI-13b)}$$

In order to have a smoother fit at the inner edge of the shear layer the second derivative of the velocity with respect to $\tilde{y}$ is also required to be zero. Hence an additional boundary condition at $\tilde{y} = \tilde{\delta}_{(-)}$ is

$$\frac{\partial^2 \tilde{g}_{(-)}}{\partial \tilde{\zeta}^2_{(-)}} = 0 \qquad \text{(VI-13c)}$$

For a reasonably smooth fit between the layers, the velocity and its first and second derivatives with respect to $\tilde{y}$ must be continuous. The continuity conditions at $\tilde{y} = 0$ are

$$\tilde{g}_{(+)}(0) = \tilde{g}_{(-)}(0) \qquad \text{(VI-14a)}$$

$$\frac{\partial \tilde{g}_{(+)}}{\partial \tilde{\zeta}_{(+)}}(0) = \left(\frac{\tilde{\delta}_{(+)}}{\tilde{\delta}_{(-)}}\right) \frac{\partial \tilde{g}_{(-)}}{\partial \tilde{\zeta}_{(-)}}(0) \qquad \text{(VI-14b)}$$

$$\frac{\partial^2 \tilde{g}_{(+)}}{\partial \tilde{\zeta}^2_{(+)}}(0) = \left(\frac{\tilde{\delta}_{(+)}}{\tilde{\delta}_{(-)}}\right)^2 \frac{\partial^2 \tilde{g}_{(-)}}{\partial \tilde{\zeta}^2_{(-)}}(0) \qquad \text{(VI-14c)}$$

It does not seem evident whether or not the shear sublayer will remain negligibly thin compared with the outer shear layer for the entire length of the shear layer. Therefore the conditions at the outer edge of the sublayer are not imposed at $\tilde{\zeta} = 0$ but at a presumably rather small positive value of $\tilde{\zeta}$. As will be shown later, through the requirement of equalization in pressure across the shear layer to order $Re_e^{-\frac{1}{2}}$, the dividing streamline must be displaced relative to the outer shear layer by an amount equal to the displacement thickness of the upper shear sublayer. Therefore the matching point between the upper shear sublayer and the outer shear layer is not at $\tilde{\zeta} = \frac{\tilde{\delta}_{(+)}}{\tilde{\delta}}$ but at $\tilde{\zeta} = \kappa \frac{\tilde{\delta}_{(+)}}{\tilde{\delta}}$,

where

$$\kappa = 1 - \frac{\tilde{\delta}^*_{(+)}}{\tilde{\delta}_{(+)}}$$

As noted previously, the coordinate $\tilde{y}$ is measured from the dividing streamline but $\tilde{\zeta}$ is defined by $\tilde{\zeta} = \frac{\tilde{y}}{\tilde{\delta}} - \tilde{\zeta}_0$. It will be shown in section 5 that $\tilde{\zeta}_0$ can be related to κ by $\tilde{\zeta}_0 = \frac{\tilde{\delta}_{(+)}}{\tilde{\delta}}(1 - \kappa) = \frac{\tilde{\delta}^*}{\tilde{\delta}}$.

Since the inner edge of the outer shear layer is not really at $\tilde{y} = 0$ and the upper shear sublayer is assumed rather thin, Taylor expansions about $\tilde{y} = 0$ for the outer shear layer may be used to provide approximate conditions at the matching-point. Therefore the continuity conditions between the upper shear sublayer and the outer shear layer can be approximated by

$$\tilde{g}_{(+)}(1) \cong \frac{1}{\tilde{g}(0)}\left[\tilde{g}(0) + \kappa\left(\frac{\tilde{\delta}_{(+)}}{\tilde{\delta}}\right)\frac{\partial \tilde{g}}{\partial \tilde{\zeta}}(0)\right] \qquad \text{(VI-15a)}$$

$$\frac{\partial \tilde{g}_{(+)}}{\partial \tilde{\zeta}_{(+)}}(1) \cong \frac{1}{\tilde{g}(0)}\left(\frac{\tilde{\delta}_{(+)}}{\tilde{\delta}}\right)\left[\frac{\partial \tilde{g}}{\partial \tilde{\zeta}}(0) + \kappa\left(\frac{\tilde{\delta}_{(+)}}{\tilde{\delta}}\right)\frac{\partial^2 \tilde{g}}{\partial \tilde{\zeta}^2}(0)\right] \qquad \text{(VI-15b)}$$

$$\frac{\partial^2 \tilde{g}_{(+)}}{\partial \tilde{\zeta}^2_{(+)}}(1) \cong \frac{1}{\tilde{g}(0)}\left(\frac{\tilde{\delta}_{(+)}}{\tilde{\delta}}\right)^2\left[\frac{\partial^2 \tilde{g}}{\partial \tilde{\zeta}^2}(0)\right] \qquad \text{(VI-15c)}$$

From the assumed form of the velocity profile given in this section, it is clear that an essential feature of the shear-layer analysis adopted here is the division of the shear layer into three parts. Since separate quartic profiles are

used to represent the velocity profiles in the upper and lower shear sublayer, and a quadratic profile is employed to express the outer shear layer, there are altogether sixteen unknown profile coefficients and thicknesses. The boundary and continuity conditions supply eleven relations among them. However, since the total number of relations must be equal to the number of unknown quantities appearing in the shear-layer velocity profile, five more relations are needed so that the velocity profile may be determined uniquely.

3. Momentum Integral Method

An integral method of the Kármán-Pohlhausen type is employed to furnish some of the remaining relations required for determining the unknown coefficients in the assumed representations for the velocity profile. Three relations may be obtained by taking the zeroth moment of the momentum equation for each of the three layers, i.e., by integrating the momentum equation over the thickness of each of the three layers.

In the derivation of an integral condition for the outer shear layer $\tilde{y}$ is temporarily replaced by $\tilde{y} + \tilde{\zeta}_0 \tilde{\delta}$ and $\tilde{v}$ is replaced by $\tilde{v} + \tilde{u}\, \tilde{\zeta}_0 \frac{d\tilde{\delta}}{d\tilde{x}}$. When expressed in these transformed variables, equation (VI-5) has the same form as before, and is to be integrated from 0 to $\tilde{\delta}$:

$$\int_0^{\tilde{\delta}} (\tilde{u}\, \tilde{u}_{\tilde{x}})\, d\tilde{y} + \int_0^{\tilde{\delta}} (\tilde{v}\, \tilde{u}_{\tilde{y}})\, d\tilde{y} = -\frac{d\tilde{p}}{d\tilde{x}} \int_0^{\tilde{\delta}} \frac{1}{\tilde{\rho}}\, d\tilde{y} + \int_0^{\tilde{\delta}} (\tilde{u}_{\tilde{y}\tilde{y}})\, d\tilde{y} \qquad \text{(VI-16)}$$

At the inner edge of the outer shear layer the new $\tilde{v}$ component of velocity is

very small, as shown in section 5, and is assumed to be zero. Then integration by parts, by using equation (VI-4), gives the following result:

$$\int_0^{\tilde{\delta}} \left(\tilde{v} \frac{\partial \tilde{u}}{\partial \tilde{y}} \right) d\tilde{y} = - \int_0^{\tilde{\delta}} \left(\frac{\partial \tilde{u}}{\partial \tilde{x}} \right) d\tilde{y} + \int_0^{\tilde{\delta}} \left(\tilde{u} \frac{\partial \tilde{u}}{\partial \tilde{x}} \right) d\tilde{y} \qquad \text{(VI-17)}$$

Substituting equation (VI-17) into equation (VI-16), there results

$$\int_0^{\tilde{\delta}} (\tilde{u}^2 - \tilde{u})_{\tilde{x}} \, d\tilde{y} = - \frac{d\tilde{p}}{d\tilde{x}} \int_0^{\tilde{\delta}} \frac{1}{\tilde{\rho}} \, d\tilde{y} + \frac{\partial \tilde{u}}{\partial \tilde{y}} \Big|_0^{\tilde{\delta}} \qquad \text{(VI-18)}$$

From equations (VI-9), (VI-12b) and (VI-18) the zeroth moment of the momentum equation for the outer shear layer can be written as

$$\frac{d}{d\tilde{x}} \left\{ \tilde{\delta} \int_0^1 \left[\tilde{g}^2 - \tilde{g} \right] d\tilde{\zeta} \right\} = - \frac{1}{\tilde{\delta}} \frac{\partial \tilde{g}}{\partial \tilde{\zeta}}(0) - \frac{d\tilde{p}}{d\tilde{x}} \tilde{\delta} \int_0^1 \frac{1}{\tilde{\rho}} d\tilde{\zeta} \qquad \text{(VI-19)}$$

By using equation (VI-8), $\tilde{p} = \tilde{p}(\tilde{x})$, and the Bernoulli's equation for the boundary $\bar{\theta} = \bar{\theta}_o$ of the inviscid core flow, equation (VI-19) is reduced to

$$\frac{d}{d\tilde{x}} \left\{ \tilde{\delta} \int_0^1 \left[\tilde{g}^2 - \tilde{g} \right] d\tilde{\zeta} \right\} = - \frac{1}{\tilde{\delta}} \frac{\partial \tilde{g}}{\partial \tilde{\zeta}}(0) + \left[\frac{(\gamma - 1) M_r^2 q_s \frac{dq_s}{d\tilde{x}} \tilde{\delta}}{1 - \frac{\gamma}{2} M_r^2 q_s^2} \right] \int_0^1 \left[\tilde{H} - \tfrac{1}{2} \tilde{g}^2 \right] d\tilde{\zeta} \qquad \text{(VI-20)}$$

For the upper shear sublayer, equation (VI-5) is integrated from 0 to $\tilde{\delta}_{(+)}$

$$\int_0^{\tilde{\delta}^{(+)}} (\tilde{u}\,\tilde{u}_{\tilde{x}})\,d\tilde{y} + \int_0^{\tilde{\delta}^{(+)}} (\tilde{v}\,\tilde{u}_{\tilde{y}})\,d\tilde{y}$$

$$= -\frac{d\tilde{p}}{d\tilde{x}} \int_0^{\tilde{\gamma}^{(+)}} \frac{1}{\tilde{\rho}}\,d\tilde{y} + \int_0^{\tilde{\delta}^{(+)}} (\tilde{u}_{\tilde{y}\tilde{y}})\,d\tilde{y} \qquad \text{(VI-21)}$$

where $\tilde{y}$ and $\tilde{v}$ are again measured relative to the dividing streamline. Since $\tilde{v} = 0$ along the dividing streamline, integration by parts, using equation (VI-4), gives the result

$$\int_0^{\tilde{\delta}^{(+)}} \left(\tilde{v}\,\frac{\partial \tilde{u}}{\partial \tilde{y}}\right) d\tilde{y} = -u_u \int_0^{\tilde{\delta}^{(+)}} \frac{\partial \tilde{u}}{\partial \tilde{x}}\,d\tilde{y} + \int_0^{\tilde{\delta}^{(+)}} \left(\tilde{u}\,\frac{\partial \tilde{u}}{\partial \tilde{x}}\right) d\tilde{y} \qquad \text{(VI-22)}$$

where $\tilde{u}_u$ is the velocity at the outer edge of the upper shear sublayer. Substituting equations (VI-8) and (VI-22) into equation (VI-21) and using Bernoulli's equation as before, then

$$\int_0^{\tilde{\delta}^{(+)}} \left[(\tilde{u}^2)_{\tilde{x}} - \tilde{u}_u\,\tilde{u}_{\tilde{x}}\right] d\tilde{y} = \frac{\partial \tilde{u}}{\partial \tilde{y}}\bigg|_0^{\tilde{\delta}^{(+)}}$$

$$+ \left[\frac{(\gamma-1) M_r^2 q_s \frac{dq_s}{d\tilde{x}}}{1 - \frac{\gamma}{2} M_r^2 q_s^2}\right] \int_0^{\tilde{\delta}^{(+)}} (\tilde{H} - \tfrac{1}{2}\tilde{u}^2)\,d\tilde{y} \qquad \text{(VI-23)}$$

which may be rewritten as

$$\int_0^{\tilde{\delta}^{(+)}} \left\{ \left[\left(\frac{\tilde{u}}{\tilde{g}(0)}\right)^2\right]_{\tilde{x}} - \left(\frac{\tilde{u}_u}{\tilde{g}(0)}\right)\left(\frac{\tilde{u}}{\tilde{g}(0)}\right)_{\tilde{x}} \right\} d\tilde{y} + \frac{1}{\tilde{g}(0)} \frac{d\tilde{g}}{d\tilde{x}} \int_0^{\tilde{\delta}^{(+)}} \left[2\left(\frac{\tilde{u}}{\tilde{g}(0)}\right)^2\right.$$

$$-\left(\frac{\tilde{u}_u}{\tilde{g}(0)}\right)\left(\frac{\tilde{u}}{\tilde{g}(0)}\right)\Bigg] d\tilde{y} = \frac{1}{\tilde{g}(0)} \frac{\lambda}{\partial \tilde{y}} \left(\frac{\tilde{u}}{\tilde{g}(0)}\right)\Bigg|_0^{\tilde{\delta}_{(+)}}$$

$$+ \left[\frac{(\gamma-1) M_r^2 \frac{dq_s}{d\tilde{x}} q_s}{1 - \frac{\gamma}{2} M_r^2 q_s^2}\right] \int_0^{\tilde{\delta}_{(+)}} \left[\frac{\tilde{H}}{\tilde{g}^2(0)} - \frac{1}{2}\left(\frac{\tilde{u}}{\tilde{g}(0)}\right)^2\right] d\tilde{y} \qquad \text{(VI-24)}$$

As implied by the definition (VI-9), $\tilde{g}(0)$ represents the approximate velocity profile for the outer shear layer evaluated at $\zeta = \frac{\tilde{y}}{\tilde{\delta}} = 0$, and is a function of $\tilde{x}$. From equations (VI-9), (VI-10), and (VI-24) and through the application of the Leibnitz rule, the zeroth moment of the momentum equation for the upper shear sublayer can be written as

$$\frac{d}{d\tilde{x}}\left(\tilde{\delta}_{(+)} \int_0^1 \tilde{g}^2_{(+)}\, d\zeta_{(+)}\right) - \tilde{g}_{(+)}(1) \frac{d}{d\tilde{x}}\left(\tilde{\delta}_{(+)} \int_0^1 \tilde{g}_{(+)}\, d\zeta_{(+)}\right)$$

$$= \left(-\frac{1}{\tilde{g}(0)} \frac{d\tilde{g}(0)}{d\tilde{x}}\right)\left\{\tilde{\delta}_{(+)} \int_0^1 \left[2\tilde{g}^2_{(+)} - \tilde{g}_{(+)}(1)\tilde{g}_{(+)}\right] d\zeta_{(+)}\right\} + \frac{1}{\tilde{\delta}_{(+)}\tilde{g}(0)} \frac{\partial \tilde{g}_{(+)}}{\partial \zeta_{(+)}}\Bigg|_0^1$$

$$+ \left[\frac{(\gamma-1) M_r^2 q_s \frac{dq_s}{d\tilde{x}} \tilde{\delta}_{(+)}}{1 - \frac{\gamma}{2} M_r^2 q_s^2}\right] \int_0^1 \left[\frac{\tilde{H}}{\tilde{g}^2(0)} - \frac{1}{2}\tilde{g}^2_{(+)}\right] d\zeta_{(+)} \qquad \text{(VI-25)}$$

For the lower shear sublayer, equation (VI-5) is integrated from $-\tilde{\delta}_{(-)}$ to 0:

$$\int_{-\tilde{\delta}_{(-)}}^0 (\tilde{u}\tilde{u}_{\tilde{x}})\, d\tilde{y} + \int_{-\tilde{\delta}_{(-)}}^0 (\tilde{v}\tilde{u}_{\tilde{y}})\, d\tilde{y}$$

$$= -\frac{d\tilde{p}}{d\tilde{x}} \int_{-\tilde{\delta}_{(-)}}^0 \frac{1}{\tilde{\rho}}\, d\tilde{y} + \int_{-\tilde{\delta}_{(-)}}^0 (\tilde{u}_{\tilde{y}\tilde{y}})\, d\tilde{y} \qquad \text{(VI-26)}$$

Again since $\tilde{v} = 0$ along the dividing streamline, the integration by parts, by using equation (VI-4), gives the following result:

$$\int_{-\tilde{\delta}_{(-)}}^{0} \left(\tilde{v}\,\frac{\partial \tilde{u}}{\partial \tilde{y}}\right) d\tilde{y} = -\left(\frac{\bar{q}_r}{\bar{u}_e}\right) q_s \int_{-\tilde{\delta}_{(-)}}^{0} \frac{\partial \tilde{u}}{\partial \tilde{x}}\, d\tilde{y} + \int_{-\tilde{\delta}_{(-)}}^{0} \left(\tilde{u}\,\frac{\partial \tilde{u}}{\partial \tilde{x}}\right) d\tilde{y} \tag{VI-27}$$

Substituting equations (VI-8) and (VI-27) into equation (VI-26) and using Bernoulli's equation as before,

$$\int_{-\tilde{\delta}_{(-)}}^{0} \left[(\tilde{u})^2_{\tilde{x}} - \left(\frac{\bar{q}_r}{\bar{u}_e}\right) q_s (\tilde{u})_{\tilde{x}} \right] = \frac{\partial \tilde{u}}{\partial \tilde{y}}\bigg|_{-\tilde{\delta}_{(-)}}^{0} + \left[\frac{(\gamma-1) M_r^2 q_s \frac{dq_s}{d\tilde{x}}}{1 - \frac{\gamma}{2} M_r^2 q_s^2} \right] \int_{-\tilde{\delta}_{(-)}}^{0} (\tilde{H} - \tfrac{1}{2}\tilde{u}^2)\, d\tilde{y} \tag{VI-28}$$

which may be rewritten as

$$\begin{aligned} &\int_{-\tilde{\delta}_{(-)}}^{0} \left\{ \left[\left(\frac{\tilde{u}}{\tilde{g}(0)}\right)^2 \right]_{\tilde{x}} - \left(\frac{\bar{q}_r}{\bar{u}_e}\right)\left(\frac{q_s}{\tilde{g}(0)}\right) \left[\left(\frac{\tilde{u}}{\tilde{g}(0)}\right) \right]_{\tilde{x}} \right\} d\tilde{y} \\ &\quad + \frac{1}{\tilde{g}(0)} \frac{d\tilde{g}(0)}{d\tilde{x}} \int_{\tilde{\delta}_{(-)}}^{0} \left[2\left(\frac{\tilde{u}}{\tilde{g}(0)}\right)^2 - \left(\frac{\bar{q}_r}{\bar{u}_e}\right)\left(\frac{q_s}{\tilde{g}(0)}\right)\left(\frac{\tilde{u}}{\tilde{g}(0)}\right) \right] d\tilde{y} \\ &\quad = \left[\frac{(\gamma-1) M_r^2 q_s \frac{dq_s}{d\tilde{x}}}{1 - \frac{\gamma}{2} M_r^2 q_s^2} \right] \int_{-\tilde{\delta}_{(-)}}^{0} \left[\frac{\tilde{H}}{\tilde{g}^2(0)} - \frac{1}{2}\left(\frac{\tilde{u}}{\tilde{g}(0)}\right)^2 \right] d\tilde{y} \\ &\quad + \left(\frac{1}{\tilde{g}(0)}\right) \frac{\partial}{\partial \tilde{y}} \left(\frac{\tilde{u}}{\tilde{g}(0)}\right)\bigg|_{-\tilde{\delta}_{(-)}}^{0} \end{aligned} \tag{VI-29}$$

From equations (VI-9), (VI-11), (VI-13a, b) and (VI-29) and through the applica-

tion of the Leibnitz rule, the zeroth moment of the momentum equation for the lower shear sublayer can be written as

$$\frac{d}{d\tilde{x}}\left(\tilde{\delta}_{(-)}\int_{-1}^{0}\tilde{g}_{(-)}^{2}\,d\tilde{\zeta}_{(-)}\right)-\left(\frac{q_r}{\bar{u}_e}\right)\left(\frac{q_s}{\tilde{g}(0)}\right)\frac{d}{d\tilde{x}}\left(\tilde{\delta}_{(-)}\int_{-1}^{0}\tilde{g}_{(-)}\,d\tilde{\zeta}_{(-)}\right)$$

$$=-\left\{\frac{1}{\tilde{g}(0)}\,\frac{d\tilde{g}(0)}{d\tilde{x}}\,\tilde{\delta}_{(-)}\int_{-1}^{0}\left[2\tilde{g}_{(-)}^{2}-\left(\frac{\bar{q}_r}{\bar{u}_e}\right)\left(\frac{q_s}{\tilde{g}(0)}\right)\tilde{g}_{(-)}\right]d\tilde{\zeta}_{(-)}\right\}$$

$$+\left[\frac{(\gamma-1)M_r^2 q_s\,\frac{dq_s}{d\tilde{x}}\,\tilde{\delta}_{(-)}}{1-\frac{\gamma}{2}M_r^2 q_s^2}\right]\int_{-1}^{0}\left(\frac{\tilde{H}}{\tilde{g}^2(0)}-\frac{1}{2}\,\tilde{g}_{(-)}^{2}\right)d\tilde{\zeta}_{(-)}$$

$$+\left(\frac{1}{\tilde{g}(0)\tilde{\delta}_{(-)}}\,\frac{\partial\tilde{g}_{(-)}}{\partial\tilde{\zeta}_{(-)}}\right)\Bigg|_{-1}^{0} \qquad \text{(VI-30)}$$

Each of the preceding integral conditions requires an overall momentum balance in one of the three parts of the shear layer. Two more conditions are obtained by requiring that the momentum equation also be satisfied at particular locations in the shear layer. Along the dividing streamline the momentum equation (VI-5), with $\tilde{u}(\tilde{x},\,\tilde{y})$ replaced by $\tilde{g}(0)\tilde{g}_{(+)}(0)$ according to equation (VI-10) becomes

$$\frac{d\tilde{g}_{(+)}(0)}{d\tilde{x}}=-\tilde{g}_{(+)}(0)\left(\frac{1}{\tilde{g}(0)}\,\frac{d\tilde{g}(0)}{d\tilde{x}}\right)+\left(\frac{1}{\tilde{g}_{(+)}(0)\tilde{g}(0)\tilde{\delta}_{(+)}^{2}}\right)\frac{\partial^2\tilde{g}_{(+)}}{\partial\tilde{\zeta}_{(+)}^{2}}(0)$$

$$+\left[\frac{(\gamma-1)M_r^2 q_s\,\frac{dq_s}{d\tilde{x}}}{1-\frac{\gamma}{2}M_r^2 q_s^2}\right]\left(\frac{\tilde{H}}{\tilde{g}^2(0)}-\frac{1}{2}\,\tilde{g}_{(+)}^{2}(0)\right)\frac{1}{\tilde{g}_{(+)}(0)} \qquad \text{(VI-31)}$$

The flow along the inner edge $\tilde{\zeta}=0$ of the outer shear layer is also required to satisfy the momentum equation. Then from equation (VI-5) and (VI-9) one

obtains

$$\frac{d\tilde{g}(0)}{d\tilde{x}} = \frac{1}{\tilde{g}(0)\tilde{\delta}^2}\frac{\partial^2\tilde{g}}{\partial\tilde{\zeta}^2}(0) + \left[\frac{(\gamma-1)M_r^2 q_s \frac{dq_s}{d\tilde{x}}}{1-\frac{\gamma}{2}M_r^2 q_s^2}\right]\left[\tilde{H} - \tfrac{1}{2}\tilde{g}^2(0)\right]\frac{1}{\tilde{g}(0)} \qquad \text{(VI-32)}$$

In addition to the eleven relations already obtained from the boundary and continuity conditions, the ordinary differential equations (VI-20), (VI-25), (VI-30), (VI-31) and (VI-32) are used to supply the required independent relations for the complete determination of the velocity profile in the shear layer. However, it is also necessary to provide the initial velocity profile in the shear layer.

4. Trailing-edge Expansion and Initial Development of Shear Layer

The expansion process at the trailing edge of the wedge is assumed isentropic and the total enthalpy is regarded as constant throughout the boundary layer. It can be shown that the velocity after corner expansion is

$$\tilde{u} = \left\{2\tilde{H}\left[1 - \left(\frac{\bar{p}_e}{\bar{p}_c}\right)^{\frac{\gamma-1}{\gamma}}\right] + \left(\frac{\bar{p}_e}{\bar{p}_c}\right)^{\frac{\gamma-1}{\gamma}}\left(\frac{\bar{u}_c}{\bar{u}_e}\right)^2 f_c'^2\right\}^{\frac{1}{2}} \qquad \text{(VI-33)}$$

where f_c is the Blasius solution for an incompressible flat-plate boundary layer and the subscript c refers to the condition at the trailing edge of the wedge and at the outer edge of the boundary layer.

If the length of the wedge surface is denoted by $\bar{L}_c$, then the Blasius similarity variable evaluated a very short distance upstream from the trailing edge of the wedge may be represented by

$$d\eta_c = \sqrt{\frac{\bar{u}_c}{2\bar{\nu}_c \bar{L}_c}} \left(\frac{\bar{\rho}}{\bar{\rho}_c}\right) d\bar{y}_c \qquad \text{(VI-34)}$$

where $\bar{y}_c$ is the $\bar{y}$ coordinate before the expansion, just upstream from the trailing edge of the wedge. Since there is no pressure gradient across the boundary layer, and $\tilde{H} = \tilde{h} + \frac{\tilde{u}^2}{2}$, the relation between $\bar{y}_c$ and η_c is

$$d\bar{y}_c = \sqrt{\frac{2\bar{\nu}_c \bar{L}_c}{\bar{u}_c}} \frac{1}{\tilde{h}_c} \left[\tilde{H} - \tfrac{1}{2}\left(\frac{\bar{u}_c}{\bar{u}_e}\right)^2 f'^2_c\right] d\eta_c \qquad \text{(VI-35)}$$

where $f'_c = f'_0(\eta_c)$. Since the total mass in the boundary layer immediately before and after the corner expansion must remain the same, the relation between $\bar{y}_e$ and η_c is

$$d\bar{y}_e = \sqrt{\frac{2\bar{\nu}_c \bar{L}_c}{\bar{u}_c}} \left(\frac{\bar{p}_c}{\bar{p}_e} \frac{1}{\tilde{h}_c} \frac{\bar{u}_c}{\bar{u}_e}\right) \left[\frac{\left(\tilde{H} - \frac{\tilde{u}^2}{2}\right)}{\tilde{u}} f'_c\right] d\eta_c \qquad \text{(VI-36)}$$

where $\bar{y}_e$ is the $\bar{y}$ coordinate measured from the dividing streamline after the expansion a very short distance downstream from the trailing edge of the wedge. Hence the relation between the transformed coordinate and the similarity variable is

$$d\tilde{y} = \left(\frac{2Re_e}{Re_c}\right)^{\frac{1}{2}} \left(\frac{\bar{L}_c}{\bar{r}_o} \frac{\bar{\rho}_c}{\bar{\rho}_e} \frac{\bar{u}_c}{\bar{u}_e}\right) \frac{f'_c}{\tilde{u}} \, d\eta_c \qquad \text{(VI-37)}$$

where $Re_c = \bar{u}_c \bar{L}_c / \bar{\nu}_c$. From equations (VI-33) and (VI-37) the velocity profile

after the trailing-edge expansion may be obtained in transformed coordinates.

The boundary-layer flow immediately after the trailing-edge expansion mixes with the flow below the dividing streamline which is virtually stagnant when $\tilde{x}$ is very small, i.e., very close to the wedge base. Hence the governing differential equation is the same as equation (VI-5), except that no pressure-gradient term is present, and can be written in terms of the stream function as

$$\frac{\partial\tilde{\psi}}{\partial\tilde{y}}\frac{\partial^2\tilde{\psi}}{\partial\tilde{x}\partial\tilde{y}} - \frac{\partial\tilde{\psi}}{\partial\tilde{x}}\frac{\partial^2\tilde{\psi}}{\partial\tilde{y}^2} = \frac{\partial^3\tilde{\psi}}{\partial\tilde{y}^3} \qquad \text{(VI-38)}$$

For the outer shear layer the stream function is

$$\tilde{\psi} \cong \tilde{\psi}_0(\tilde{y})$$

where $\tilde{\psi}_0'(\tilde{y}) = \sum_0^2 a_n(0)\left(\frac{\tilde{y}}{\tilde{\delta}(0)}\right)^n$. Then $a_0(0)$, $a_1(0)$, $a_2(0)$ and $\tilde{\delta}(0)$ are obtained by fitting a polynomial to the velocity profile after the corner expansion. For the flow near the dividing streamline the viscous stresses are very large and the flow is described approximately as the mixing of a uniform flow with fluid at rest. Hence it is assumed that the solution has the approximate form

$$\tilde{\psi} \sim \sqrt{2a_0(0)\tilde{x}}\, f_0(\eta) \qquad \text{(VI-39)}$$

$$\eta \cong \sqrt{\frac{a_0(0)}{2\tilde{x}}}\ \tilde{y} \qquad \text{(VI-40)}$$

The solution is obtained from the following differential equation and boundary conditions

$$f_0''' + f_0 f_0'' = 0 \qquad \text{(VI-41)}$$

$$f_0'(\infty) \to 1\ ;\ f_0'(-\infty) \to 0\ ;\ f_0(0) = 0 \qquad \text{(VI-42)}$$

Therefore for a fixed small positive $\tilde{x}$ and for $\tilde{\eta} \geq 0$,

$$\tilde{g}_{(+)}\left(\tilde{\zeta}_{(+)}\right) \cong f_0'(\tilde{\eta}) \qquad \text{(VI-43)}$$

Similarly for $\tilde{\eta} \leq 0$,

$$\tilde{g}_{(-)}\left(\tilde{\zeta}_{(-)}\right) \cong f_0'(\tilde{\eta}) \qquad \text{(VI-44)}$$

Initial values are provided for the profile parameters of the upper and lower shear sublayer by fitting polynomials to the upper and lower parts of $f_0'(\eta)$.

5. The Location of Dividing Streamline

Since the velocity in the inviscid core flow is not exactly zero, the pressure is not exactly constant, and therefore the shear layer is not exactly straight. In a first approximation the curvature of the shear layer will be such that the pressure in the external flow balances the pressure in the recirculating flow. The velocity in the inviscid core flow is $\frac{\bar{u}}{u_e} = O(M_r)$ and so the nondimensional shear-layer curvature is $O(M_r^2)$. If the pressure gradient is known from the solution of (IV), the shear-layer curvature can be calculated to this order.

The pressure variation across the shear layer must be zero not only to order M_r^2 but also to higher order in Reynolds number. Lock[38], in his study of the mixing of parallel streams, notes that the dividing streamline is not necessarily straight. Ting[39] shows that for the mixing of a uniform supersonic stream with a parallel uniform subsonic stream the dividing streamline is displaced toward the subsonic portion of the flow by an amount equal to the displacement thickness of the viscous layer above the dividing streamline, so that the pressure is kept the same across the mixing layer up to an appropriate order of magnitude. The location of the dividing streamline is important in the study of the shear layer in the wake, because it has an influence on the shear-stress distribution and velocity distribution.

Since the velocity distribution in the outer shear layer and in the recirculating flow is very complex, it seems necessary to retain the approximation that M_r is small. It is assumed that the outer shear layer may be approximated by a uniform shear flow at supersonic speed

$$\bar{u} = \bar{u}_u + \bar{\Omega}\bar{y}$$

where $\bar{\Omega}$ is the vorticity and is a constant. This approximation is consistent with previous assumptions, since only the portion of the outer shear layer near $\bar{y} = 0$ needs to be correctly represented here. The recirculating flow is assumed to have zero velocity. Since the recirculating flow will actually have velo-

city $\frac{\bar{u}}{\bar{u}_e} = O(M_r)$, then $\bar{p} = \bar{p}_e [1 + O(M_r^2)]$ in the recirculation region, and the velocity at the inner edge of the outer shear layer will actually be $\bar{u} = \bar{u}_u [1 + O(M_r^2)]$. The nondimensional variables for the uniform shear flow are defined as

$$\hat{x} = \frac{\bar{x}}{\bar{r}_o} \; ; \; \hat{y} = \frac{\bar{y}}{\bar{r}_o}$$

$$\hat{\psi} = \frac{\bar{\psi}}{\bar{u}_u \bar{r}_o} \; ; \; \hat{u} = \frac{\bar{u}}{\bar{u}_u} \; ; \; \hat{v} = \frac{\bar{v}}{\bar{u}_u} \; ; \; \hat{N} = \frac{\bar{\Omega}\, \bar{r}_o}{\bar{u}_u}$$

The nondimensional variables for the recirculating flow are defined as

$$x = \frac{\bar{x}}{\bar{r}_o} \; ; \; y = \frac{\bar{y}}{\bar{r}_o}$$

$$\psi = \frac{\bar{\psi}}{\bar{u}_u \bar{r}_o} \; ; \; u = \frac{\bar{u}}{\bar{u}_u} \; ; \; v = \frac{\bar{v}}{\bar{u}_u}$$

The nondimensional variables for the mixing layer are defined as

$$x\dagger = \frac{\bar{x}}{\bar{r}_o} \; ; \; y\dagger = \frac{\sqrt{Re_u}}{\bar{r}_o}\, \bar{y} \; ; \; Re_u = \frac{\bar{u}_u}{\bar{u}_e} Re_e$$

$$\psi\dagger = \frac{\bar{\psi}}{\bar{u}_u \bar{r}_o} \; ; \; u\dagger = \frac{\bar{u}}{\bar{u}_u} \; ; \; v\dagger = \frac{\bar{v}}{\bar{u}_u}$$

Following the same procedure as for the mixing of two parallel streams given by Ting[39], the flow variables may be expanded as

$$\left.\begin{aligned}
\hat{\psi} &\sim \hat{\psi}_0 + \epsilon\hat{\psi}_1 + \dots \\
\hat{u} &\sim \hat{u}_0 + \epsilon\hat{u}_1 + \dots \\
\hat{v} &\sim \epsilon\hat{v}_1 + \epsilon^2\hat{v}_2 + \dots \\
\frac{\bar{p} - \bar{p}_e}{\bar{\rho}_u \bar{u}_u^2} &\sim p_0 + \epsilon p_1 + \dots
\end{aligned}\right\} \quad \text{(VI-45)}$$

$$\left.\begin{aligned}
\psi &\sim \psi_0 + \epsilon\psi_1 + \dots \\
u &\sim u_0 + \epsilon u_1 + \dots \\
v &\sim \epsilon v_1 + \epsilon^2 v_2 + \dots \\
\frac{\bar{p} - \bar{p}_e}{\bar{\rho}_u \bar{u}_u^2} &\sim p_0 + \epsilon p_1 + \dots
\end{aligned}\right\} \quad \text{(VI-46)}$$

$$\left.\begin{aligned}
\psi^\dagger &\sim \epsilon\psi_1^\dagger + \epsilon^2\psi_2^\dagger + \dots \\
u^\dagger &\sim u_0^\dagger + \epsilon u_1^\dagger + \dots \\
v^\dagger &\sim \epsilon v_1^\dagger + \epsilon^2 v_2^\dagger + \dots \\
\frac{\bar{p} - \bar{p}_e}{\bar{\rho}_u \bar{u}_u^2} &\sim p_0^\dagger + \epsilon p_1^\dagger + \dots
\end{aligned}\right\} \quad \text{(VI-47)}$$

where $\epsilon = Re_u^{-\frac{1}{2}}$, $\bar{\rho}_u$ is the density of the uniform shear flow, and $p_0 = p_0(x) = O(M_r^2)$.

Substituting equation (VI-47) into the Navier-Stokes equations and collecting coefficients of like powers of ϵ gives the following form for the $y^\dagger$ component of the momentum equation:

$$\epsilon\, p_{1\,y^\dagger}^\dagger + \ldots = O(\epsilon^2)$$

The matching conditions for the pressure at the outer and the inner edge of the mixing layer give

$$p_1^\dagger(\tilde{x}, \infty) = \hat{p}_1(\hat{x}, 0)$$
$$p_1^\dagger(\tilde{x}, -\infty) = p_1(x, 0)$$

There results a compatibility condition

$$\hat{p}_1(\hat{x}, 0) = p_1(x, 0) \qquad \text{(VI-48)}$$

Equation (VI-48) states that the pressure difference across the mixing layer should be $O(\epsilon)$. This condition is used at a later stage for the determining of the location of the dividing streamline relative to the outer shear layer.

The nondimensional Navier-Stokes equations for incompressible flow may be written as

$$\left(\psi_y \frac{\partial}{\partial x} - \psi_x \frac{\partial}{\partial y}\right)\nabla^2\psi = \epsilon^2 \nabla^2 \nabla^2 \psi \qquad \text{(VI-49)}$$

From equations (VI-45) and (VI-49) the following set of equations can be obtained:

$$\left(\hat{\psi}_{0\hat{y}} \frac{\partial}{\partial \hat{x}} - \hat{\psi}_{0\hat{x}} \frac{\partial}{\partial \hat{y}}\right) \nabla^2 \hat{\psi}_0 = 0 \qquad \text{(VI-50a)}$$

$$\left(\hat{\psi}_{0\hat{y}} \frac{\partial}{\partial \hat{x}} - \hat{\psi}_{0\hat{x}} \frac{\partial}{\partial \hat{y}}\right) \nabla^2 \hat{\psi}_1 + \left(\hat{\psi}_{1\hat{y}} \frac{\partial}{\partial \hat{x}} - \hat{\psi}_{1\hat{x}} \frac{\partial}{\partial \hat{y}}\right) \nabla^2 \hat{\psi}_0 = 0 \qquad \text{(VI-50b)}$$

Equation (50a) can be reduced to

$$\nabla^2 \hat{\psi}_0 = \hat{N} = \text{constant} \qquad \text{(VI-51a)}$$

Since the following boundary conditions must be satisfied

$$\hat{\psi}_0(\hat{x}, \hat{y}) = \hat{y} + \tfrac{1}{2}\hat{N}\hat{y}^2 \qquad \text{upstream} \qquad \text{(VI-51b)}$$

$$\hat{\psi}_0(\hat{x}, 0) = 0 \qquad \text{(VI-51c)}$$

the solution is

$$\hat{\psi}_0(\hat{x}, \hat{y}) = \hat{y} + \frac{\hat{N}}{2}\hat{y}^2 \qquad \text{(VI-52)}$$

As noted previously, terms $O(M_r^2)$ in the coefficient of $\hat{y}$ have been neglected.

Substituting equation (VI-46) into equation (VI-49), there results a set of

differential equations

$$\left(\psi_{0y}\,\frac{\partial}{\partial y} - \psi_{0x}\,\frac{\partial}{\partial y}\right)\nabla^2\psi_0 = 0 \qquad \text{(VI-53a)}$$

$$\left(\psi_{0y}\,\frac{\partial}{\partial x} - \psi_{0x}\,\frac{\partial}{\partial y}\right)\nabla^2\psi_1 + \left(\psi_{1y}\,\frac{\partial}{\partial x} - \psi_{1x}\,\frac{\partial}{\partial y}\right)\nabla^2\psi_0 = 0 \qquad \text{(VI-53b)}$$

Since $\frac{\bar{u}}{u_e} = O(M_r)$ in the recirculation region, equation (VI-53a) can be written as

$$\nabla^2\psi_0 = O(M_r) \qquad \text{(VI-54a)}$$

Since

$$\psi_0(x,0) = 0 \qquad \text{(VI-54b)}$$

in the present approximation the solution will be estimated as:

$$\psi_0(x,y) = O(M_r) \qquad \text{(VI-55)}$$

Substituting equation (VI-47) into equation (VI-49), there results a set of differential equations

$$\frac{\partial}{\partial y^\dagger}\left(\psi_1^\dagger{}_{y^\dagger y^\dagger y^\dagger} + \psi_1^\dagger{}_{x^\dagger}\,\psi_1^\dagger{}_{y^\dagger y^\dagger} - \psi_1^\dagger{}_{y^\dagger}\,\psi_1^\dagger{}_{x^\dagger y^\dagger}\right) = 0 \qquad \text{(VI-56a)}$$

$$\frac{\partial}{\partial y^\dagger}\left(\psi^\dagger{}_{2y^\dagger y^\dagger y^\dagger} + \psi^\dagger{}_{1x^\dagger}\,\psi^\dagger{}_{2y^\dagger y^\dagger} - \psi^\dagger{}_{1y^\dagger}\,\psi^\dagger{}_{2x^\dagger y^\dagger} + \psi^\dagger{}_{2x^\dagger}\,\psi^\dagger{}_{1y^\dagger y^\dagger} - \psi^\dagger{}_{2y^\dagger}\,\psi^\dagger{}_{1x^\dagger y^\dagger}\right) = 0 \qquad \text{(VI-56b)}$$

The matching condition as $y\dagger \to \infty$ and $y \to 0$ is

$$\psi\dagger_{1y\dagger}(x\dagger, \infty) = \psi_{0y}(x, 0)$$

The matching condition as $y\dagger \to -\infty$ and $y \to 0$ is

$$\psi\dagger_{1y\dagger}(x\dagger, -\infty) = \psi_{0y}(x, 0) = 0$$

Hence the following asymptotic relations are obtained

$$\psi\dagger_1(x\dagger, y\dagger) \sim y\dagger \hat{\psi}_{0\hat{y}}(\hat{x}, 0) + o(y\dagger) \qquad \text{as } y\dagger \to \infty$$

(VI-57a)

$$\psi\dagger_1(x\dagger, y\dagger) \sim o(y\dagger) \qquad \text{as } y\dagger \to -\infty$$

(VI-57b)

By using equation (VI-57), equation (VI-56a) can be reduced to

$$\psi\dagger_{1y\dagger y\dagger y\dagger} + \psi\dagger_{1x\dagger}\psi\dagger_{1y\dagger y\dagger} - \psi\dagger_{1y\dagger}\psi\dagger_{1x\dagger y\dagger} = -\hat{\psi}_{0\hat{y}}(\hat{x}, 0)\hat{\psi}_{0\hat{x}\hat{y}}(\hat{x}, 0)$$

(VI-58)

Since $\psi_0(x, y)$ is a function of y alone, equation (VI-58) can be reduced to

$$\psi\dagger_{1y\dagger y\dagger y\dagger} + \psi\dagger_{1x\dagger}\psi\dagger_{1y\dagger y\dagger} - \psi\dagger_{1y\dagger}\psi\dagger_{1x\dagger y\dagger} = 0$$

(VI-59)

Two of the boundary conditions are

$$\psi^{\dagger}_{1y^{\dagger}}(x^{\dagger}, \infty) = 1 \qquad \text{(VI-60a)}$$

$$\psi^{\dagger}_{1y^{\dagger}}(x^{\dagger}, -\infty) = 0 \qquad \text{(VI-60b)}$$

Equations (VI-59) and (VI-60) have a solution of the form

$$\psi^{\dagger}_{1} = \sqrt{2x^{\dagger}}\, f(\eta^{\dagger}), \quad \eta^{\dagger} = \frac{y^{\dagger}}{\sqrt{2x^{\dagger}}}$$

where $f(\eta^{\dagger})$ satisfies the differential equation and boundary conditions

$$f''' + f f'' = 0 \qquad \text{(VI-61a)}$$

$$f'(\infty) = 1 \qquad \text{(VI-61b)}$$

$$f'(-\infty) = 0 \qquad \text{(VI-61c)}$$

Equation (VI-58) actually applies to the mixing layer with the streamline $\psi^{\dagger} = 0$ slightly displaced relative to the outer shear layer. Let $x^{\dagger}$ and $y^{\dagger}$ be measured along and normal to $\psi^{\dagger} = 0$ respectively. Then, since the curvature of the line $\psi^{\dagger} = 0$ affects only the higher approximations to the equation for the mixing region, equation (VI-59) remains unchanged. A third boundary condition is obtained from the requirement that the pressure difference across

the mixing layer be of order ϵ^2. Therefore, the velocity profiles in the first approximation of the mixing region should be so oriented that the pressures induced in the inviscid stream by the effect of displacement thickness are balanced across the mixing layer. Since equations (VI-61a, b, c) are invariant under the transformation

$$\eta^\dagger \rightarrow \eta^\dagger + \beta^\dagger$$

the third boundary condition may be assumed as

$$f(0) = 0 \qquad \text{(VI-61d)}$$

The solution obtained by using boundary condition $f(0) = 0$ differs from those using $f(\beta^\dagger) = 0$ only in the location of the line $\psi^\dagger = 0$. The solution of equations (VI-61a, b, c, d) for $\eta^\dagger \rightarrow \infty$ is

$$f(\eta^\dagger) \sim (\eta^\dagger + \beta^\dagger_u) + \text{exponential} \qquad \text{(VI-62)}$$

Where $\beta^\dagger_u$ is proportional to the displacement thickness of the upper part of the shear sublayer which is measured from $\psi^\dagger = 0$. Similarly the solution for $\eta^\dagger \rightarrow -\infty$ is

$$f(\eta^\dagger) \sim (\eta^\dagger + \beta^\dagger_l) + \text{exponential} \qquad \text{(VI-63)}$$

where $\beta_1^\dagger$ is proportional to the displacement thickness of the lower part of the shear sublayer, which is measured from $\psi^\dagger = 0$.

By using equations (VI-53b), (VI-54a) and (VI-63) the flow below the mixing layer due to displacement thickness is described by

$$\nabla^2 \psi_1 = 0 \qquad \text{(VI-64a)}$$

$$\psi_1(x,0) = -\beta_1 \sqrt{2x} \qquad \text{for } x > 0 \qquad \text{(VI-64b)}$$

From Bernoulli's equation p_1 may be expressed as

$$p_1 = -u_0 u_1 \qquad \text{(VI-65a)}$$

Since $\epsilon\psi_1$, ϵu_1 and ϵv_1 are of order ϵ and u_0 is of order M_r, ϵp_1 will be estimated as

$$\epsilon p_1 = O(M_r \epsilon)$$
$$= o(\epsilon) \qquad \text{(VI-65b)}$$

Therefore one gets

$$p_1(x,0) = p_1(x,0) = p_1^\dagger(x^\dagger, y^\dagger) = 0 \qquad \text{(VI-66)}$$

if terms of order M_r are neglected compared to unity.

For the uniform shear flow, the next approximation is governed by the

linearized equations[28] for irrotational supersonic flow:

$$\frac{\partial \hat{u}_1}{\partial \hat{y}} - \frac{\partial \hat{v}_1}{\partial \hat{x}} = 0 \qquad \text{(VI-67a)}$$

$$(1 + \hat{N}\hat{y})\,\hat{u}_{1\hat{x}} + \hat{N}\hat{v}_1 = -\hat{p}_{1\hat{x}} \qquad \text{(VI-67b)}$$

$$(1 + \hat{N}\hat{y})\,\hat{v}_{1\hat{x}} = -\hat{p}_{1\hat{y}} \qquad \text{(VI-67c)}$$

From equation (VI-66) one obtains $\hat{p}_{1\hat{x}} = 0$, $\hat{p}_{1\hat{y}} = 0$. Hence equations (VI-67a, b, c) become

$$\frac{\partial \hat{u}_1}{\partial \hat{y}} = \frac{\partial \hat{v}_1}{\partial \hat{x}} = 0 \qquad \text{(VI-68a)}$$

$$(1 + \hat{N}\hat{y})\,\hat{u}_{1\hat{x}} + \hat{N}\hat{v}_1 = 0 \qquad \text{(VI-68b)}$$

From Bernoulli's equation, p_1 may be expressed as[28]

$$\hat{p}_1 \cong -\hat{u}_0\hat{u}_1 \qquad \text{(VI-69)}$$

Since $\hat{p}_1 = 0$ and $\hat{u}_0 \neq 0$, there results

$$\hat{u}_1 = 0 \qquad \text{(VI-70)}$$

Hence equation (VI-68b) reduces to

$$\hat{N}\hat{v}_1 = 0 \qquad \text{(VI-71)}$$

Since $\hat{N}$ = constant, it is required for the uniform shear flow at supersonic speed that

$$\hat{v}_1(\hat{x}, \hat{y}) = \hat{v}_1(\hat{x}, 0) = v^{\dagger}_1(x^{\dagger}, \infty) = 0 \qquad \text{(VI-72)}$$

This relation means that the line $\psi^{\dagger} = 0$ is displaced by an amount equal to the displacement thickness of the upper shear sublayer. In other words, it is required that there be no effect of displacement thickness on the uniform shear flow. If this result is applied to the problem discussed in the previous sections, one can make the approximation that for $\tilde{y}$ measured from the dividing streamline, the inner edge of the outer shear layer is at $\tilde{y} = \zeta_0\tilde{\delta}$, where $\zeta_0 = \tilde{\delta}^*_{(+)}/\tilde{\delta}$, and the $\tilde{v}$ component of velocity is negligibly small at the inner edge of the outer shear layer.

It is evident that the approximation (VI-72) is not highly accurate, because the error is $O(M_r)$. However, the only purpose here is to obtain an estimate for κ, which in turn will be used to estimate the effect of nonzero sublayer thickness on the outer shear layer. Since this effect is expected to be small, it is not necessary that the value of κ be extremely accurate.

VII

NUMERICAL SOLUTION

1. The Derivation of the Equations for Computation

In the discussion of the conservation of angular momentum for the entire recirculating flow, it was observed that for a steady motion the accelerating torque from the shear layer should always be equal to the retarding torque from the base boundary layer. In order to determine these torques it is necessary to find the distribution of the shear stress both along the base of the wedge and along the dividing streamline.

Since the distribution of the shear stress along the base of the wedge can be determined by the solution of equations (V-1) and (V-2) for the base boundary layer, the solution of the system of approximating ordinary differential equations (V-29) and (V-30) is needed. For fairly good accuracy the velocity of the inviscid core flow evaluated along the base of the wedge can be approximated by

$$q_b = \left\{ 2\bar{\theta}_o(\theta^2 - \theta) + \frac{8}{\pi^2}\sum_0^5\left[\frac{1}{(2n+1)^2}\right]\sin(2n+1)\pi\theta \right.$$

$$+ \frac{8}{\pi^2}\sum_0^5\left[\frac{7.4\bar{\theta}_o}{(2n+1)^2\pi^2} + \frac{36\bar{\theta}_o}{(2n+1)^4\pi^4} - \frac{\pi\bar{\theta}_o}{2(2n+1)}\right]\sin(2n+1)\pi\theta$$

$$\left. + \frac{8}{\pi^2}\sum_1^5\left[\frac{23.9\bar{\theta}_o}{(2n\pi)^2}\right]\sin 2n\pi\theta \right\} \qquad \text{(VII-1)}$$

because the series in q_b converge quite rapidly. The transformed coordinate along the $\overline{X}$ direction, given by equation (V-22), can be approximated by $X \cong \int_0^\theta q_b \, d\theta$. Hence

$$\dot{q}_b = \frac{dq_b}{dX} = \frac{1}{q_b} \frac{dq_b}{d\theta} \qquad \text{(VII-2)}$$

Equations (V-29) and (V-30) can be rewritten as

$$\frac{d\Theta_0}{d\theta} = -\frac{1}{q_b} \frac{dq_b}{d\theta} (9\Theta_0 + 7\Theta_1) + \left(\frac{34}{\Theta_0} - \frac{32}{\Theta_1} \right) q_b \qquad \text{(VII-3)}$$

$$\frac{d\Theta_0}{d\theta} = -\frac{1}{q_b} \frac{dq_b}{d\theta} (4\Theta_0 + 6\Theta_1) + \left(\frac{20}{\Theta_0} - \frac{16}{\Theta_1} \right) q_b \qquad \text{(VII-4)}$$

These equations are ordinary differential equations with θ as the independent variable. The initial conditions for Θ_0 and Θ_1 can be obtained by substituting $X \cong \frac{1}{2} C_1 \theta^2$ into equation (V-39). Then, for θ fixed but small, the following approximation is obtained

$$\Theta_0 \cong 0.815 \sqrt{C_1}\, \theta \qquad \text{(VII-5)}$$

$$\Theta_1 \cong 1.292 \sqrt{C_1}\, \theta \qquad \text{(VII-6)}$$

where C_1 may be obtained from the Taylor expansion of q_b about $\theta = 0$, and

$$C_1 \cong \left[-2\bar{\theta}_o + \frac{8}{\pi} \sum_0^5 \frac{1}{(2n+1)} + \frac{8}{\pi^2} \sum_0^5 \left(\frac{7.4\bar{\theta}_o}{(2n+1)\pi} - \frac{\pi^2 \bar{\theta}_o}{2} + \frac{36\bar{\theta}_o}{(2n+1)^3 \pi^3} \right) + \frac{8}{\pi^2} \sum_1^5 \frac{23.9\bar{\theta}_o}{2n\pi} \right]$$

Hence the Runge-Kutta method can be used to provide solutions for Θ_0 and Θ_1.

Since

$$Y = \frac{\sqrt{Re_r}}{\bar{L}_r \bar{q}_r} \bar{q}_b \bar{Y}, \quad U = \frac{\bar{U}}{\bar{q}_b}, \quad \text{and } \Theta^{-1} = \frac{\partial U}{\partial Y}\Big|_{Y=0}$$

the shear stress along the base of the wedge, $\bar{\tau}_b$, can be written as

$$\bar{\tau}_b = \bar{\mu}_r \frac{\partial \bar{U}}{\partial \bar{Y}}\Big|_{\bar{Y}=0}$$

$$= \frac{\bar{\mu}_r \bar{q}_r \sqrt{Re_r}}{\bar{L}_r} \frac{q_b^2}{\Theta_0} \qquad \text{(VII-7)}$$

the local skin-friction coefficient along the base of the wedge, C_F, has the form

$$C_F = \frac{2\bar{\tau}_b}{\bar{\rho}_r (\bar{q}_r q_b)^2}$$

$$= \frac{2}{\Theta_0} \frac{1}{\sqrt{Re_r}} \qquad \text{(VII-8)}$$

The distribution of the shear stress along the dividing streamline can be obtained from the solution of the shear-layer equations (VI-1), (VI-2) and (VI-3).

An integral method of the Kármán-Pohlhausen type is used to reduce this set of partial differential equations to a set of approximating ordinary differential equations. The velocity profiles are approximated by polynomials with undetermined coefficients, given by equations (VI-9), (VI-10), and (VI-11). Since

$$\tilde{y} = \frac{\sqrt{Re_e}}{\bar{r}_o} \int_0^{\bar{y}} \tilde{\rho}\, d\bar{y},\ \tilde{u} = \frac{\bar{u}}{\bar{u}_e},\ \frac{\partial \tilde{u}}{\partial \tilde{y}}\Big|_{\tilde{y}=0} = \frac{a_0}{\delta_{(+)}} \frac{\partial \tilde{g}_{(+)}}{\partial \zeta_{(+)}}(0)$$

the distribution of the shear-stress along the dividing streamline, $\bar{\tau}_d$, can be written as

$$\tilde{\tau}_d = \bar{\mu}_e \frac{\partial \bar{u}}{\partial \bar{y}}\Big|_{\bar{y}=0}$$

$$= \frac{\bar{\mu}_e \bar{u}_e Re_e^{\frac{1}{2}}}{\bar{r}_o} \frac{a_0 b_1}{\delta_{(+)}} \qquad \text{(VII-9)}$$

The local skin friction coefficient along the dividing streamline, c_f, has the form:

$$c_f = \frac{2\tilde{\tau}_d}{\bar{\rho}_e \bar{u}_e^2}$$

$$= \frac{2}{\sqrt{Re_e}} \frac{a_0 b_1}{\delta_{(+)}} \qquad \text{(VII-10)}$$

where a_0, b_1, and $\tilde{\delta}_{(+)}$ are given by the solutions of the system of equations (VI-20), (VI-25), (VI-30), (VI-31) and (VI-32) with the boundary and continuity

conditions (VI-12) through (VI-15).

Since, in the continuity condition between the outer shear layer and the upper shear layer, the location of the outer edge of the shear sublayer is needed, the location of the dividing streamline must be determined. It has been shown that the dividing streamline is displaced by an amount equal to the displacement thickness of the upper shear sublayer. This satisfies the requirement of zero pressure gradient across the shear layer to order $(Re_e^{-\frac{1}{2}})$.

The displacement thickness for the upper shear sublayer, $\tilde{\delta}^*_{(+)}$, is expressed as

$$\frac{\tilde{\delta}^*_{(+)}}{\tilde{\delta}_{(+)}} = \int_0^1 \left(1 - \frac{\bar{u}}{\bar{u}_u}\right) d\tilde{\zeta}_{(+)}$$

$$= \int_0^1 \left(1 - \frac{\bar{u}_d}{\bar{u}_e}\,\frac{\bar{u}_e}{\bar{u}_u}\,\frac{\bar{u}}{\bar{u}_d}\right) d\tilde{\zeta}_{(+)}$$

$$= \int_0^1 \left(1 - \frac{\tilde{g}(0)\,\tilde{g}_{(+)}}{\tilde{g}(\kappa\Delta)}\right) d\tilde{\zeta}_{(+)}$$

$$= 1 - \frac{a_0}{\left[1 - (1-a_0)(1-\Delta)^2\right]}\left[b_0 + \frac{b_1}{2} + \frac{b_2}{3} + \frac{b_3}{4} + \frac{b_4}{5}\right] \qquad \text{(VII-11)}$$

where $\bar{u}_d = \bar{u}_e \tilde{g}(0)$ is the velocity at the outer edge of the upper shear, $\bar{u}_u = \bar{u}_e \tilde{g}(\kappa\Delta)$ is the velocity at the outer edge of the upper shear sublayer, $\Delta = \tilde{\delta}_{(+)} / \tilde{\delta}$

The outer edge of the upper shear sublayer is at

$$\tilde{\zeta} = \kappa\Delta \qquad \text{(VII-12)}$$

where $\kappa = \left(1 - \frac{\tilde{\delta}^*_{(+)}}{\tilde{\delta}_{(+)}}\right)$. Since $\frac{\tilde{\delta}^*_{(+)}}{\tilde{\delta}_{(+)}}$ can be shown to be nearly constant, $\frac{d}{d\tilde{x}}\left(\frac{\tilde{\delta}^*_{(+)}}{\tilde{\delta}_{(+)}}\right)$ may be assumed negligibly small in the computation. This will simplify the computation and is within the accuracy needed. Hence equations (VI-15a, b, c) can be rewritten in the following form:

$$\tilde{g}_{(+)}(1) \cong \left[1 + \frac{2\kappa\,\Delta(1-a_0)}{a_0}\right]$$

$$\frac{\partial \tilde{g}_{(+)}}{\partial \tilde{\zeta}_{(+)}}(1) \cong \Delta\left[\frac{2(1-a_0)}{a_0} - \frac{\kappa\,\Delta(1-a_0)}{a_0}\right]$$

$$\frac{\partial^2 \tilde{g}_{(+)}}{\partial \tilde{\zeta}^2_{(+)}}(1) \cong -\left[\frac{\Delta^2(1-a_0)}{a_0}\right]$$

For simplicity, define

$$\kappa_0 = \frac{2\kappa\,\Delta(1-a_0)}{a_0} \qquad \text{(VII-13)}$$

$$\kappa_1 = \kappa_0 - \frac{\kappa_0\Delta}{2} \qquad \text{(VII-14)}$$

$$\kappa_2 = -\kappa_0\Delta \qquad \text{(VII-15)}$$

$$\kappa_3 = \kappa_0 - \frac{\kappa_1}{2} + \frac{\kappa_2}{12} \qquad \text{(VII-16)}$$

$$\kappa_4 = \frac{\kappa_3}{1+\Delta} \qquad \text{(VII-17)}$$

$$\kappa_5 = \kappa_4 \Delta \tag{VII-18}$$

$$\kappa_6 = \frac{1 - \left(\frac{\bar{q}_r}{\bar{u}_e}\right)\left(\frac{q_s}{a_0}\right)}{1+\Delta} \tag{VII-19}$$

These quantities are functions of a_0, $\tilde{\delta}$, $\tilde{\delta}_{(+)}$, $\tilde{\delta}_{(-)}$ and q_s. The velocity of the inviscid core flow evaluated along the dividing streamline can be approximated by

$$q_s = \left\{(1-x) - \frac{8}{\pi^2}\,\frac{1}{1-x}\sum_0^5 \left[\left(\frac{1}{(2n+1)^2} - \frac{\pi x^2}{2\bar{\theta}_o(2n+1)} + \frac{7.4\bar{\theta}_o}{(2n+1)^2\pi^2} + \frac{36\bar{\theta}_o}{(2n+1)^4\pi^4}\right)\exp\left[-(2n+1)\,\pi x/\bar{\theta}_o\right] - \left(\frac{23.9\bar{\theta}_o}{(2n\pi)^2}\right)\exp\left(-2n\pi x/\bar{\theta}_o\right)\right]\right\} \tag{VII-20}$$

Therefore, based on the boundary and continuity conditions, the profile coefficient can be expressed in terms of a_0, b_2, $\tilde{\delta}$, $\tilde{\delta}_{(+)}$ and $\tilde{\delta}_{(-)}$:

$$a_1 = 2(1-a_0) \tag{VII-21}$$

$$a_2 = -(1-a_0) \tag{VII-22}$$

$$b_0 = 1 - \kappa_6 - \frac{b_2\delta}{6} + \kappa_3 - \kappa_4 \tag{VII-23}$$

$$b_1 = 2\kappa_6 + \left(\frac{b_2}{3}\right)(\delta - 1) + 2\kappa_4 \qquad \text{(VII-24)}$$

$$b_3 = -2\kappa_6 - \frac{b_2(\delta+1)}{3} + \kappa_1 - \frac{\kappa_2}{3} - 2\kappa_4 \qquad \text{(VII-25)}$$

$$b_4 = \kappa_6 + \frac{b_2(2+\delta)}{6} - \frac{\kappa_1}{2} + \frac{\kappa_2}{4} + \kappa_4 \qquad \text{(VII-26)}$$

$$c_0 = 1 - \kappa_6 - \frac{b_2\delta}{6} + \kappa_3 - \kappa_4 \qquad \text{(VII-27)}$$

$$c_1 = 2\kappa_6\delta + \frac{b_2\delta(\delta-1)}{3} + 2\kappa_5 \qquad \text{(VII-28)}$$

$$c_2 = b_2\delta \qquad \text{(VII-29)}$$

$$c_3 = -2\kappa_6\delta + b_2\left(\delta^2 + \frac{\delta}{3}\right) - 2\kappa_5 \qquad \text{(VII-30)}$$

$$c_4 = -\kappa_6\delta + b_2\left(\frac{\delta^2}{3} + \frac{\delta}{6}\right) - \kappa_5 \qquad \text{(VII-31)}$$

where $\delta = \frac{\tilde{\delta}_{(-)}}{\tilde{\delta}_{(+)}}$.

Substituting equations (VII-9), (VII-21) and (VII-22) into equations (VI-20) and (VI-31), there results

$$\frac{d\tilde{\delta}}{d\tilde{x}} = -\left(\frac{15}{3a_0^2 - a_0 - 2}\right)\left[\tilde{\delta}\,\frac{da_0}{d\tilde{x}}\left(\frac{6a_0 - 1}{15}\right) + \left(\frac{2(1-a_0)}{\tilde{\delta}}\right) - \kappa_7\tilde{\delta}\left(\tilde{H} - \frac{8+4a_0+3a_0^2}{30}\right)\right] \qquad \text{(VII-32)}$$

$$\frac{da_0}{d\tilde{x}} = \kappa_7 \left[\frac{\tilde{H}}{a_0} - \tfrac{1}{2} a_0 \right] - \frac{(1-a_0)}{\tilde{\delta}^2 a_0} \qquad \text{(VII-33)}$$

where $\kappa_7 = \dfrac{(\gamma-1) M_r^2 q_s \dfrac{dq_s}{d\tilde{x}}}{1 - \dfrac{\gamma}{2} M_r^2 q_s^2}$. Equations (VI-32) and (VI-33) are two differential equations in two dependent variables. The initial value for $\tilde{\delta}$ and a_0 can be approximated by appropriate curve fitting of the expanded velocity profile, which is found by assuming an isentropic expansion to the base pressure of the Blasius profile evaluated at the trailing edge of the wedge. This expanded velocity profile can be obtained from the solution of the following equations:

$$\frac{df_c}{d\eta_c} = f_c^{(1)} \qquad \text{(VII-34)}$$

$$\frac{df_c^{(1)}}{d\eta_c} = f_c^{(2)} \qquad \text{(VII-35)}$$

$$\frac{df_c^{(2)}}{d\eta_c} = -f_c f_c^{(2)} \qquad \text{(VII-36)}$$

$$\tilde{u} = \left\{ 2\tilde{H} \left[1 - \left(\frac{\bar{p}_e}{p_c} \right)^{\frac{\gamma-1}{\gamma}} \right] + \left(\frac{\bar{p}_e}{p_c} \right)^{\frac{\gamma-1}{\gamma}} \frac{\bar{u}_c}{u_e}^2 f_c^{(1)} 2 \right\}^{\frac{1}{2}} \qquad \text{(VII-37)}$$

$$\frac{d\tilde{y}}{dy_c} = \left(\frac{2Re_e}{Re_c} \right)^{\frac{1}{2}} \left(\frac{\bar{L}_c}{r_o} \frac{\bar{\rho}_c}{\rho_e} \frac{\bar{u}_c}{u_e} \right) \frac{f_c^{(1)}}{\tilde{u}} \qquad \text{(VII-38)}$$

Equations (VII-34), (VII-35) and (VII-36) are obtained from the Blasius equation. Equations (VII-37) and (VII-38) are obtained from equations (VI-33) through (VI-37)

and $y_c = \frac{\bar{y}_c}{L_c}$. The initial conditions for the system of differential equations (VII-34), (VII-35), (VII-36) and (VII-38) are

$$f_c(0) = f_c^{(1)}(0) = 0$$
$$f_c^{(2)} = 0.4696$$
$$\tilde{y}(0) = 0$$

Hence the Runge-Kutta method can be used to provide solutions for $\tilde{u}(\eta_c)$ and $\tilde{y}(\eta_c)$. A plot of $\tilde{u}(\tilde{y})$ gives the expanded velocity profile in the coordinate system of the modified Howarth transformation. For $\tilde{x} = 0$, it is assumed that

$$\tilde{u}(\tilde{y}) \cong 1 - (1 - a_0(0))\left(1 - \frac{\tilde{y}}{\tilde{\delta}(0)}\right)^2 \qquad \text{(VII-39)}$$

Therefore $a_0(0)$ and $\tilde{\delta}(0)$ can be determined approximately from the plot of the expanded velocity profile. The system of ordinary differential equations (VII-32) and (VII-33) can be solved numerically by using the Runge-Kutta method.

Substituting equations (VI-9), (VI-10) and (VI-11) into equations (VI-25), (VI-30) and (VI-32), there results

$$\frac{d}{d\tilde{x}}\left\{\tilde{\delta}_{(+)}\left[b_0^2 + b_0 b_1 + \frac{1}{3}\left(2b_0 b_2 + b_1^2\right) + \frac{1}{2}\left(b_0 b_3 + b_1 b_2\right) + \right.\right.$$
$$+ \frac{1}{5}\left(2b_0 b_4 + b_2^2 + 2b_1 b_3\right) + \frac{1}{3}\left(b_1 b_4 + b_2 b_3\right)$$
$$\left.\left. + \frac{1}{7}\left(b_3^2 + 2b_2 b_4\right) + \frac{1}{4} b_3 b_4 + \frac{1}{9} b_4^2\right]\right\}$$
$$- \left(1 + 2\kappa \frac{(1-a_0)\Delta}{a_0}\right) \frac{d}{d\tilde{x}}\left[\tilde{\delta}_{(+)}\left(b_0 + \frac{b_1}{2} + \frac{b_2}{3} + \frac{b_3}{4} + \frac{b_4}{5}\right)\right]$$

$$= \left(-\frac{1}{a_0}\frac{da_0}{d\tilde{x}}\tilde{\delta}_{(+)}\right)\left\{2b_0^2 + 2b_0b_1 + \frac{2}{3}\left(2b_0b_2 + b_1^2\right)\right.$$

$$+ \left(b_0b_3 + b_1b_2\right) + \frac{2}{5}\left(2b_0b_4 + b_2^2 + 2b_1b_3\right)$$

$$+ \frac{2}{3}\left(b_1b_4 + b_2b_3\right) + \frac{2}{7}\left(b_3^2 + 2b_2b_4\right) + \frac{1}{2}b_3b_4 + \frac{2}{9}b_4^2$$

$$\left. - \left[1 + 2\kappa\frac{(1-a_0)}{a_0}\left(\frac{\tilde{\delta}_{(+)}}{\tilde{\delta}}\right)\right]\left(b_0 + \frac{b_1}{2} + \frac{b_2}{3} + \frac{b_3}{4} + \frac{b_4}{5}\right)\right\}$$

$$+ \frac{1}{\tilde{\delta}_{(+)}a_0}\left\{\left(\frac{\tilde{\delta}_{(+)}}{\tilde{\delta}}\right)\left[\frac{2(1-a_0)}{a_0} - \kappa\left(\frac{\delta_{(+)}}{\tilde{\delta}}\right)\left(\frac{1-a_0}{a_0}\right)\right] - b_1\right\}$$

$$+ \kappa_7\tilde{\delta}_{(+)}\left\{\frac{\tilde{H}}{a_0^2} - \frac{1}{2}\left[b_0^2 + b_0b_1 + \frac{1}{3}\left(2b_0b_2 + b_1^2\right)\right.\right.$$

$$+ \frac{1}{2}\left(b_0b_3 + b_1b_2\right) + \frac{1}{5}\left(2b_0b_4 + b_2b_3\right) + \frac{1}{7}\left(b_3^2 + 2b_2b_4\right)$$

$$\left.\left. + \frac{1}{4}b_3b_4 + \frac{1}{9}b_4^2\right]\right\} \qquad \text{(VII-40)}$$

$$\frac{d}{d\tilde{x}}\left\{\tilde{\delta}_{(+)}\left[c_0^2 - c_0c_1 + \frac{1}{3}\left(2c_0c_2 + c_1^2\right)\right.\right.$$

$$- \frac{1}{2}\left(c_0c_3 + c_1c_2\right) + \frac{1}{5}\left(2c_0c_4 + c_2^2 + 2c_1c_3\right)$$

$$\left.\left. - \frac{1}{3}\left(c_1c_4 + c_2c_3\right) + \frac{1}{7}\left(c_3^2 + 2c_2c_4\right) - \frac{1}{4}c_3c_4 + \frac{1}{9}c_4^2\right]\right\}$$

$$- \left(\frac{\bar{q}_r}{\bar{u}_e}\right)\left(\frac{q_s}{a_0}\right)\frac{d}{d\tilde{x}}\left[\tilde{\delta}_{(+)}\left(c_0 - \frac{c_1}{2} + \frac{c_2}{3} - \frac{c_3}{4} + \frac{c_4}{5}\right)\right]$$

$$= -\left(\frac{1}{a_0}\frac{da_0}{d\tilde{x}}\tilde{\delta}_{(+)}\right)\left[2c_0^2 - 2c_0c_1 + \frac{2}{3}\left(2c_0c_2 + c_1^2\right) - \left(c_0c_3 + c_1c_2\right)\right.$$

$$+ \frac{2}{5}\left(2c_0c_4 + c_2^2 + 2c_1c_3\right) - \frac{2}{3}\left(c_1c_4 + c_2c_3\right) + \frac{2}{7}\left(c_3^2 + 2c_2c_4\right)$$

$$\left. - \frac{1}{2}c_3c_4 + \frac{2}{9}c_4^2\right] - \left[\left(\frac{\bar{q}_r}{\bar{u}_e}\right)\left(\frac{q_s}{a_0}\right)\tilde{\delta}_{(+)}\right]\left(c_0 - \frac{c_1}{2} + \frac{c_2}{3} - \frac{c_3}{4} + \frac{c_4}{5}\right)$$

$$+ \frac{c_1}{a_0\tilde{\delta}_{(-)}} + \kappa_7\tilde{\delta}_{(-)}\left\{\frac{\tilde{H}}{a_0^2} - \frac{1}{2}\left[c_0^2 - c_0c_1 + \frac{1}{3}\left(2c_0c_2 + c_1^2\right)\right.\right.$$

$$- \frac{1}{2}\left(c_0c_3 + c_1c_2\right) + \frac{1}{5}\left(2c_0c_4 + c_2^2 + c_2^2 + 2c_1c_3\right) - \frac{1}{3}\left(c_1c_4 + c_2c_3\right)$$

$$\left.\left. + \frac{1}{7}\left(c_3^2 + 2c_2c_4\right) - \frac{1}{4}c_3c_4 + \frac{1}{9}c_4^2\right]\right\} \qquad \text{(VII-41)}$$

$$\frac{db_0}{d\tilde{x}} = -\frac{b_0}{a_0}\frac{da_0}{d\tilde{x}} + \kappa_7\left(\frac{\tilde{H}}{a_0^2b_0} - \frac{b_0}{2}\right) \qquad \text{(VII-42)}$$

By using equations (VII-13) through (VII-33) equations (VII-40), (VII-41) and (VII-42) may be reduced to a system of three ordinary differential equations with dependent variables b_2, $\tilde{\delta}_{(+)}$, and $\tilde{\delta}_{(-)}$. Since this system of ordinary differential equations involves all the profile coefficients and thicknesses and their derivatives with respect to $\tilde{x}$ in a very complicated manner, these equations will be rearranged so that the numerical solution can be conveniently obtained by using a digital computer. In general equations (VII-40), (VII-41) and (VII-42) can be written as

$$Q_{11}\frac{db_2}{d\tilde{x}} + Q_{12}\frac{d\tilde{\delta}_{(+)}}{d\tilde{x}} + Q_{13}\frac{d\tilde{\delta}_{(-)}}{d\tilde{x}} = Q_1 \qquad \text{(VII-43)}$$

$$Q_{21}\frac{db_2}{d\tilde{x}} + Q_{22}\frac{d\tilde{\delta}_{(+)}}{d\tilde{x}} + Q_{23}\frac{d\tilde{\delta}_{(-)}}{d\tilde{x}} = Q_2 \qquad \text{(VII-44)}$$

$$Q_{33}\frac{db_2}{d\tilde{x}} + Q_{32}\frac{d\tilde{\delta}_{(+)}}{d\tilde{x}} + Q_{33}\frac{d\tilde{\delta}_{(-)}}{d\tilde{x}} = Q_3 \qquad \text{(VII-45)}$$

where the Q_{mn}'s are functions of b_2, $\tilde{\delta}_{(+)}$, $\tilde{\delta}_{(-)}$, a_0, $\tilde{\delta}$, and q_s, and the Q_m's are functions of b_2, $\tilde{\delta}_{(+)}$, $\tilde{\delta}_{(-)}$, a_0, $\tilde{\delta}$, q_s, $\frac{da_0}{d\tilde{x}}$, $\frac{dq_s}{d\tilde{x}}$. The Q_{mn}'s are given in the Appendix. Defining

$$G_{11} = \frac{Q_{12}}{Q_{11}} - \frac{Q_{22}}{Q_{21}}$$

$$G_{12} = \frac{Q_{13}}{Q_{11}} - \frac{Q_{23}}{Q_{21}}$$

$$G_1 = \frac{Q_1}{Q_{11}} - \frac{Q_2}{Q_{21}}$$

$$G_{21} = \frac{Q_{22}}{Q_{21}} - \frac{Q_{32}}{Q_{31}}$$

$$G_{22} = \frac{Q_{23}}{Q_{21}} - \frac{Q_{33}}{Q_{31}}$$

$$G_2 = \frac{Q_2}{Q_{21}} - \frac{Q_3}{Q_{31}}$$

then one can obtain

$$\frac{db_2}{d\tilde{x}} = \left(\frac{Q_1}{Q_{11}}\right) - \left(\frac{Q_{12}}{Q_{11}}\right) \frac{\left[\frac{G_1}{G_{12}} - \frac{G_{12}}{G_{22}}\right]}{\left[\frac{G_{11}}{G_{12}} - \frac{G_{21}}{G_{22}}\right]} - \left(\frac{Q_{13}}{Q_{11}}\right) \frac{\left[\frac{G_1}{G_{11}} - \frac{G_{12}}{G_{21}}\right]}{\left[\frac{G_{12}}{G_{11}} - \frac{G_{22}}{G_{21}}\right]} \qquad \text{(VII-46)}$$

$$\frac{d\tilde{\delta}_{(+)}}{d\tilde{x}} = \frac{\left[\frac{G_1}{G_{12}} - \frac{G_{12}}{G_{22}}\right]}{\left[\frac{G_{11}}{G_{12}} - \frac{G_{21}}{G_{22}}\right]} \qquad \text{(VII-47)}$$

$$\frac{d\tilde{\delta}_{(-)}}{d\tilde{x}} = \frac{\left[\frac{G_1}{G_{11}} - \frac{G_{12}}{G_{21}}\right]}{\left[\frac{G_{12}}{G_{11}} - \frac{G_{22}}{G_{21}}\right]} \qquad \text{(VII-48)}$$

The initial values for $\tilde{b}_2$, $\tilde{\delta}_{(+)}$, and $\tilde{\delta}_{(-)}$ may be approximated by appropriate curve fitting of the similarity velocity profile, for the mixing between a uniform stream and a fluid at rest, evaluated at a fixed but small $\tilde{x} = \tilde{x}_0$. Therefore, for $\tilde{y} \geq 0$, equation (VI-43) can be written as

$$\sum_0^4 b_n(\tilde{x}_0) \left(\frac{\tilde{y}}{\tilde{\delta}_{(+)}}\right)^n \cong f_0' \left(\sqrt{\frac{a_0(0)}{2\tilde{x}_0}}\ \tilde{y}\right)$$

for $\tilde{y} \leq 0$, equation (VI-44) can be written as

$$\sum_0^4 c_n(\tilde{x}_0) \left(\frac{\tilde{y}}{\tilde{\delta}_{(-)}}\right)^n \cong f_0' \left(\sqrt{\frac{a_0(0)}{2\tilde{x}_0}}\ \tilde{y}\right)$$

Since $b_n(\tilde{x}_0)$ and $c_n(\tilde{x}_0)$ are given by equations (VII-13) through (VII-31), which are functions of $b_2(\tilde{x}_0)$, $\tilde{\delta}_{(+)}(\tilde{x}_0)$, $\tilde{\delta}_{(-)}(\tilde{x}_0)$, $a_0(0)$, and $\tilde{\delta}(0)$, and since $f_0'\left(\sqrt{\frac{a_0(0)}{2\tilde{x}_0}}\ \tilde{y}\right)$, $a_0(0)$, and $\tilde{\delta}(0)$ are known, $b_2(\tilde{x}_0)$, $\tilde{\delta}_{(+)}(\tilde{x}_0)$, and $\tilde{\delta}_{(-)}(\tilde{x}_0)$ can be determined approximately from the plot of $f_0'\left(\sqrt{\frac{a_0(0)}{2\tilde{x}_0}}\ \tilde{y}\right)$. Hence the system of ordinary differential equations (VII-46), (VII-47) and (VII-48) can be solved numerically by using the Runge-Kutta method.

Since the shear stress distribution along the base of the wedge and the dividing streamline can be determined, and since the dividing streamline is assumed straight, the conservation of angular momentum of the recirculation region requires that

$$\left(\int_0^{\bar{L}_r} \bar{\tau}_b\, d\bar{X}\right)\bar{R}_b = \left(\int_0^{\bar{r}_o} \bar{\tau}\, dx\right)\bar{R}_d \qquad \text{(VII-49)}$$

where $\bar{R}_b$ and $\bar{R}_d$ are the perpendicular distance from the base of the wedge and the dividing streamline to the center of rotation respectively, which, for a given wake angle, can be determined from the solution of the inviscid core flow. From equations (VII-7) and (VII-0), the above equation can be rewritten as

$$\left(\frac{\bar{\mu}_e \bar{u}_e Re_e^{\frac{1}{2}} \bar{R}_d}{\bar{r}_o}\right)\int_0^1 \frac{a_0 b_1}{\delta_{(+)}}\, dx = \left(\frac{\bar{\mu}_r \bar{q}_r Re_r^{\frac{1}{2}} \bar{R}_b}{\bar{L}_r}\right)\int_0^1 \frac{q_b^2}{\theta_0}\, dX \qquad \text{(VII-50)}$$

By using the linear viscosity law, $\frac{\bar{L}_r}{\bar{r}_o} \cong \bar{\theta}_o$, $p\dagger_{\tilde{y}\dagger} = O(\epsilon)$, and the equation of state, the above equation reduces to

$$\bar{q}_r^{3/2} = \left(\frac{\bar{T}_e}{\bar{T}_r}\right)^{\frac{1}{2}} \left(\bar{\theta}_o\right)^{-\frac{1}{2}} \left(\frac{\bar{R}_d}{\bar{R}_b}\right) \left[\frac{\int_0^1 \frac{a_0 b_1}{\delta_{(+)}}\, dx}{\int_0^1 \frac{q_b^2}{\bar{\theta}_0}\, dX}\right] \bar{u}_e^{3/2} \qquad \text{(VII-51)}$$

Since $\bar{q}_r = \bar{\omega}_r \bar{L}_r/2$ and $\bar{\omega}_r = \bar{\omega}_0$, the equilibrium rate of rotation for the inviscid core fluid can be obtained for a given wake angle:

$$\bar{\omega}_0 = \left(\frac{2}{\bar{L}_r}\right)\left(\frac{\bar{T}_e}{\bar{T}_r}\right)^{1/3} \left(\bar{\theta}_o\right)^{-1/3} \left(\frac{\bar{R}_d}{\bar{R}_b}\right)^{2/3} \left[\frac{\int_0^1 \frac{a_0 b_1}{\delta_{(+)}}\, dx}{\int_0^1 \frac{q_b^2}{\bar{\theta}_0}\, dX}\right] \bar{u}_e \qquad \text{(VII-52)}$$

Accordingly, for a given $\bar{\theta}_o$, there exists an equilibrium $\bar{\omega}_0$ which in turn provides a velocity profile for the shear layer at $x = 1$. Hence the pressure at the rear stagnation point can be obtained from the local Mach number at $x = 1$ and $y = 0$. Since $\bar{u} = a_0(1)\, b_0(1)\, \bar{u}_e$ and $\bar{T} = \frac{\bar{u}_e^2}{\bar{c}_p}\left[\tilde{H} - \frac{1}{2} a_0^2(1)\, b_0^2(1)\right]$, then

$$\left[M_d(\bar{\theta}_o)\right]_{x=1} = \frac{a_0(1) b_0(1)}{\sqrt{(\gamma-1)\left(\tilde{H} - \frac{1}{2} a_0^2(1)\, b_0^2(1)\right)}} \qquad \text{(VII-53)}$$

and the recompression ratio for the dividing streamline is

$$\frac{\bar{p}_{stagnation}}{\bar{p}_b} = \left\{1 + \frac{\gamma-1}{2}\left[M_d(\theta_o)\right]_{x=1}^2\right\}^{\frac{\gamma}{\gamma-1}} \qquad \text{(VII-54)}$$

2. Evaluation of Results and Comparison with Experimental Data

The theoretical model studied previously concerns the laminar near wake behind a slender wedge as $Re_e \to \infty$. However, for finite but relatively large R_e with a laminar near wake, this model should provide reasonably accurate results. Computation have been carried out for the flow over a wedge with $\bar{\theta}_c = 6^o$ and $\bar{L}_c = 0.399$ under the following upstream conditions:

$$M_\infty = 2.61 \text{ and } 3.51 \; ; \; Re_c = 2 \times 10^5$$

For these given conditions, the experimental results show that the near wake is laminar but very close to the transition range; the wake angle is quite small; the lip-shock strength is relatively small; the recompression region is not too long and the boundary-layer thickness is still small. Above all, the prevailing reason for choosing these upstream conditions is that these are the available experimental conditions closest to the theoretical model, and a comparison can be made between the theoretical and the experimental results. Based on the above given conditions, it can be shown that, for a flow with total temperature equal to 1000^oR, the flow properties after the wedge shock are

$$M_c = 2.34, \quad \bar{T}_c = 477.3^oR \; , \quad \bar{\rho}_c = 0.678 \times 10^{-4} \text{ slug/ft}^3$$

$$u_c = 2500 \text{ ft/sec}, \quad \bar{u}_c = 0.338 \times 10^{-6} \text{ lb-sec/ft}^2 \text{ for } M_\infty = 2.61$$

$$M_c = 3.14, \quad \bar{T}_c = 336.5^oR, \quad \bar{\rho}_c = 0.422 \times 10^{-4} \text{ slug/ft}^3$$

$$\bar{u}_c = 2810 \text{ ft/sec}, \quad \bar{\mu}_c = 0.236 \times 10^{-6} \text{ lb-sec/ft}^2 \text{ for } M_\infty = 3.51$$

The flow properties corresponding to the conditions at the outer edge of the shear layer and the recirculation region may be obtained provided that the wake angle

is known. The flow properties after the corner expansion are

$$\left.\begin{aligned} &M_e = 3.01, \quad \bar{T}_e = 356^{\circ}R, \quad \bar{\rho}_e = 0.323 \times 10^{-4} \ \text{slug/ft}^3 \\ &\bar{u}_e = 2780 \ \text{ft/sec}, \quad \bar{\mu}_e = 0.25 \times 10^{-6} \ \text{lb-sec/ft}^2 \\ &Re_e = 0.998 \times 10^5 \end{aligned}\right\} \begin{aligned} &\text{for } M_\infty = 2.61 \\ &\bar{\theta}_o = 8.7^{\circ} \end{aligned}$$

$$\left.\begin{aligned} &M_e = 4.28, \quad \bar{T}_e = 211^{\circ}R, \quad \bar{\rho}_e = 0.133 \times 10^{-4} \ \text{slug/ft}^3 \\ &\bar{u}_e = 3074 \ \text{ft/sec}, \quad \bar{\mu}_e = 0.15 \times 10^{-6} \ \text{lb-sec/ft}^2 \\ &Re_e = 0.602 \times 10^5 \end{aligned}\right\} \begin{aligned} &\text{for } M_\infty = 3.51 \\ &\bar{\theta}_o = 10.7^{\circ} \end{aligned}$$

The flow properties in the recirculation region are

$$\bar{T}_r = 1000^{\circ}R, \quad \bar{\mu}_r = 0.71 \times 10^{-6} \ \text{lb-sec/ft}^2$$

and

$$\bar{\rho}_r = 0.115 \times 10^{-4} \ \text{slug/ft}^3 \qquad \text{for } M_\infty = 2.61$$

$$\bar{\rho}_r = 0.281 \times 10^{-5} \ \text{slug/ft}^3 \qquad \text{for } M_\infty = 3.51$$

Since the complete solution for the inviscid core flow is given by equation (IV-29), the streamlines in the inviscid core flow for $\bar{\theta}_o = 10^{\circ}$ are drawn. Figure (4a) shows the streamline pattern when coordinates are nondimensionalized by the wake length. Figure (4b) shows the streamline pattern with the abscissa normalized by the length of the wake and the ordinate normalized by the base height. The flow velocity is relatively high in a region within a distance equal to the base height from the base of the wedge, and decreases gradually toward the rear stagnation point. It can be shown that the distance between the center of rotation and the base of the wedge increases as $\bar{\theta}_o$ increases.

Figure 5 through figure 8 are drawn for $M_\infty = 2.61$, $Re_c = 2 \times 10^5$,

and for $\bar{\theta}_o = 8.7^o$. This $\bar{\theta}_o$ satifies the reattachment condition and the requirement of conservation of angular momemtum in the recirculation region. For a given $\bar{\theta}_o$, equations (VII-1) through (VII-6) can provide a numerical solution for the base boundary layer. The shear stress along the base of the wedge is shown in figure 5. This increases very rapidly with θ for $\theta < 0.2$, because the inviscid core flow has a large acceleration for $r = 1$ and $\theta < 0.2$. Since the inviscid core flow decelerates for $r = 1$ and $\theta > 0.5$, the shear stress diminishes rather rapidly and approaches zero near $\theta = 0.8$. Figure 6 shows the velocity profiles at $\theta = 0, 0.15, 0.30, 0.45$, and 0.60. The boundary-layer thickness grows gradually for $\theta \leq 0.5$ but increases very fast for $\theta > 0.5$. The integral method used appears to predict separation, which may occur near $\theta = 0.8$. The stagnation-point velocity profile obtained from the similarity solution is also shown in order that a comparison can be made between the similarity solution and the solution from the method of integral relations for $\theta = 0$. It is evident that the method of integral relations gives a fairly accurate velocity profile for $U < 0.9$. The accuracy will certainly be improved, if the order of approximation K in (V) is increased.

When $\bar{\theta}_o$ is given, the initial velocity profile for the shear layer can be determined. Therefore the numerical solution can be obtained for the shear layer equations (VII-46) through (VII-48). Figure 7 shows the shear stress distribution along the dividing streamline. Initially the shear stress is very large, because the inviscid core flow velocity is very small, at $\theta = 1$ and for $r \to 1$,

and the shear sublayer is extremely thin. Since the inviscid core flow has large acceleration for $\theta = 1$ and $r > 0.85$ (or $\frac{\bar{x}}{r_o} < 0.15$), and since the thickness of the shear sublayer grows fairly rapidly for $r > 0.85$, the shear stress along the dividing streamline declines rather quickly. The shear stress decreases slowly for $r < 0.85$, because the shear sublayer grows rather slowly and the velocity of the inviscid core flow decreases gradually. Figure 8 gives the velocity profiles for the shear-layer at $x = 0.05$, 0.2, 0.45, 0.7, and 1.0. For x small the change in velocity profile is large near the dividing streamline. As x increases this change in velocity profile spreads out to a larger region on each side of the dividing streamline. The velocity profile for the portion of the shear layer with high kinetic energy changes fairly slowly throughout the whole near-wake region.

Figure 9 shows the curves used to obtain the wake angle, which in turn determines the base pressure. The solid curve is obtained from equation (VII-54), which furnishes the recompression ratio along the dividing streamline for $M_\infty = 2.61$ and for an equilibrium rate of rotation for the inviscid core flow. When a uniform supersonic flow is turned through a given angle from a specified initial static pressure, the final value of the pressure depends on the initial value of the Mach number, and the final pressure has a minimum value for a particular initial Mach number. Hence a minimum compression ratio can be determined and is shown by the dotted line. The intersection between the solid and the dotted curves provides an appropriate wake angle and recompression ratio,

which in turn gives the base pressure. This intersection point satifies the re-attachment condition. Since figure 9 gives $\bar{\theta}_o = 8.7^o$, and $\bar{p}/\bar{p}_b = 1.52$, the corresponding equilibrium rate of rotation for inviscid core flow is $\bar{\omega}_0 \cong -60000$ rad/sec., and $\bar{p}_b/\bar{p}_\infty = 0.538$. Hence $\bar{q}_r = 1250$ ft/sec., $Re_r = 0.844 \times 10^3$, $M_r = 0.806$. The experimental results given by Hama for $Re_c = 2 \times 10^6$ and $M_\infty = 2.61$ show that $\bar{\theta}_o \cong 7.5^o$; $\bar{p}_b/\bar{p}_\infty \cong 0.56$ and the lip-shock strength is approximately equal to 1.25. Consequently, the computed and the experimental results agree fairly well for this case.

For $Re_c = 2 \times 10^6$ and $M_\infty = 3.51$, the theoretical model predicts that $\bar{\theta}_o \cong 10.7^o$, $\bar{p}_b/\bar{p}_\infty = 0.36$, $\bar{q}_r = 1190$ ft/sec., and $Re = 0.196 \times 10^3$ and $M_r = 0.78$. The experimental results given by Hama show that $\bar{\theta}_o \cong 8.5^o$, $\bar{p}_b/\bar{p}_\infty = 0.45$ and the lip-shock strength is approximately equal to 1.4. The predicted results are less accurate for this case.

VIII

CONCLUSIONS

A theoretical description has been presented for the flow in the laminar near wake of a slender wedge at supersonic speed and high Reynolds number. This study consists of separate analyses for the various near-wake regions having different physical character. The solutions for these regions must be matched through the condition of the conservation of angular momentum for the recirculation region and the proposed reattachment condition, so that the near-wake flow is uniquely determined.

As the Reynolds number approaches infinity as a limit, the thickness of the laminar viscous layers enclosing the recirculating flow is of order $Re_e^{-\frac{1}{2}}$, and the flow in the interior of the recirculation region may be considered as inviscid and nonconducting. The typical velocity of the recirculating flow must be of the same order as that of the external flow, although numerically it is considerably smaller. The Reynolds number Re_r for the recirculation region differs from Re_e through factors involving powers of M_e. Therefore, in the limit $Re_e \to \infty$ with M_e fixed, Re_r will also approach infinity. Since M_r is fairly small, in the zeroth-order approximation the recirculating flow may be regarded as incompressible. The inviscid incompressible recirculating flow has constant vorticity and constant temperature. The effect of compressibility is estimated to be rather small.

The inviscid incompressible recirculating flow in the right triangular region is characterized by the small wake angle $\bar{\theta}_o$. Hence the stream function

$\bar{\psi}$ may be expanded in a power series in $\bar{\theta}_o$, and an approximate solution may be obtained analytically. The zeroth-order solution for $\bar{\psi}$ is symmetric about = the first-order solution for $\bar{\psi}$ does not have this symmetry. It is not possible to obtain a second-or higher-order solution, because the representation for one of the boundary conditions is not a uniformly convergent series. The flow velocity is high in a region within a distance of the order of the base height from the base of the wedge. The maximum flow velocity is approximately $0.85\,\bar{q}_r = 0.85\,(\bar{\omega}_r \bar{L}_r/2)$, and the distance between the base of the wedge and the center of rotation increases as $\bar{\theta}_o$ increases. It should be mentioned that the formulation in terms of a right triangular region assumes that secondary eddies either do not occur or have negligible effect.

In general the shear stress along the base is large for $\theta < 0.5$, because the flow is accelerating. The shear stress declines rather rapidly for $\theta > 0.5$ due to the adverse pressure gradient. The boundary-layer thickness grows gradually for $\theta < 0.5$ and more rapidly for $\theta > 0.5$. Although the integral method predicts boundary-layer separation near $\theta = 0.8$, it is believed that, due to the suction effect of the shear layer near the trailing edge of the wedge, the separation will be delayed.

The development of the shear layer is investigated by including the effects of the finite initial thickness, the trailing-edge expansion, the nonzero inner-edge velocity, and the equalization of the pressure across the shear layer up to $O(Re_e^{-1})$. However, it is not necessary to consider the details of the cor-

ner expansion, because only a small distance is required for the completion of the expansion, and because the lip-shock strength is rather small (pressure ratio 1.25 for $M_\infty = 2.61$ and 1.40 for $M_\infty = 3.51$). The portion of the velocity profile with high kinetic energy remains nearly unchanged throughout the near-wake region, but the portion of the velocity profile near the dividing streamline is changed greatly. These results suggest that it is indeed appropriate to divide the shear layer into an outer shear layer and a shear sublayer, and that the changes in the outer shear layer actually could have been neglected. Initially the thickness of the shear sublayer grows rapidly, and the shear stress along the dividing streamline declines rapidly.

The proposed reattachment condition is based on the minimum pressure increase attainable at the rear stagnation point from the turning of a streamline in the shear layer to a direction parallel to the wake center line. This condition and the requirement that angular momentum be conserved in the recirculation region are used to obtain a unique solution for the base pressure and hence for the near-wake flow. For $M_\infty = 2.61$ and $Re_c = 2 \times 10^5$, the predicted values for $\bar{\theta}_o$ and $\bar{p}_b/\bar{p}_\infty$ are fairly close to the experimental results[2]. However, for $M_\infty = 3.51$ and $Re_c = 2 \times 10^5$, the predicted values are less satisfactory, because of the smaller value of Re_r.

The deviation of the predicted values for $M_\infty = 2.61$ from the experimental results is probably caused mainly by the inadequacy of the proposed reattachment condition. The experimental results show that the flow is only

partially recompressed at reattachment. The theoretical reattachment condition proposed by Chapman[9] assumes that the recompression is completed, and is bound to result in disagreement between the predicted and the measured values of the base pressure. The present reattachment condition is intended to remedy this inadequacy. However, since the predicted base pressure is too low it seems that this reattachment condition does not provide sufficient recompression. By requiring that a different streamline be turned to a direction parallel to the wake center line, one can obtain values of $\bar{\theta}_o$ and $\bar{p}_b / \bar{p}_\infty$ which are significantly closer to the experimental results.

It is known that the separation along the base occurs somewhere below the trailing edge, that the dividing streamline is slightly curved, and that the center of rotation is displaced because of the base boundary layer. The errors which result from neglecting these effects will influence the geometry of the inviscid recirculating flow. The corresponding changes in $\bar{\theta}_o$ and $\bar{p}_b$ arise primarily from a change in the length of the near wake, and can be shown to be quite small, of the order of a few per cent.

For $M_\infty = 2.61$ and $Re_c = 2 \times 10^5$, the thickness of the base boundary layer at a distance of half the base height from the wake center line is approximately 0.07", and the thickness of the lower shear sublayer at $x = \frac{1}{2}$ is approximately 0.05". Since the base height is 0.5", these values indicate that there exists a quite large region of inviscid recirculating flow. Even for $M_\infty = 3.51$ and $Re_c = 2 \times 10^5$ a significant portion of the recirculating flow may be des-

cribed as approximately inviscid. Therefore, for a relatively large Reynolds number the present model does give a fairly good representation of the actual flow. For large M_∞, however, the trailing-edge expansion region and the recompression region are no longer small, the lip shock is stronger, the wake Reynolds number is smaller, and the wake angle is larger. These features are all incorporated in the analysis carried out by Weiss.[19]

In order to understand the near-wake flow more thoroughly it would be necessary to study the recompression and the trailing-edge expansion regions. As mentioned before, the present reattachment condition does not give sufficient pressure recovery. To obtain a more accurate reattachment condition and to verify the assumption of isentropic recompression within a narrow region, it would be necessary to study the recompression region in more detail. The separation processes, the behavior of the base boundary layer approaching the separation point, and the formation of the lip shock could be better understood through the investigation of the trailing-edge expansion region. The dependence of $\bar{p}_b$ and $\bar{\theta}_o$ on Reynolds number does not appear in the current approximation. A first approximation for this dependence could presumably be derived after studying the recompression region and the trailing-edge expansion region.

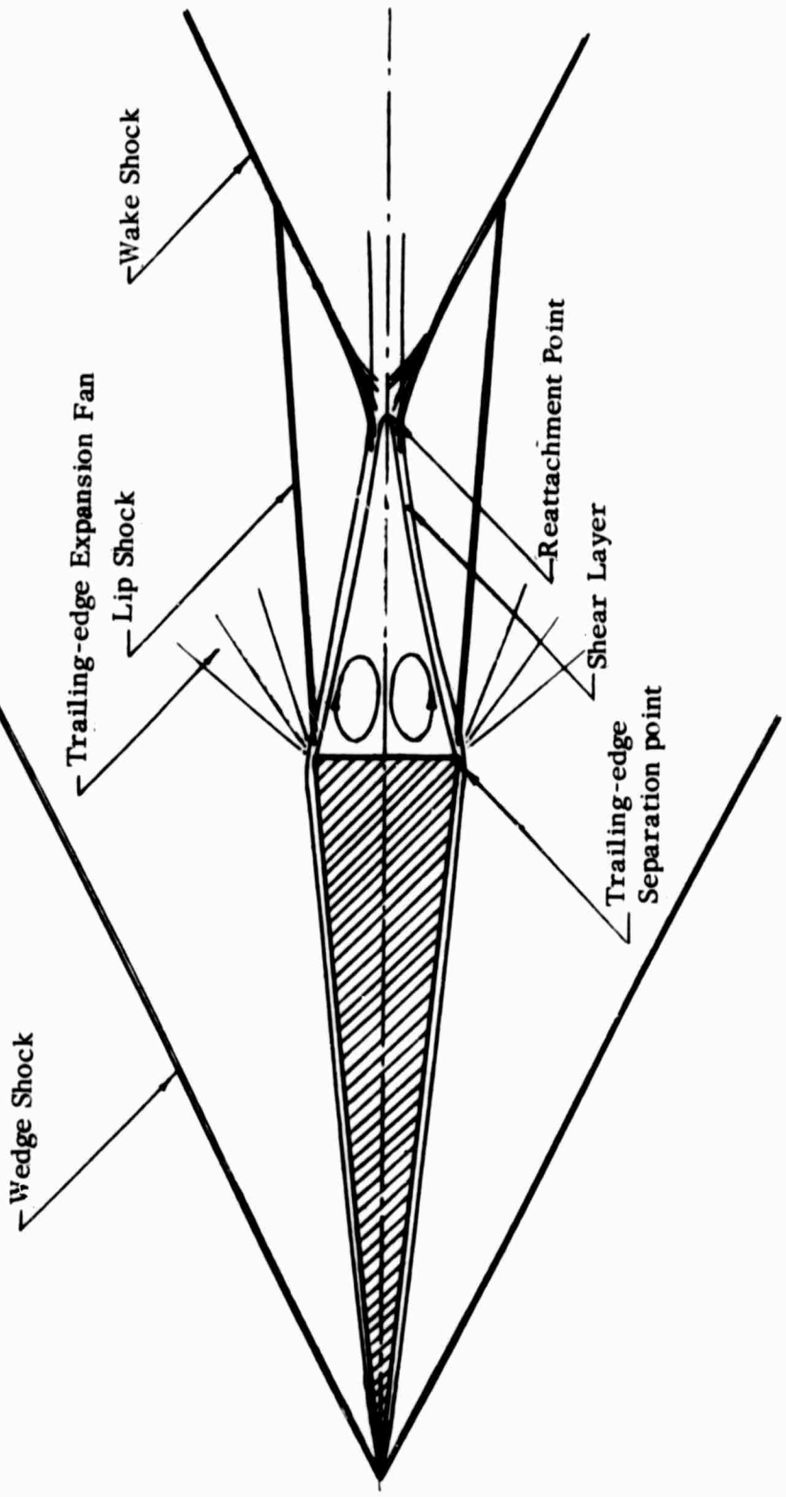

Figure 1: Slender Wedge in Supersonic Flow

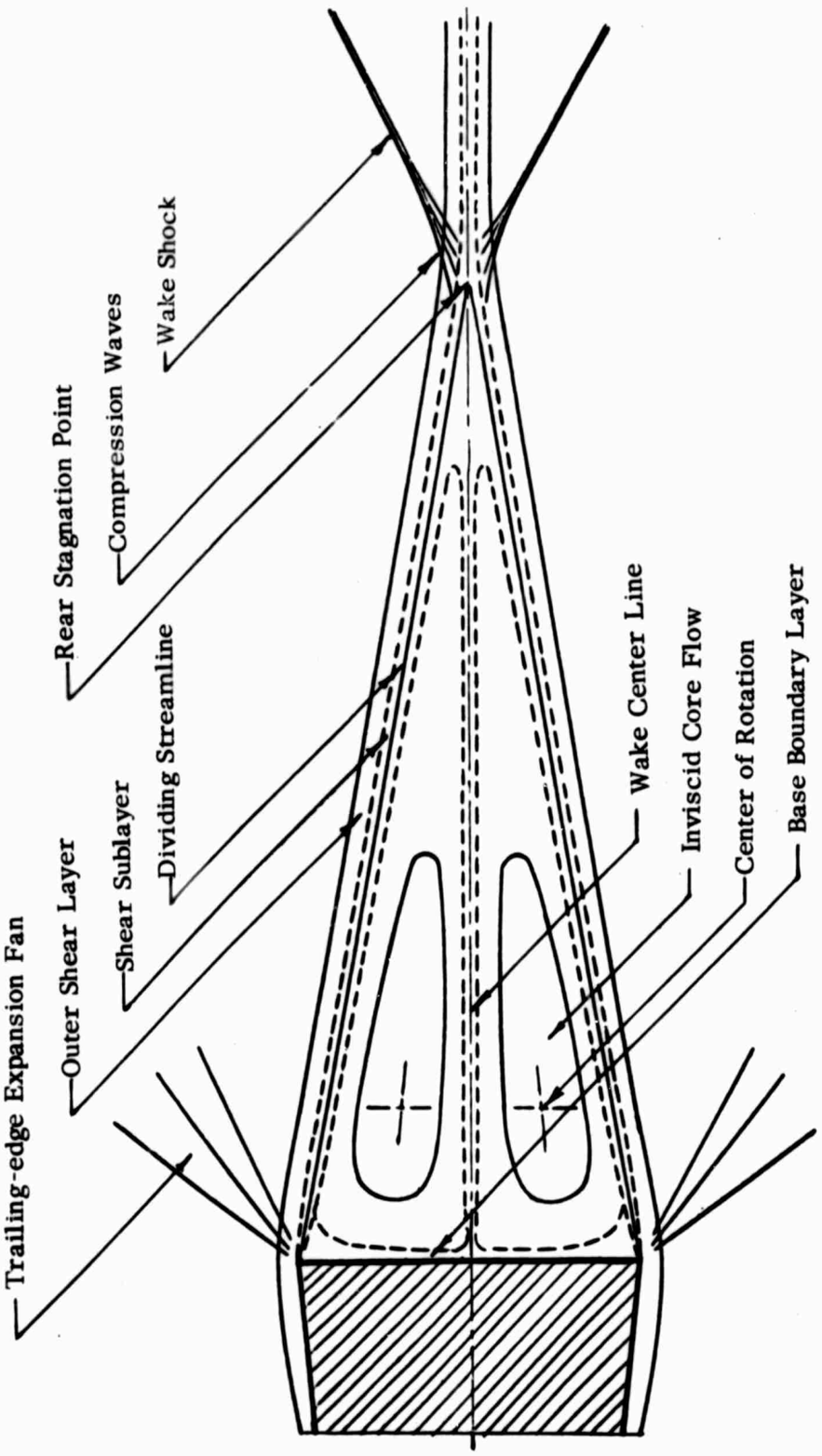

Figure 2: Proposed Model for the Near Wake of Slender Wedge in Supersonic Flow

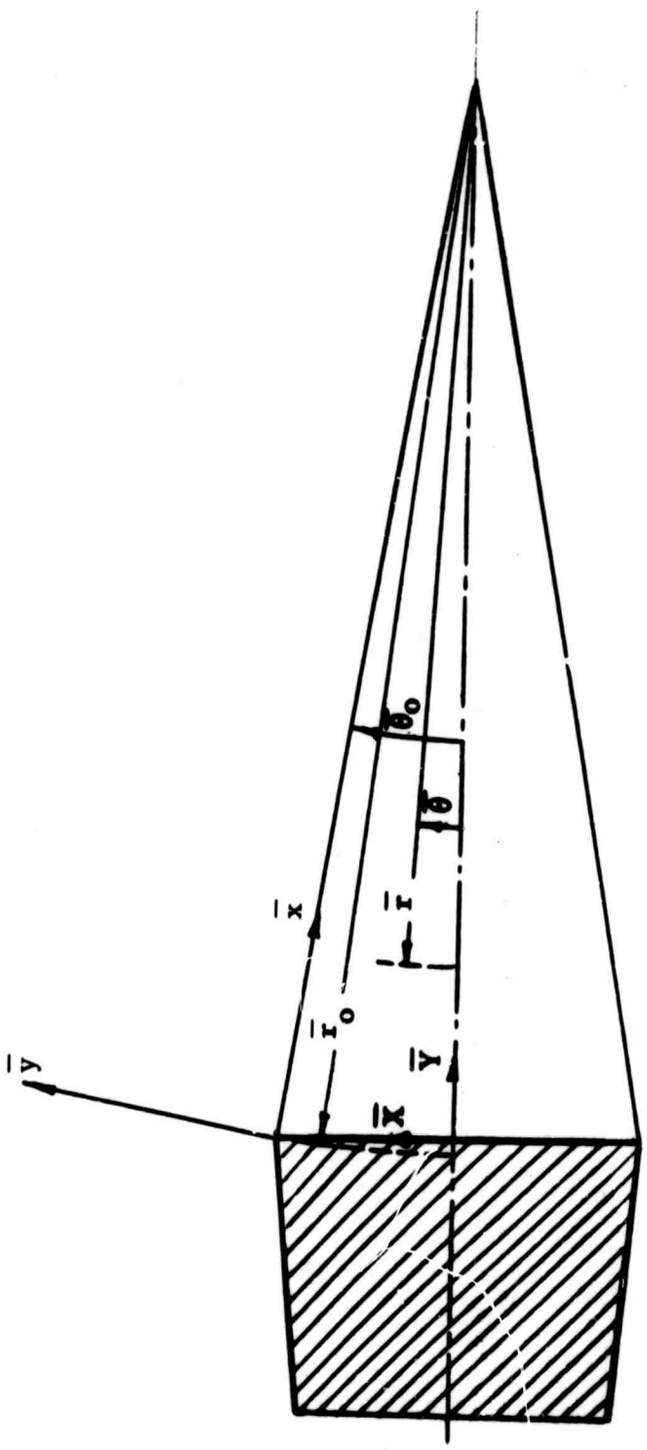

Figure 3: Coordinate Systems

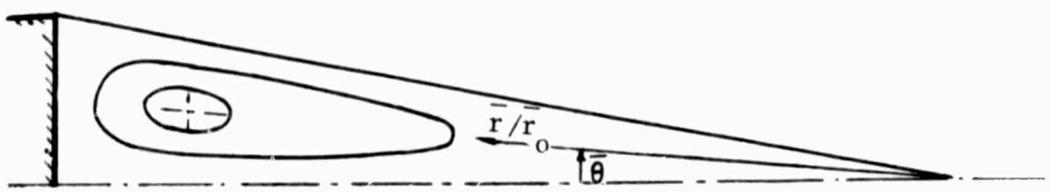

(a) Streamline Pattern Drawn to Scale

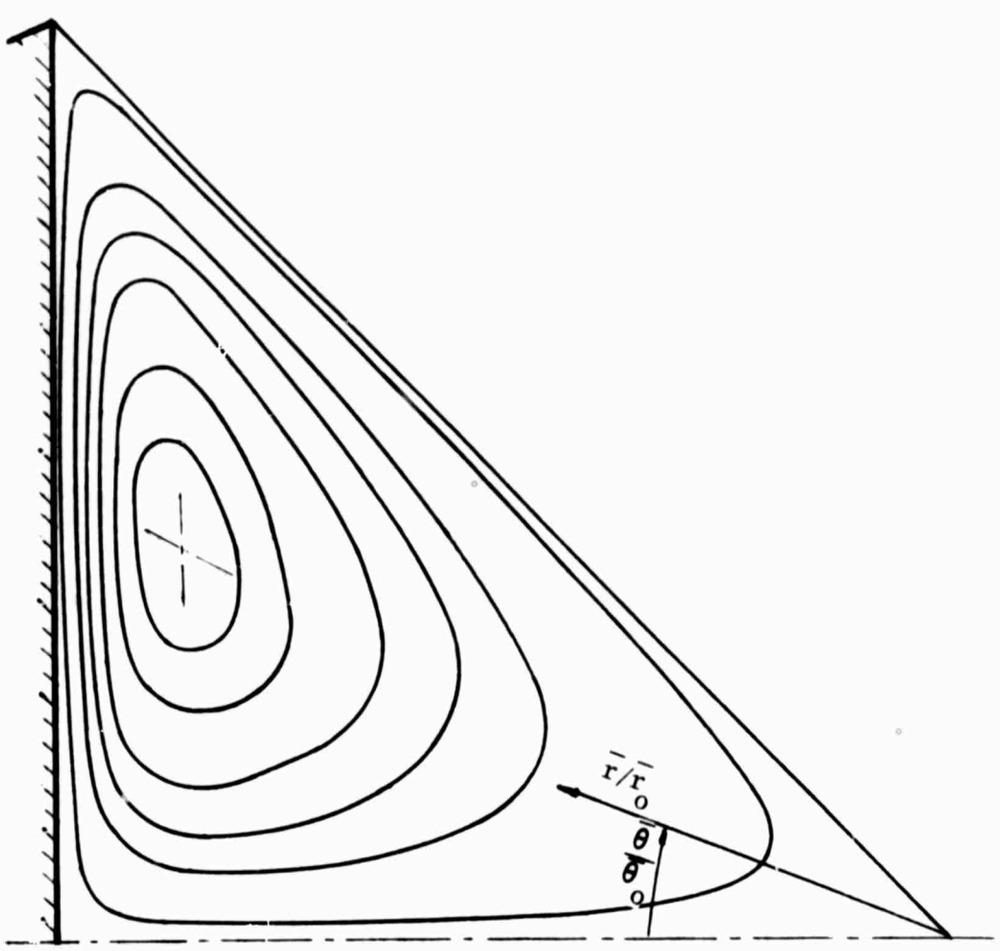

(b) Streamline Pattern with Stretched Vertical Coordinate

Figure 4: Streamlines in the Inviscid Core Flow

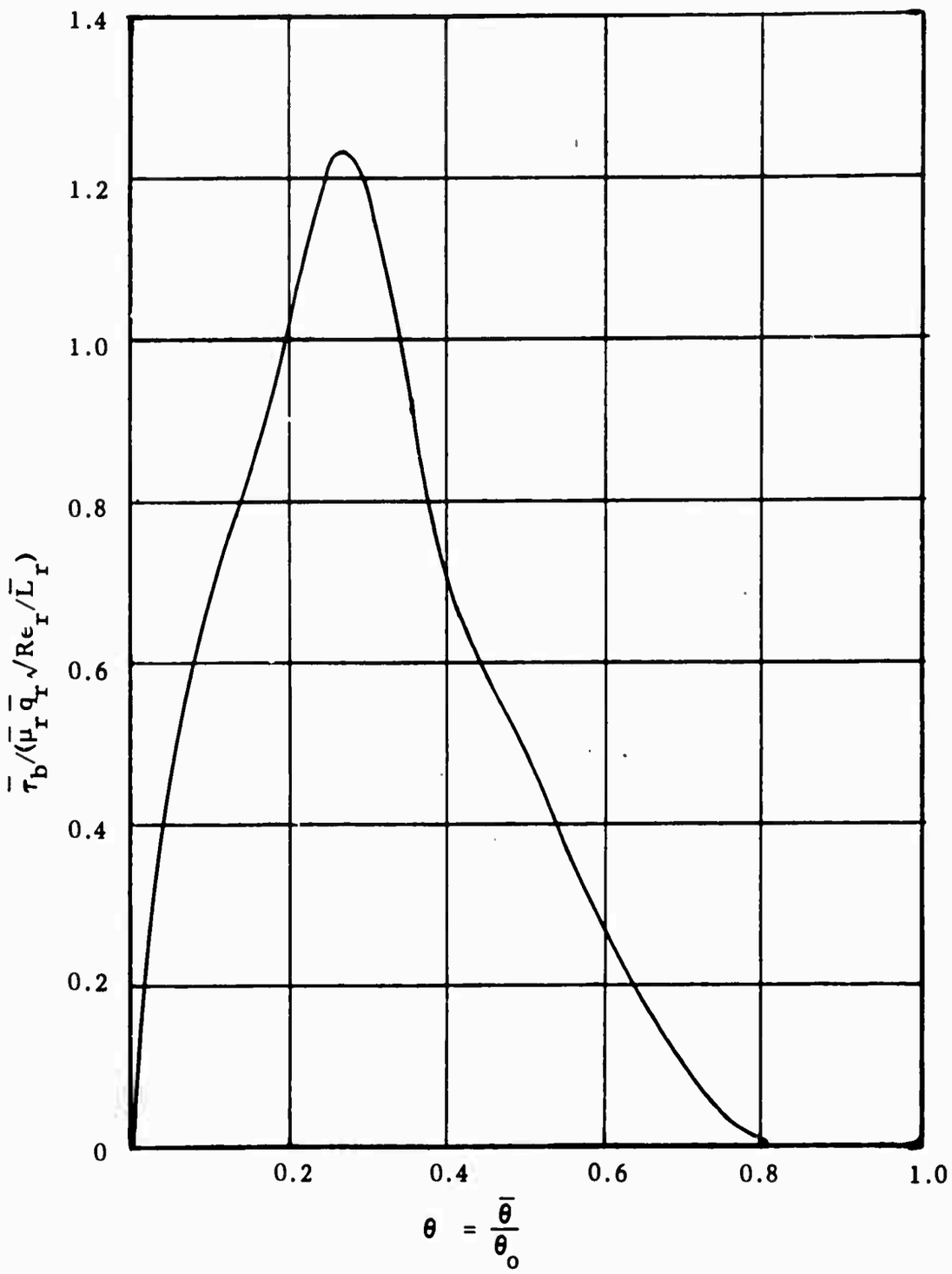

Figure 5: Shear Stress Distribution along the Base of the Wedge

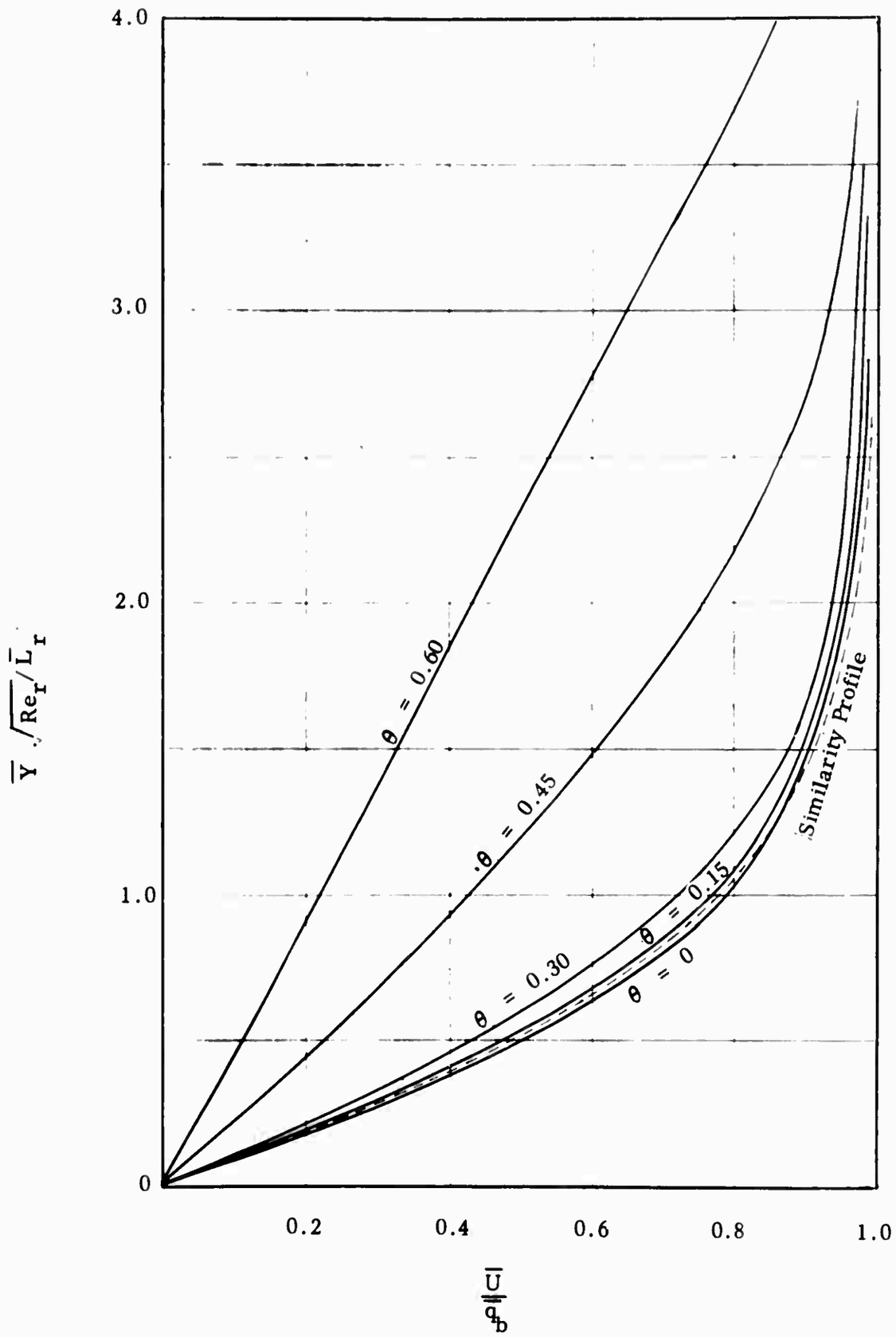

Figure 6: Velocity Profiles of the Base Boundary Layer

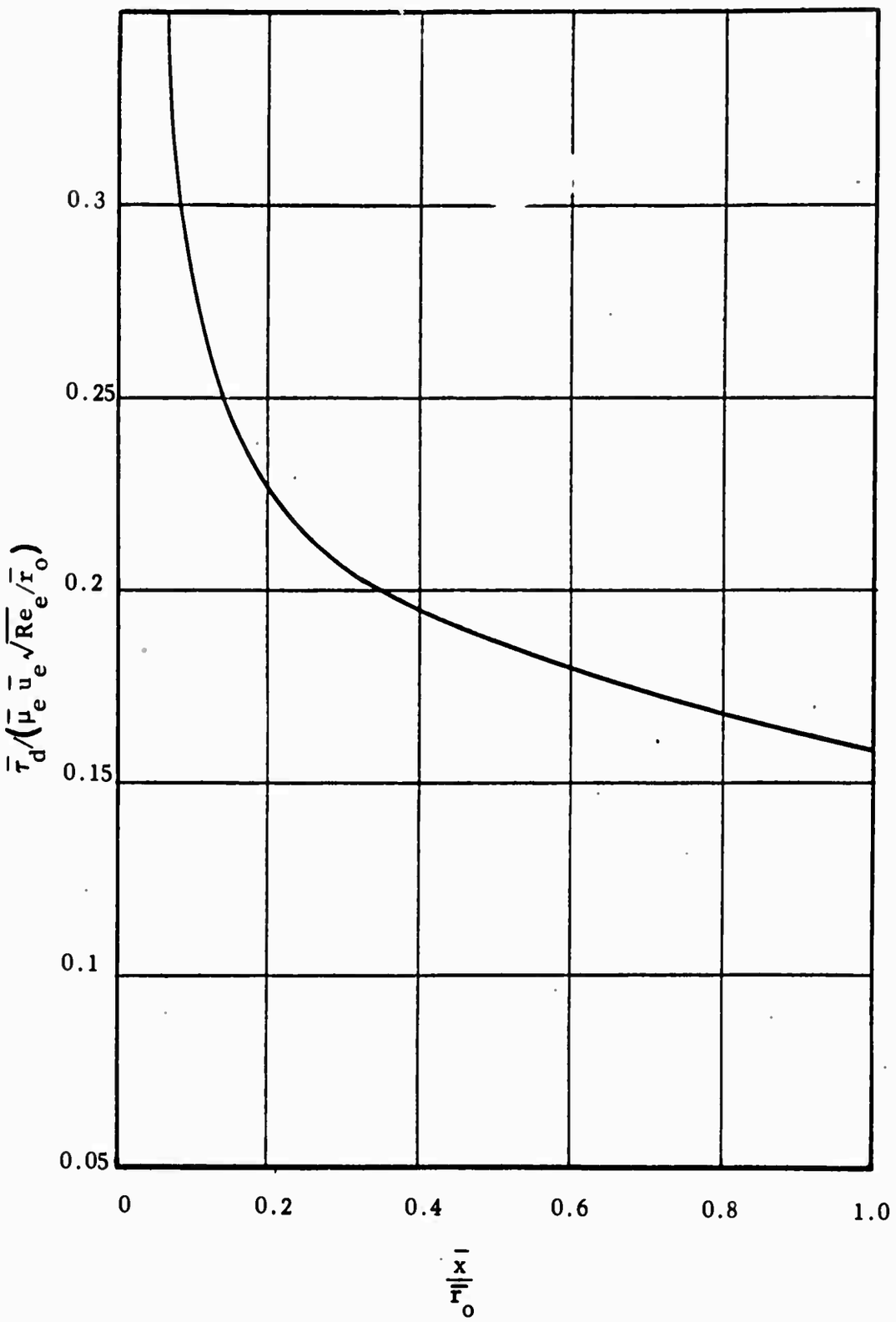

Figure 7: Shear Stress Distribution along the Dividing Streamline

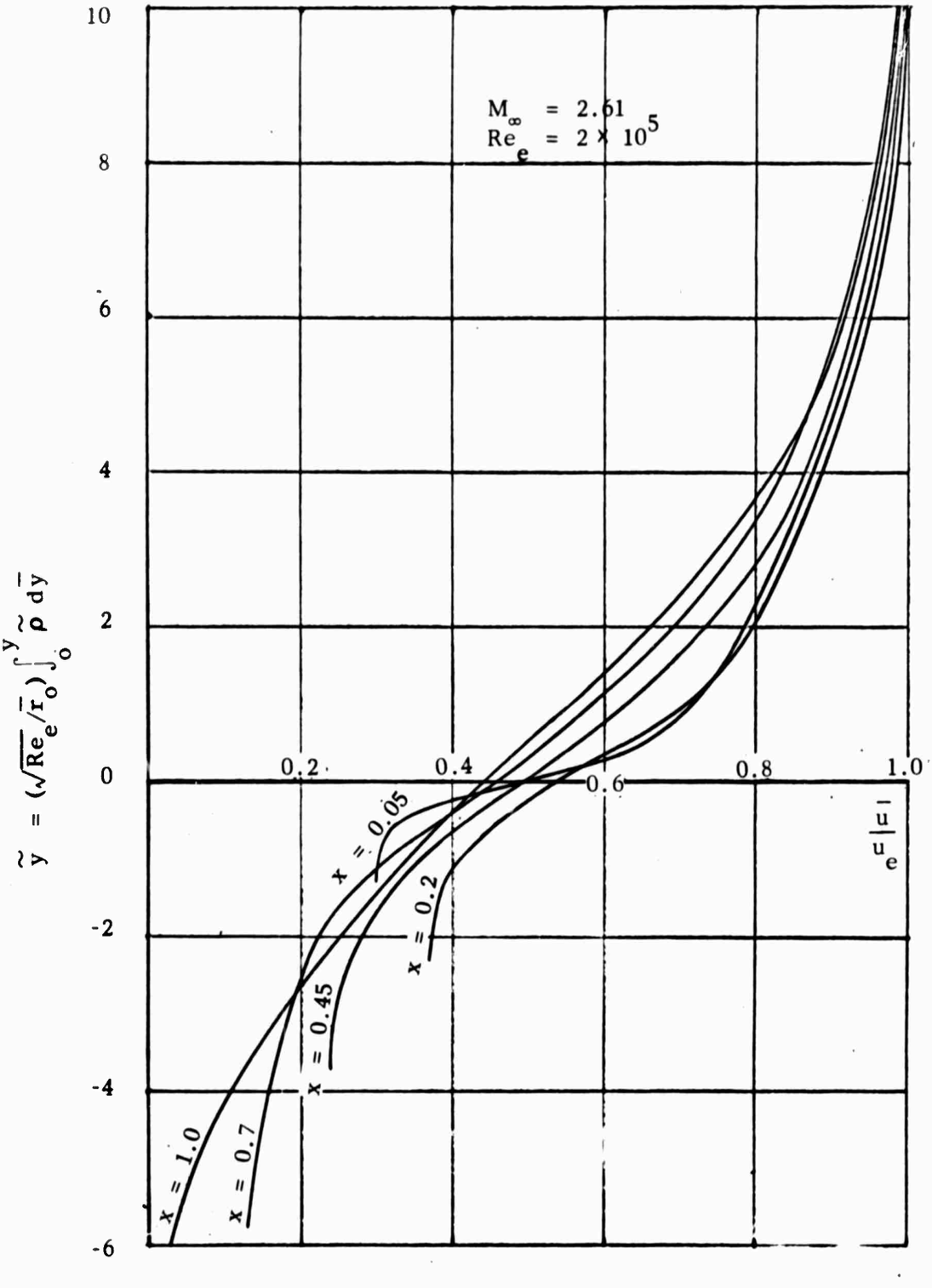

Figure 8: Velocity Profiles of the Laminar Free Shear Layer

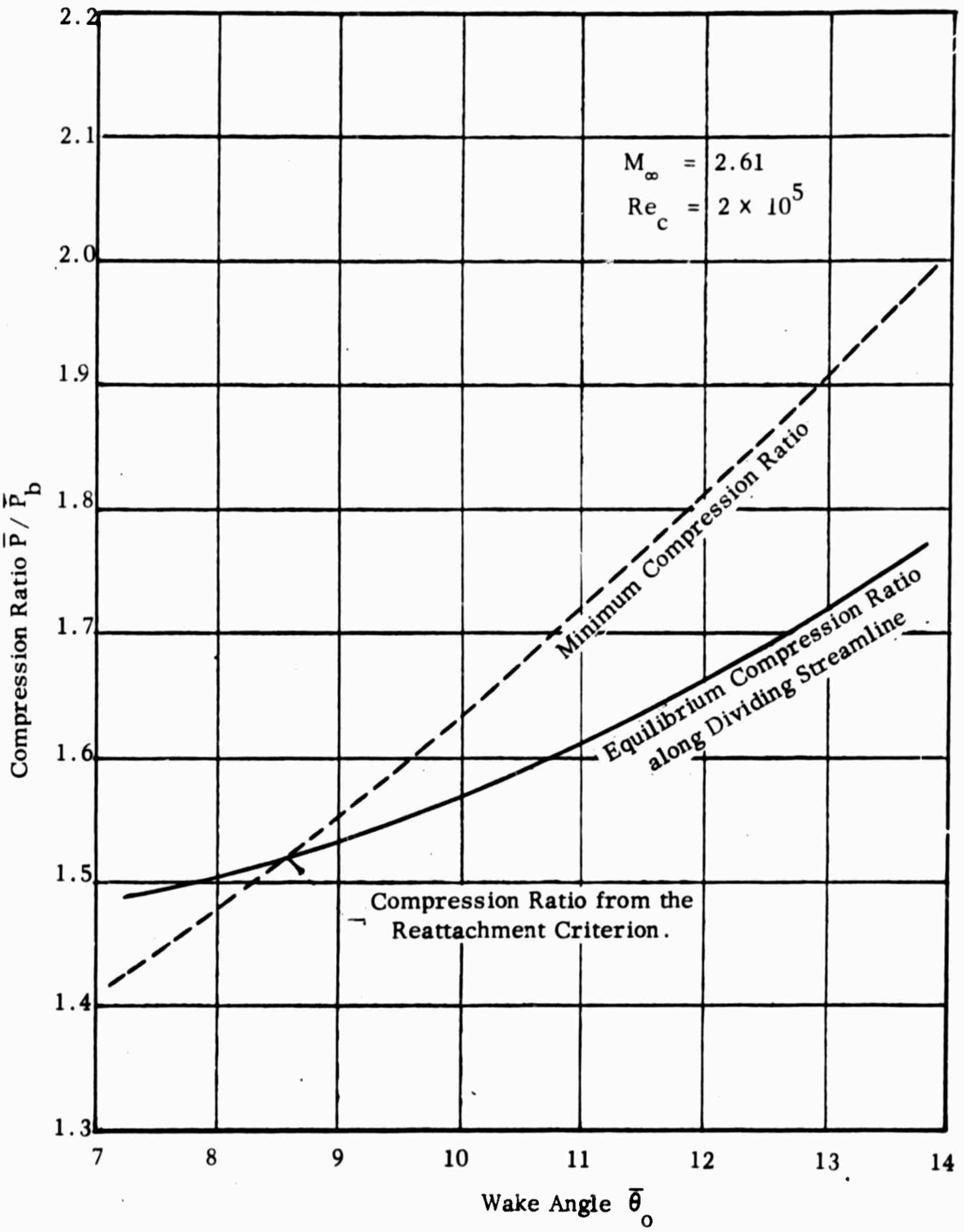

Figure 9: Determination of a Unique Compression Ratio for the Dividing Streamline

REFERENCES

1. Lykoudis, P. S., "A Review of Hypersonic Wake Studies," AAIA J. 4, 557-590. (1966)

2. Hama, F. R., "Experimental Investigations of Wedge Base Pressure and Lip Shock," Tech. Report No. 32-1033, Jet Propulsion Laboratory, Calif. Inst. of Tech., Pasadena, Calif., (1966)

3. Hama, F. R., "Estimation of the Strength of Lip Shock," AIAA J. 4, 166-167. (1966)

4. Batt, R. G., "Experimental Investigation of Wakes Behind Two-Dimensional Slender Bodies at Mach Number Six," Ph.D. Thesis, Cal. Ins. Tech., (1967)

5. Martellucci, A., Trucco, H. and Agrone, A., "Measurements of the Turbulent Near Wake of a Cone at Mach 6," AIAA J. 4, 385-391. (1966)

6. Todisco, A. and Pallone, A., "Near Wake Flow Field Measurements," AIAA J. 3, 2075-2081. (1965)

7. Chapman, D. R., "Laminar Mixing of a Compressible Fluid," NACA TN 1800. (1950)

8. Chapman, D. R., "An Analysis of Base Pressure at Supersonic Velocities and Comparison with Experiments," NACA TN 2137. (1951)

9. Chapman, D. R., Kuehn, D. M. and Larson, H. H., "Investigation of Separated Flows in Supersonic and Subsonic Streams with Emphasis on the Effect of Transition," NACA TN 3866. (1957)

10. Baum, E., King, H. H. and Denison, M. R., "Recent Studies of the Laminar Base-Flow Region," AIAA J. 2, 1527-1535. (1964)

11. Toba, K., "Analysis of Free Shear Layer with Finite Initial Thickness and Its Application to Base Flow," Douglas Report SM,-45943. (1964)

12. Reeves, B. L. and Lees, "Theory of the Laminar Near Wake of Blunt Bodies in Hypersonic Flow," AIAA J. 3, 2061-2074. (1965)

13. Stewartson, K., "Further Solutions of the Falkner - Skan Equations," Proc. Cambridge Phil. Soc. 50, 454-465. (1954)

14. Golik, R. J., Webb, W. H. and Lees, L., "Further Results of Viscous Interaction Theory for the Laminar Supersonic Near Wake," AIAA Paper No. 67-61. (1967)

15. Dean, W. R., "Note on the Motion of Liquid Near a Position of Separation," Proc. Cambridge Phil. Soc. 46, 293-306. (1950)

16. Oswatitsch, K., "The Separation Condition of Boundary Layers," Grumman Research Department Translation TR-28. (1964)

17. Reeves, B. L. and Buss, H., "On the Flow in Regions of Laminar Separation," AIAA Paper No. 67-64. (1967)

18. Reeves, B. L. and Buss, H., "A Theoretical Model of Laminar Hypersonic Near Wake Behind Blunt-Based Slender Bodies," AVCO Report AVSSD-0422-67RR. (1967)

19. Weiss, R., "A New Theoretical Solution of the Laminar Hypersonic Near Wake," AIAA J. 5, 2142-2149. (1967)

20. Prandtl, L., "Motion of Fluid with Very Little Viscosity," NACA TM 452. (1928)

21. Prandtl, L., "The Generation of Vortices in Fluids of Small Viscosity," J. Royal Aero. Soc. 31, 720-740. (1927)

22. Batchelor, G. K., "On Steady Laminar Flow with Closed Streamlines at Large Reynolds Numbers," J. Fluid Mech. 1, 177-190. (1956)

23. Batchelor, G. K., "A Proposal Concerning Laminar Wakes Behind Blunt Bodies at Large Reynolds Numbers," J. Fluid Mech. 1, 388-395. (1956)

24. Lenard, M., "A Theoretical Model of the High Reynolds Number Laminar Near Wake Flow Field Behind Axisymmetric Bodies in Hypersonic Flight," G. E., Fluid Mech. Component Fundamentals Memo. No. 111. (1966)

25. Guderley, K. G. and Greene, D. E., "Mathematical Theory of Steady Compressible Swirl Flows with Closed Streamlines at High Reynolds Numbers," ARL 67-0140, Aerospace Research Laboratories, Office of Aerospace Research, United States Air Force, Wright-Patterson Air Force Base, Ohio, (1967).

26. Weinbaum, S., "On Singular Points in the Laminar Two-Dimensional Near Wake Flow Field," G. E. Tech. Mem. No. 36. (1967)

27. Olsson, G. R. and Messiter, A. F., "The Hypersonic Laminar Boundary Layer Approaching the Base of a Slender Body," AIAA Paper No. 68-67. (1968)

28. Liepmann, H. W. and A. Roshko, Elements of Gasdynamics, John Wiley and Sons, Inc., New York, 1960.

29. Lagerstrom, P. A., "Laminar Flow Theory," Theory of Laminar Flows, ed. F. K. Moore, Princeton University Press, Princeton, New Jersey, 1964.

30. Van Dyke, M.D., Perturbation Methods in Fluid Mechanics, Academic Press, New York, 1964.

31. Burggraf, O. R., "Analytical and Numerical Studies of the Structure of Steady Separated Flows," J. Fluid Mech. 24, 113-151. (1966)

32. Churchill, R. V., Fourier Series and Boundary Value Problems. McGraw - Hill, New York,

33. Schlichting, H., Boundary Layer Theory, (4th ed.), McGraw - Hill, New York, 1960.

34. Rosenhead, L. (ed), Laminar Boundary Layers, Oxford Univ. Press, Oxford, England, 1963.

35. Belotserkovskii, O. M. and Chushkin, P. I., "The Numerical Solution of Problems in Gas Dynamics," Basic Developments in Fluid Dynamics, ed. M. Holt, Academic Press, New York, 1965.

36. Kubota, T. and Dewey, C. F., Jr, "Momentum Integral Methods for the Laminar Free Shear Layer," AIAA J. 2. 629-637. (1964)

37. Kuethe, A. M. and Schetzer, J. D., Foundations of Aerodynamics, (2nd ed) John Wiley & Sons, Inc., New York, 1959.

38. Lock, R. C., "The Velocity Distribution in the Laminar Boundary Layer Between Parallel Streams," Quar. Journ. Mech. and Appl. Math. 4, 42-63. (1957)

39. Ting, L., "On the Mixing of Two Parallel Streams," Journal of Mathematics and Physics, 38, 153-165. (1959)

APPENDIX

COEFFICIENTS OF THE SHEAR-LAYER EQUATIONS

Define

$$\frac{db_n}{dq_s} = b_{n0}, \quad \frac{db_n}{da_0} = b_{n1}, \quad \frac{db_n}{d\tilde{\delta}} = b_{n2}, \quad \frac{db_n}{db_2} = b_{n3},$$

$$\frac{db_n}{d\tilde{\delta}_{(+)}} = b_{n4}, \quad \frac{db_n}{d\tilde{\delta}_{(-)}} = b_{n5}$$

$$\frac{dc_n}{dq_s} = c_{n0}, \quad \frac{dc_n}{da_0} = c_{n1}, \quad \frac{dc_n}{d\tilde{\delta}} = c_{n2}, \quad \frac{dc_n}{db_2} = c_{n3},$$

$$\frac{dc_n}{d\tilde{\delta}_{(+)}} = c_{n4}, \quad \frac{dc_n}{d\tilde{\delta}_{(-)}} = c_{n5}$$

$$\frac{d\kappa_n}{dq_s} = \kappa_{n0}, \quad \frac{d\kappa_n}{da_0} = \kappa_{n1}, \quad \frac{d\kappa_n}{d\tilde{\delta}} = \kappa_{n2}, \quad \frac{d\kappa_n}{db_2} = \kappa_{n3},$$

$$\frac{d\kappa_n}{d\tilde{\delta}_{(+)}} = \kappa_{n4}, \quad \frac{d\kappa_n}{d\tilde{\delta}_{(-)}} = \kappa_{n5}$$

Then from equations (VII-13) through (VII-31) one can obtain

$$\kappa_{00} = 0$$

$$\kappa_{01} = -\frac{2\kappa\Delta}{\tilde{\delta}\, a_0^2}$$

$$\kappa_{02} = - \frac{2\kappa \tilde{\delta}_{(+)}(1-a_0)}{\tilde{\delta}^2 a_0}$$

$$\kappa_{03} = 0$$

$$\kappa_{04} = \frac{2\kappa (1-a_0)}{\tilde{\delta} a_0}$$

$$\kappa_{05} = 0$$

$$\kappa_{10} = 0$$

$$\kappa_{11} = - \frac{2\Delta}{a_0} + \frac{\kappa \Delta^2}{a_0^2}$$

$$\kappa_{12} = - \frac{2\Delta(1-a_0)}{a_0} + \frac{2\kappa \Delta^2 (1-a_0)}{\tilde{\delta} a_0}$$

$$\kappa_{13} = 0$$

$$\kappa_{14} = \frac{2(1-a_0)}{\tilde{\delta} a_0} - \frac{2\kappa \Delta (1-a_0)}{\tilde{\delta} a_0}$$

$$\kappa_{15} = 0$$

$$\kappa_{20} = 0$$

$$\kappa_{21} = \frac{2\Delta^2}{a_0^2}$$

$$\kappa_{22} = \frac{4\Delta^2(1-a_0)}{\delta a_0}$$

$$\kappa_{23} = 0$$

$$\kappa_{24} = -\frac{4\Delta(1-a_0)}{\delta a_0}$$

$$\kappa_{25} = 0$$

$$\kappa_{30} = 0$$

$$\kappa_{31} = \kappa_{01} - \frac{\kappa_{11}}{2} + \frac{\kappa_{21}}{12}$$

$$\kappa_{32} = \kappa_{02} - \frac{\kappa_{12}}{2} + \frac{\kappa_{22}}{12}$$

$$\kappa_{33} = 0$$

$$\kappa_{34} = \kappa_{04} - \frac{\kappa_{14}}{2} + \frac{\kappa_{24}}{12}$$

$$\kappa_{35} = 0$$

$$\kappa_{40} = 0$$

$$\kappa_{41} = \frac{\kappa_{31}}{1+\delta}$$

$$\kappa_{42} = \frac{\kappa_{32}}{1+\delta}$$

$$\kappa_{43} = 0$$

$$\kappa_{44} = \frac{\kappa_{34}}{1+\delta} + \frac{\kappa_4 \delta}{(1+\Delta)\tilde{\delta}_{(+)}}$$

$$\kappa_{45} = -\frac{\kappa_4}{(1+\delta)\tilde{\delta}_{(+)}}$$

$$\kappa_{50} = 0$$

$$\kappa_{51} = \frac{\kappa_{31}\delta}{(1+\delta)}$$

$$\kappa_{52} = \frac{\kappa_{32}\delta}{(1+\delta)}$$

$$\kappa_{53} = 0$$

$$\kappa_{54} = \frac{\kappa_{34}\delta}{(1+\delta)} + \left(\frac{\kappa_5}{\tilde{\delta}_{(+)}}\right)\left[-\frac{\delta}{(1+\delta)} + \frac{\delta^2}{(1+\delta)^2}\right]$$

$$\kappa_{55} = \left(\frac{\kappa_5}{\tilde{\delta}_{(+)}}\right)\left[\frac{1}{(1+\delta)} - \frac{\delta}{(1+\delta)^2}\right]$$

$$\kappa_{60} = -\left(\frac{\bar{q}_r}{\bar{u}_e}\right)\left[\frac{1}{(1+\delta)a_0}\right]$$

$$\kappa_{61} = \left(\frac{\bar{q}_r}{\bar{u}_e}\right)\left(\frac{q_s}{a_0}\right)\left[\frac{1}{(1+\delta)a_0}\right]$$

$$\kappa_{52} = 0$$

$$\kappa_{63} = 0$$

$$\kappa_{64} = \left[1 - \left(\frac{\bar{q}_r}{\bar{u}_e}\right)\left(\frac{q_s}{a_0}\right)\right]\left[\frac{\delta}{(1+\delta)^2\,\tilde{\delta}_{(+)}}\right]$$

$$\kappa_{65} = -\left[1 - \left(\frac{\bar{q}_r}{\bar{u}_e}\right)\left(\frac{q_s}{a_0}\right)\right]\left[\frac{1}{(1+\delta)\delta_{(+)}}\right]$$

$$b_{00} = -\kappa_{60}$$

$$b_{01} = -\kappa_{61} + \kappa_{31} - \kappa_{41}$$

$$b_{02} = \kappa_{32} - \kappa_{42}$$

$$b_{03} = -\frac{\delta}{6}$$

$$b_{04} = -\kappa_{64} + \frac{b_2 \delta}{6\tilde{\delta}_{(+)}} + \kappa_{34} - \kappa_{44}$$

$$b_{05} = -\kappa_{65} - \kappa_{45} - \frac{b_2}{6\tilde{\delta}_{(+)}}$$

$$b_{10} = 2\kappa_{60}$$

$$b_{11} = 2\kappa_{61} + 2\kappa_{41}$$

$$b_{12} = 2\kappa_{42}$$

$$b_{13} = \frac{1}{3}(\delta - 1)$$

$$b_{14} = 2\kappa_{64} - \frac{b_2 \delta}{3\tilde{\delta}_{(+)}} + 2\kappa_{44}$$

$$b_{15} = 2\kappa_{65} + \frac{b_2}{3\tilde{\delta}_{(+)}} + 2\kappa_{45}$$

$$b_{20} = 0$$

$$b_{21} = 0$$

$$b_{22} = 1$$

$$b_{23} = 0$$

$$b_{24} = 0$$

$$b_{25} = 0$$

$$b_{30} = -2\kappa_{60}$$

$$b_{31} = -2\kappa_{61} + \kappa_{11} - \frac{\kappa_{21}}{3} - 2\kappa_{41}$$

$$b_{32} = \kappa_{12} - \frac{\kappa_{22}}{3} - 2\kappa_{42}$$

$$b_{33} = -\frac{\tilde{\delta}_{(-)}}{3\delta_{(+)}} - 1$$

$$b_{34} = -2\kappa_{64} + \frac{b_2\tilde{\delta}_{(-)}}{3\tilde{\gamma}^2_{(+)}} + \kappa_{14} - \frac{\kappa_{24}}{3} - 2\kappa_{44}$$

$$b_{35} = -2\kappa_{65} - \frac{b_2}{3\delta_{(+)}} - 2\kappa_{45}$$

$$b_{40} = \kappa_{60}$$

$$b_{41} = \kappa_{61} - \frac{\kappa_{11}}{2} + \frac{\kappa_{21}}{4} + \kappa_{41}$$

$$b_{42} = -\frac{\kappa_{12}}{2} + \frac{\kappa_{22}}{4} + \kappa_{42}$$

$$b_{43} = \frac{1}{6}(2 + \delta)$$

$$b_{44} = \kappa_{64} + \frac{b_2\delta}{6\delta_{(+)}} - \frac{\kappa_{14}}{2} + \frac{\kappa_{24}}{2} + \kappa_{44}$$

$$b_{45} = \kappa_{65} + \frac{b_2}{6\delta_{(+)}} + \kappa_{45}$$

$$c_{00} = -\kappa_{60}$$

$$c_{01} = -\kappa_{61} + \kappa_{31} - k_{41}$$

$$c_{02} = \kappa_{32} - \kappa_{42}$$

$$c_{03} = -\frac{1}{6}\delta$$

$$c_{04} = -\kappa_{64} + \frac{b_2\delta}{6\tilde{\delta}_{+)}} + \kappa_{34} - \kappa_{44}$$

$$c_{05} = -\kappa_{65} - \frac{b_2}{6\tilde{\delta}_{(+)}} - \kappa_{45}$$

$$c_{10} = 2\kappa_{60}\delta$$

$$c_{11} = 2\kappa_{61}\,\delta + 2\kappa_{51}$$

$$c_{12} = 2\kappa_{52}$$

$$c_{13} = \frac{1}{3}\,\delta\,(\delta - 1)$$

$$c_{14} = 2\kappa_{64}\delta - \frac{2\delta\left[1 - \left(\frac{\bar{q}_r}{\bar{u}_e}\right)\left(\frac{q_s}{a_0}\right)\right]}{\tilde{\delta}_{(+)}(1+\delta)} + 2\kappa_{54} - (2\delta - 1)\,\frac{b_2\delta}{3\tilde{\delta}_{(+)}}$$

$$c_{15} = 2\kappa_{65}\delta + \frac{2\left[1 - \left(\frac{\bar{q}_r}{\bar{u}_e}\right)\left(\frac{q_s}{a_0}\right)\right]}{(1+\delta)\,\delta_{(+)}} + 2\kappa_{55} + \frac{b_2}{3\delta_{(+)}}(2\delta - 1)$$

$$c_{20} = 0$$

$$c_{21} = 0$$

$$c_{22} = 0$$

$$c_{23} = \delta^2$$

$$c_{24} = \frac{2b_2\delta^2}{\delta_{(+)}}$$

$$c_{25} = \frac{2b_2\delta}{\delta_{(+)}}$$

$$c_{30} = -2\kappa_{60}\delta$$

$$c_{31} = -2\kappa_{61} - 2\kappa_{51}$$

$$c_{32} = -2\kappa_{52}$$

$$c_{33} = \delta^2 + \frac{1}{3}\delta$$

$$c_{34} = -2\kappa_{64}\delta + 2\kappa_{6}\delta - 2\kappa_{54} - \frac{b_2}{\delta_{(+)}}\left(2\delta^2 + \frac{1}{3}\delta\right)$$

$$c_{35} = -2\kappa_{65}\delta - \frac{2\kappa_6}{\delta_{(+)}} - 2\kappa_{55} + \left(\frac{b_2}{\delta_{(+)}}\right)\left(2\delta + \frac{1}{3}\right)$$

$$c_{40} = -\kappa_{60}\delta$$

$$c_{41} = -\kappa_{61}\delta - \kappa_{51}$$

$$c_{42} = -\kappa_{52}$$

$$c_{43} = \frac{1}{3}\delta^2 + \frac{1}{6}\delta$$

$$c_{44} = -\kappa_{64}\delta + \frac{\kappa_6\delta}{\delta_{(+)}} - \kappa_{54} - \left(\frac{2\delta}{3} - \frac{\delta}{6}\right)\left(\frac{b_2}{\delta_{(+)}}\right)$$

$$c_{45} = -\kappa_{65}\delta - \frac{\kappa_6}{\delta_{(+)}} - \kappa_{55} - \left(\frac{2\delta}{3} + \frac{1}{6}\right)\left(\frac{b_2}{\delta_{(+)}}\right)$$

Again define

$$M = b_0^2 + b_0b_1 + \frac{1}{3}\left[2b_0b_2 + b_1^2\right] + \frac{1}{2}\left[b_0b_3 + b_1b_2\right] + \frac{1}{5}\left[2b_0b_4 + b_2^2 + 2b_1b_3\right]$$

$$+ \frac{1}{3}\left[b_1b_4 + b_2b_3\right] + \frac{1}{7}\left[b_3^2 + 2b_2b_4\right] + \frac{1}{4}b_3b_4 + \frac{1}{9}b_4^2$$

$$\frac{dM}{db_0} = 2b_0 + b_1 + \frac{2}{3}b_2 + \frac{1}{2}b_3 + \frac{2}{5}b_4$$

$$\frac{dM}{db_1} = b_0 + \frac{2}{3}b_1 + \frac{1}{2}b_2 + \frac{2}{5}b_3 + \frac{1}{3}b_4$$

$$\frac{dM}{db_2} = \frac{2}{3}b_0 + \frac{1}{2}b_1 + \frac{2}{5}b_2 + \frac{1}{3}b_3 + \frac{2}{7}b_4$$

$$\frac{dM}{db_3} = \frac{1}{2}b_0 + \frac{2}{5}b_1 + \frac{1}{3}b_3 + \frac{2}{7}b_3 + \frac{1}{4}b_4$$

$$\frac{dM}{db_4} = \frac{2}{5}b_0 + \frac{1}{3}b_1 + \frac{2}{7}b_2 + \frac{1}{4}b_3 + \frac{2}{9}b_4$$

$$M_0 = \frac{dM}{dq_s} = \sum_{n=0}^{4} \frac{dM}{db_n} b_{n0}$$

$$M_1 = \frac{dM}{da_0} = \sum_{n=0}^{4} \frac{dM}{db_n} b_{n1}$$

$$M_2 = \frac{dM}{d\tilde{\delta}} = \sum_{n=0}^{4} \frac{dM}{db_n} b_{n2}$$

$$M_3 = \frac{dM}{db_2} = \sum_{n=0}^{4} \frac{dM}{db_n} b_{n3}$$

$$M_4 = \frac{dM}{d\tilde{\delta}_{(+)}} = \sum_{n=0}^{4} \frac{dM}{db_n} b_{n4}$$

$$M_5 = \frac{dM}{d\tilde{\delta}_{(-)}} = \sum_{n=0}^{4} \frac{dM}{db_n} b_{n5}$$

$$D = c_0^2 - c_0c_1 + \frac{1}{3}\left[2c_0c_2 + c_1^2\right] - \frac{1}{2}\left[c_0c_3 + c_1c_2\right] + \frac{1}{5}\left[2c_0c_4 + c_2^2 + 2c_1c_3\right]$$

$$- \frac{1}{3}\left[c_1c_4 + c_2c_3\right] + \frac{1}{7}\left[c_3^2 + 2c_2c_4\right] - \frac{1}{4}c_3c_4 + \frac{1}{9}c_4^2$$

$$\frac{dD}{dc_0} = 2c_0 - c_1 + \frac{2}{3}c_2 - \frac{1}{2}c_3 + \frac{2}{5}c_4$$

$$\frac{dD}{dc_1} = -c_0 + \frac{2}{3}c_1 - \frac{1}{2}c_2 + \frac{2}{5}c_3 - \frac{1}{3}c_4$$

$$\frac{dD}{dc_2} = \frac{2}{3}c_0 - \frac{1}{2}c_1 + \frac{2}{5}c_2 - \frac{1}{3}c_3 + \frac{2}{7}c_4$$

$$\frac{dD}{dc_3} = -\frac{1}{2}c_0 + \frac{2}{5}c_1 - \frac{1}{3}c_2 + \frac{2}{7}c_3 - \frac{1}{4}c_4$$

$$\frac{dD}{dc_4} = \frac{2}{5}c_0 - \frac{1}{3}c_1 + \frac{2}{7}c_2 - \frac{1}{4}c_3 + \frac{1}{9}c_4$$

$$D_0 = \frac{dD}{dq_s} = \sum_{n=0}^{4} \frac{dD}{dc_n} c_{n0}$$

$$D_1 = \frac{dD}{da_0} = \sum_{n=0}^{4} \frac{dD}{dc_n} c_{n1}$$

$$D_2 = \frac{dD}{d\delta} = \sum_{n=0}^{4} \frac{dD}{dc_n} c_{n2}$$

$$D_3 = \frac{dD}{db_2} = \sum_{n=0}^{4} \frac{dD}{dc_n} c_{n3}$$

$$D_4 = \frac{dD}{d\tilde{\delta}_{(+)}} = \sum_{n=0}^{4} \frac{dD}{dc_n} c_{n4}$$

$$D_5 = \frac{dD}{d\tilde{\delta}_{(-)}} = \sum_{n=0}^{4} \frac{dD}{dc_n} c_{n5}$$

$$N = \sum_{n=0}^{4} (n+1)\, b_n$$

$$N_0 = \frac{dN}{dq_s} = \sum_{n=0}^{4} (n+1)\, b_{n0}$$

$$N_1 = \frac{dN}{da_0} = \sum_{n=0}^{4} (n+1)\, b_{n1}$$

$$N_2 = \frac{dN}{d\tilde{\delta}} = \sum_{n=0}^{4} (n+1)\, b_{n2}$$

$$N_3 = \frac{dN}{db_2} = \sum_{n=0}^{4} (n+1)\, b_{n3}$$

$$N_4 = \frac{dN}{d\tilde{\delta}_{(+)}} = \sum_{n=0}^{4} (n+1)\, b_{n4}$$

$$N_5 = \frac{dN}{d\tilde{\delta}_{(-)}} = \sum_{n=0}^{4} (n+1)\, b_{n5}$$

$$E = \sum_{n=0}^{4} (n+1)\, (-1)^n\, c_n$$

$$E_0 = \frac{dE}{dq_s} = \sum_{n=0}^{4} (n+1)\, (-1)^n\, C_{n0}$$

$$E_1 = \frac{dE}{da_0} = \sum_{n=0}^{4} (n+1)(-1)^n c_{n1}$$

$$E_2 = \frac{dE}{d\tilde{\delta}} = \sum_{n=0}^{4} (n+1)(-1)^n c_{n2}$$

$$E_3 = \frac{dE}{db_2} = \sum_{n=0}^{4} (n+1)(-1)^n c_{n3}$$

$$E_4 = \frac{dE}{d\tilde{\delta}_{(+)}} = \sum_{n=0}^{4} (n+1)(-1)^n c_{n4}$$

$$E_5 = \frac{dE}{d\tilde{\delta}_{(-)}} = \sum_{n=0}^{4} (n+1)(-1)^n c_{n5}$$

$$Q_{11} = \tilde{\delta}_{(+)} (M_3 - \kappa_3 N_3)$$

$$Q_{12} = M - \kappa_3 N + \tilde{\delta}_{(+)} (M_4 - \kappa_3 N_4)$$

$$Q_{13} = \tilde{\gamma}_{(+)} (M_5 - \kappa_3 N_5)$$

$$Q_1 = -\tilde{\delta}_{(+)} (2M - \kappa_3 N_1) \frac{1}{a_0} \frac{da_0}{d\tilde{x}} + \frac{\kappa_1}{a_0 \tilde{\delta}_{(+)}} - \frac{b_1}{\tilde{\delta}_{(+)} a_0}$$

$$+ \kappa_7 \tilde{\delta}_{(+)} \left(\frac{\tilde{H}}{a_0^2} - \frac{1}{2} M \right) - \tilde{\delta}_{(+)} (M_0 - \kappa_3 N_0) \frac{dq_s}{d\tilde{x}}$$

$$- \tilde{\gamma}_{(+)} (M_1 - \kappa_3 N_1) \frac{da_0}{d\tilde{x}} - \tilde{\gamma}_{(+)} (M_2 - \kappa_3 N_2) \frac{d\tilde{\delta}}{d\tilde{x}}$$

$$Q_{21} = \tilde{\delta}_{(-)} \left(D_3 - \frac{\bar{q}_r q_s E_3}{\bar{u}_e a_0} \right)$$

$$Q_{22} = \tilde{\delta}_{(-)} \left(D_4 - \frac{\bar{q}_r q_s E_4}{\bar{u}_e a_0} \right)$$

$$Q_{23} = D - \frac{\bar{q}_r q_s E}{\bar{u}_e a_0} + \tilde{\delta}_{(-)} \left(D_5 - \frac{\bar{q}_r q_s E_5}{\bar{u}_e a_0} \right)$$

$$Q_2 = - \frac{2}{a_0} \frac{da_0}{d\tilde{x}} \tilde{\delta}_{(-)} \left(D - \frac{\bar{q}_r q_s E}{\bar{u}_e a_0} \right) + \frac{c_1}{\delta_{(-)} a_0}$$

$$- \tilde{\delta}_{(-)} \left(D_0 - \frac{\bar{q}_r q_s E_0}{\bar{u}_e a_0} \right) \frac{dq_s}{d\tilde{x}} + \kappa_7 \tilde{\delta}_{(-)} \left(\frac{\tilde{H}}{a_0^2} - \tfrac{1}{2} D \right)$$

$$- \tilde{\delta}_{(-)} \left(D_1 - \frac{\bar{q}_r q_s E_1}{\bar{u}_e a_0} \right) \frac{da_0}{d\tilde{x}} - \tilde{\delta}_{(-)} \left(D_2 - \frac{\bar{q}_r q_s E_2}{\bar{u}_e a_0} \right) \frac{d\delta}{d\tilde{x}}$$

$$Q_{31} = c_0 c_{03}$$

$$Q_{32} = c_0 c_{04}$$

$$Q_{33} = c_0 c_{05}$$

$$Q_3 = - \frac{c_0^2}{a_0} \frac{da_0}{d\tilde{x}} + \frac{2c_2}{a_0 \tilde{\delta}_{(-)}^2} + \kappa_7 \left(\frac{\tilde{H}}{a_0^2} - \frac{c_0^2}{2} \right)$$

$$- c_0 c_{00} \frac{dq_s}{d\tilde{x}} + c_0 c_{01} \frac{da_0}{d\tilde{x}} + c_0 c_{02} \frac{d\tilde{\delta}}{d\tilde{x}}$$

BLANK PAGE

UNCLASSIFIED

Security Classification

DOCUMENT CONTROL DATA - R & D

(Security classification of title, body of abstract and indexing annotation must be entered when the overall report is classified)

1. ORIGINATING ACTIVITY *(Corporate author)*
Willow Run Laboratories, Institute of Science and Technology,
The University of Michigan, Ann Arbor

2a. REPORT SECURITY CLASSIFICATION
Unclassified

2b. GROUP

3. REPORT TITLE
THE LAMINAR NEAR WAKE BEHIND A SLENDER WEDGE AT SUPERSONIC SPEED AND HIGH REYNOLDS NUMBER

4. DESCRIPTIVE NOTES *(Type of report and inclusive dates)*

5. AUTHOR(S) *(First name, middle initial, last name)*
Ching-Ju Chang and Arthur F. Messiter

6. REPORT DATE	7a. TOTAL NO. OF PAGES	7b. NO. OF REFS
November 1968	xiv + 159	39

8a. CONTRACT OR GRANT NO.	9a. ORIGINATOR'S REPORT NUMBER(S)
DAHC15 67 C 0062	8430-2-T
b. PROJECT NO. ARPA Order 236	
c.	9b. OTHER REPORT NO(S) *(Any other numbers that may be assigned this report)*
d.	

10. DISTRIBUTION STATEMENT

11. SUPPLEMENTARY NOTES	12. SPONSORING MILITARY ACTIVITY
	Advanced Research Projects Agency, Department of Defense, Washington, D. C.

13. ABSTRACT

The theoretical study presented is concerned with predicting the flow details in the region immediately behind a slender wedge moving at supersonic speed. An asymptotic solution is obtained for the laminar near wake, which is valid in the limit as Reynolds number based on external flow properties tends to infinity, with the external Mach number held fixed. In this limit, the interior of the recirculating flow is approximately incompressible and inviscid; the viscous layer is a continuous thin layer with large transverse velocity gradient; and the typical velocity of the recirculating flow must be of the same order as that of the external flow, although numerically it is small.

For the inviscid core, it is shown from consideration of the dissipative terms that the temperature and vorticity are nearly constant. These results demonstrate the fact that, even though the core flow is inviscid and nonconducting, and the primary effects of diffusive exchanges are limited to the continuous viscous layer enclosing the recirculating flow, the accumulative effects of very small diffusive exchanges are experienced throughout the entire recirculation region.

There exists an equilibrium vorticity for the inviscid core so as to satisfy the condition of conservation of angular momentum for the recirculating flow. At the rear stagnation point, a tentative reattachment condition similar to Chapman's is used but based on the minimum pressure increase attainable at the rear stagnation point from the turning of a streamline in the shear layer to a direction parallel to the wake center line. Based on these two conditions, a unique solution for the near wake flow can be obtained for a given upstream flow condition. Numerical results are in general agreement with the available experimental data.

DD FORM 1 NOV 68 1473

UNCLASSIFIED

Security Classification

14 KEY WORDS	LINK A		LINK B		LINK C	
	ROLE	WT	ROLE	WT	ROLE	WT
Guided missiles						
Supersonic speed						
Reynolds number						
Flow						
Mach number						